Université d'Ottawa · University of Ottawa

Université d'Ottawa • University of Ottawa

FACULTÉ DES ÉTUDES SUPÉRIEURES ET POSTDOCTORALES

FACULTY OF GRADUATE AND POSTDOCTORAL STUDIES

Sylvia BALABANIAN

AUTEUR DE LA THÈSE - AUTHOR OF THESIS

M. Sc. (Biochemistry)

GRADE - DEGREE

Department of Biochemistry

FACULTÉ, ÉCOLE, DÉPARTEMENT - FACULTY, SCHOOL, DEPARTMENT

TITRE DE LA THÈSE - TITLE OF THE THESIS

Gene and Protein Expression Profiling of a Presymptomatic Type III Spinal Muscular Atrophy Mouse Model

A. MacKenzie

DIRECTEUR DE LA THÈSE - THESIS SUPERVISOR

CO-DIRECTEUR DE LA THÈSE - THESIS CO-SUPERVISOR

EXAMINATEURS DE LA THÈSE - THESIS EXAMINERS

Jocelyn Côté

D. Franks

J.-M. De Koninck, Ph.D.

LE DOYEN DE LA FACULTÉ DES ÉTUDES SUPÉRIEURES ET POSTDOCTORALES

DEAN OF THE FACULTY OF GRADUATE AND POSTDOCTORAL STUDIES

Gene and Protein Expression Profiling of a Presymptomatic Type III Spinal Muscular Atrophy Mouse Model

Sylvia Balabanian

Thesis submitted to the
Faculty of Graduate and Postdoctoral Studies
In partial fulfillment of the requirements
For the MSc degree in Biochemistry
With specialization in Human Molecular Genetics

Department of Biochemistry, Microbiology and Immunology
Faculty of Medicine
University of Ottawa

Your file Votre référence
ISBN: 0-494-01405-9
Our file Notre référence
ISBN: 0-494-01405-9

ACKNOWLEDGEMENTS

I would like to thank Dr. Alex MacKenzie for giving me the opportunity to study in his laboratory. I have greatly appreciated his encouragement and inspiration.

I would also like to thank Dr. Nathalie Gendron for her constant intellectual and personal support and Dr. Rashmi Kothary for his help throughout my project.

I would like to thank the SMA group especially Dan Kaplansky and Shannon Hayward-McClelland for their help with the animal colony, Lily Lin and April Doyle for their assistance in the lab and Phil Griffin for his technical advice.

I would like to extend my thanks to everyone at the Solange Gauthier Karsh Laboratory for having a sense of humour which always kept my spirits high.

Finally, I would like to thank my family for their unconditional love.

Abstract

In order to determine the molecular events leading up to motor neuron degeneration in SMA this study profiled the changes at the mRNA and protein levels in spinal cords of *Smn*$^{+/-}$ mice with those of *Smn*$^{+/+}$ littermates. The *Smn*$^{+/-}$ mice show 50% motor neuron loss by 6 months of age and are used as a model for mild SMA in humans. We have isolated RNA from spinal cords of 5-week-old mice in order to perform representational difference analysis (RDA) and microarray analysis using Affymetrix MOE430 arrays. Subtle but reproducible changes occur in the transcriptome of SMA mice. Genes involved in RNA metabolism, apoptosis regulation and transcriptional regulation were shown to be the most affected in the *Smn* $^{+/-}$ mice. These changes in expression were characterized by semi-quantitative RT-PCR and Western blot analysis at various timepoints. The differences in protein levels in 5-week-old *Smn*$^{+/-}$ and *Smn*$^{+/+}$ spinal cords were examined using apoptosis and kinase protein screens from Kinetworks Bioinformatics. Results demonstrated similar protein expression levels in the *Smn*$^{+/-}$ and *Smn*$^{+/+}$ samples. Although the signaling pathways and apoptotic protein levels do not seem to be significantly altered in the SMA mouse spinal cord at the 5-week presymptomatic stage we believe that the cells present the first signs of the apoptotic process indicating that they are responding to the stress of Smn depletion.

TABLE OF CONTENTS

LIST OF TABLES

LIST OF FIGURES

1. Introduction

1.1 Spinal Muscular Atrophy

1.1.1 Epidemiology

Childhood spinal muscular atrophies (SMA) are a group of inherited neurodegenerative disorders caused by the loss of motor neurons in the anterior horn of the spinal cord leading to muscular weakness with muscular atrophy. The estimated heterozygote frequency is 1/40 (Pearn J, 1973). With an incidence between 1 in 6 000 and 1 in 10 000 in newborns and fatality between 1 in 16 000 and 1 in 25 000 infants in Europe and North America it is the most common monogenic disease fatal to infants and one of the most common forms of neuromuscular disorder in childhood (Pearn J, 1978).

1.1.2 Clinical Classification

Due to the clinical variability of SMA, the International SMA Consortium classified the disease into three groups based on the age of onset and clinical course (Munstat, 1991). This subdivision into three groups is subjective and there is heterogeneity within each group and an overall continuum of clinical course (Dubowitz, 1995). Type I SMA (also called Werdnig-Hoffmann disease) is the most severe form with onset either at birth or within six months of age and death before the age of two years from respiratory failure (Werdnig 1894, Hoffmann 1900). Patients with type II SMA (intermediate form) develop muscular weakness by 18 months of age and can sit but will never be able to stand or walk without support. Type III SMA also known as Kugelberg-Welander disease, has an onset between 18 months and 30 years of age with the patient achieving the ability to walk but developing a variable degree of proximal muscle weakness (Kugelberg and Welander 1956). Type IV

SMA, the mildest form, is considered to have an age of onset occurring after 30 years (Pearn et al., 1978).

1.1.3 Diagnosis and Treatment

A firm diagnosis of SMA is typically established after performing a physical examination, electromyography (EMG), genetic testing and, in cases when the investigations are not confirmatory, a muscle biopsy.

All four forms of SMA are characterized by a symmetric weakness in the proximal muscles of the arms and legs, a loss of deep tendon reflexes and muscular fasciculations. Sensation is unaffected and SMA patients appreciate feelings like tickling and light touch. Blood creatine kinase (CK) levels are normal or slightly elevated in SMA patients, distinguishing it from muscular dystrophy where CK levels are very high.

The EMG test can usually provide evidence of a neurogenic atrophy associated with anterior horn cell degeneration. Children with symptomatic SMA show muscle denervation but no sensory denervation and normal motor nerve conduction velocity with slightly slower conduction in the more severe cases (Munsat et al. 1969, Hausmanowa-Petrusewicz 1970 and Moosa and Dubowitz 1970).

Homozygous deletion of survival of motor neurons (*SMN*) gene is commonly used to confirm the clinical diagnosis of SMA. Detection of a homozygous deletion of *SMN* is especially important for diagnosing SMA in children with classic clinical signs and symptoms of SMA, but who in addition have other unusual features either in the brain or outside the nervous system (Burglen et al., 1995; Rudnik-Shoneborn et al., 1996). On the milder end of the spectrum are type IV patients with substantially later onset and milder

degrees of weakness who have previously been excluded because of overlap with other motor neuron diseases.

Treatment of all forms of SMA is symptomatic and supportive, and includes treating pneumonia, curvature of the spine, and respiratory infections, if present. Also, physical therapy, orthotic supports, and rehabilitation are useful. As yet, there is no cure for this neuromuscular disorder (Iannaconne et al., 2004).

1.1.4 Pathology

The pathological hallmark of all forms of SMA is the paucity of the anterior horn cells of the spinal cord and the lower brainstem, with the few surviving motor neurons exhibiting swelling of the perikarya and chromatolysis (Murayama et al., 1991). Ultrastructural analysis shows that mitochondria and clumps of membranous bodies collect in the cell soma of chromatolytic neurons, with adjacent accumulation of neurofilaments (Chou & Fakadej, 1971). Axonal degeneration occurs anterograde, with resulting denervation of the myocytes within its motor unit. This can sometimes lead to the reinnervation of muscle, where adjacent uninjured motor neurons sprout leads to fiber type grouping of myocytes, while the injured axon attempts axonal sprouting. The typical histologic finding in SMA muscle is large numbers of atrophic fibers, often a few micrometers in diameter, resulting from denervation of muscle in early childhood (Cotran et al., 1999). All forms of SMA are characterized by progressive muscle weakness with predominant involvement of the proximal muscle groups.

The widely held notion has been that SMA is a neuropathy principally involving the cell body with secondary degeneration of the axons. However, there are some reasons to believe neuronopathy may follow from pathology expressed initially in the distant axon.

Electrophysiologic and pathologic reviews of animal models of motor neuron disease suggest a precendent for primary abnormalities in the distal axon of motor neurons (Pinter et al., 1995; Cork et al., 1989; Schmalbruch et al., 1991). Studies in zebrafish show that reduced levels of Smn protein lead to disturbed motor axon outgrowth and pathfinding (McWhorter et al., 2003). Finally, motorneurons isolated from an SMA mouse model exhibit normal survival, but reduced axon growth (Rossoll et al., 2003). Recent evidence suggesting axonal growth defects in SMA models has shifted the focus of SMA pathology from the motorneuron cell body to the distal axon.

1.2 Molecular Genetics of Spinal Muscular Atrophy

1.2.1 Locus of the Survival of Motor Neuron Gene

All four forms of SMA have been mapped to 5q12-13 in humans (Brzustowicz et al., 1990; Melki et al. 1990). Positional cloning strategies show that this genomic region is characterized by an inverted duplication with each element containing four genes: the *SMN* gene (Lefebvre et al. 1995), the gene encoding neuronal apoptosis inhibitor protein (*NAIP*) (Roy et al., 1995), the gene encoding p44, a subunit of the basal transcription factor TFIIH (Burglen et al., 1997), and the H4F5 gene (Scharf et al., 1998).

The *NAIP* and *SMN* genes are duplicated with a telomeric *SMN* gene (*SMN1*) and a centromeric *SMN* gene (*SMN2*), and *NAIP* is duplicated either with exon 5 (*NAIP5*) or without exon 5 (*NAIPD*). The nearly identical genes, *SMN1* and *SMN2*, can be distinguished by five nucleotide changes in exons 7 and 8 (Lefebvre et al., 1995). The critical difference between *SMN1* and *SMN2* is a C to T transition that affects splicing of exon 7 and generates mostly an unstable isoform lacking exon 7 (Lorson et al., 1999; Monani et al., 1999). The loss of the *SMN1* gene, which is observed in 95% of SMA patients (Lefebvre et al. 1995),

occurs by two different mechanisms: deletion (Wirth et al., 1995), or conversion of *SMN1* to *SMN2* (Campbell et al., 1997). Patients in which *SMN1* was neither deleted nor converted to *SMN2*, carry either a point mutation (Y272C) or short deletions in the consensus splice sites of introns 6 and 7 of *SMN1* (Lefebvre et al., 1995). A point mutation (E134K) within the SMN Tudor domain that prevents Sm binding has also been observed (Buhler et al., 1999). All SMA patients retain at least one intact copy of the *SMN2* gene. This implies that complete absence of *SMN* genes in human, as confirmed in mice, is embryonic lethal (Schrank et al., 1997). *SMN2* can produce low levels of full-length transcript and studies have shown a positive correlation between phenotype severity and *SMN2* copy number (McAndrew et al., 1997; Campbell et al., 1997). Thus the *SMN2* gene acts as a modifier of phenotype in SMA.

1.2.2 *SMN* Is Highly Conserved During Evolution

Orthologues of *SMN* have been identified in yeast (*Schizosaccharomyces pombe*), nematode (*Caenorhabditis elegans*), fly (*Drosophila melangostar*), zebrafish, and mouse (Bertrandy et al., 1999; DiDonato et al., 1997; Miguel-Aliaga et al., 2000; Owen et al, 2000; Schrank et al., 1997). No spontaneous mutations have been found in these species and only chimpanzees, mankind's closest relative, have 2-7 copies of the *SMN* gene, although the mutations found in the human *SMN2* gene are not present in any of the multiple copies of the chimpanzee *SMN* gene (Rochette et al., 2001).

1.2.3 Functions of SMN Protein in the Cell

SMN is a ubiquitously expressed protein. Exon 3 of *SMN* has homology to a Tudor domain (Mohagheg et al., 1999), a conserved domain found in several RNA-binding proteins

(Ponting, 1997). The central Tudor domain facilitates the SMN-Sm protein interaction (Selenko et al., 2001). SMN is localized in the cytoplasm and nuclear structures called gems and Cajal bodies (Liu et al., 1996). In both the nucleus and cytoplasm SMN is a member of a multiprotein complex comprising spliceosomal U snRNPs Sm proteins, profilins (Giesemann et al., 1999), a number of novel proteins: Gemin2, Gemin3 a putative DEAD-box helicase, Gemin4, Gemin5 a WD repeat protein, Gemin6 and U snRNAs (Fisher et al., 1997; Yong et al, 2002). Through these interactions it is thought that SMN plays a central role in pre-mRNA splicing by promoting the assembly of snRNPs in the cytoplasm (Fisher et al., 1997), the transport of snRNPs in the nucleus (Narayanan et al., 2002) and the nuclear regeneration of snRNPs and spliceosomes (Pellizzoni et al., 1998), as well as the modulation of Sm protein composition of U snRNPs (Meister et al., 2000). In motor neurons SMN is also localized in axons (Pagliardini et al., 2000; Jablonka et al., 2001; Fan & Simard, 2002), but unlike nuclear SMN it does not co-localize with Gemin 2 (Jablonka et al., 2001). Instead, axonal SMN interacts with hnRNPR and hnRNPQ (Mourelatos et al., 2001; Rossoll et al., 2002), RNA binding proteins that recognize and bind to mRNA and may be involved in their axonal transport (Rossoll et al., 2002). A recent study by Zhang et al. (2003) implicated the active role for SMN in neurite outgrowth. The domain encoded by exon 7 is required for the localization of the Smn protein associated with RNPs in motor neuron axons in an SMA mouse model, and this deficit results in significantly shorter neuritis (Rossoll et al., 2002). Binding of Smn to hnRNP R and localization of these proteins in motor axons suggest that Smn could be involved in the transport of crucial mRNAs in motor axons.

SMN has been shown to interact directly or indirectly with p53 (Young et al., 2001) and Bcl-2 (Iwahashi et al., 1997), suggesting that SMN plays a role in apoptosis. SMN has also

been implicated in the regulation of transcription through interaction with transcription factors (Strasswimmer et al., 1999; Campbell et al., 2000; Williams et al., 2000) and RNA polymerase II (Pellizzoni et al., 2001). SMN has been shown to interact with other proteins including nucleolar proteins, Osteoclast Stimulatory Factor (Kurihara, 2001), and ZPR1 (Gangwani et al, 2001) suggesting other as yet undefined roles of SMN.

SMN is expressed in all tissues and its function is essential to cell survival, however only motor neurons appear to be sensitive to a reduction in SMN levels. There are three hypotheses that attempt to explain how a deficiency of *SMN1* leads to a defect specifically in motor neurons (i) large amounts of SMN protein may be required for particular pre-mRNA splicing or transcriptional process in motor neurons, and a loss of SMN function would result in a defect restricted to some RNA molecules in these cells; (ii) SMN may have a specific function related to RNA metabolism or transcription in motor neurons through an interacting protein specific to these cells; (iii) SMN may have another function, so far unknown. Further molecular investigations are clearly needed for the identification of those SMN functions which, when reduced or lost, cause motor neuron attrition and thus SMA.

1.3 Animal Models of Spinal Muscular Atrophy

1.3.1 The Murine *Smn* Knockout Model Is Embryonic Lethal

The first model, developed in Germany, consisted of knocking out the murine *Smn* gene through homologous recombination in embryonic stem cells. The homozygote deletion of *Smn* in the mouse is lethal at the blastocyte stage when levels of maternal Smn have dropped, demonstrating an essential role for Smn (Schrank et al., 1997).

1.3.2 Three *SMN2* Transgenic Mouse Models

Three transgenic mouse models carrying the human *SMN2* gene have been generated (Hsieh-Li et al., 2000; Monani et al., 2000; Monani et al., 2003). One group's model is based on the production of two mouse lines, one carrying a deletion of mouse *Smn* exon 7 through homologous recombination and the other expressing human *SMN2* gene after microinjection of a genomic DNA fragment which also contains part of centromeric *NAIP* and intact *H4F5* genes (Hsieh-Li et al., 2000). Mice carrying both homozygous deletion of *Smn* exon 7 and the human genomic transgene developed a variety of symptoms including lower body weight, short and enlarged tails, edema, chronic necrosis of the tail and hindlimbs, and a variable age of survival in the same littermates. The most severe form, called type 1, was characterized by the absence of furry hair and death within 10 days of age. Intermediate phenotype (classified type 2) was characterized by poor activity and death within 4 weeks of age. Mutant mice called type 3 survived normally and were characterized by short and enlarged tails. The different phenotypes observed within the same littermates have been correlated with the *SMN2* transgene copy. The necrosis of tail and hindlimbs in some mutant mice are intriguing and unexpected phenotypes. Fine characterization of the neuromuscular system of these mutant mice has not been performed yet.

A similar approach was adopted by another group who created mouse lines carrying a transgene containing the human *SMN2* gene without any neighbouring genes (Monani et al., 2000). They selected lines containing either low or high copy number of *SMN2* transgene. Mice carrying low copy number of the *SMN2* gene and a homozygous null *Smn* allele ($Smn^{-/-}$) developed a severe phenotype leading to death either *in utero* or in the first 6 hours after birth, or survival up to 6 days of age. Interestingly, surviving mutant mice carrying low

copy number of *SMN2* displayed abnormal motor behaviour associated with moderate motor neuron degeneration in the spinal cord (up to 35%) at the latest stage of the disease. They also showed evidence of motor axon loss and sprouting, muscle atrophy and abnormal EMG patterns. Phenotypic features in the mice included muscle weakness and a decreased life span. The only abnormal phenotype displayed by mutant mice ($Smn^{-/-}$) carrying a high copy number of *SMN2* transgene is a short, thick tail suggesting that neuronal death was a late manifestation of the disease phenotype. In addition, mutant mice carrying a high copy number of *SMN2* transgene confirmed that *SMN2* was able to rescue the embryonic lethality of the *Smn* knockout mice and demonstrated that an increased copy number of *SMN2* reduced the severity of the phenotype, consistent with data observed in human SMA.

The third transgene model was created by Monani et al. in 2003. They introduced a transgene carrying an A2G into *Smn*-null mice and reported that it is unable to rescue embryonic lethality. An A2G missense mutation in exon 1 of the *SMN* gene disrupts self-association and presumably prevents the formation of SMN oligomers (Lyu et al., 1990; Chakrabartty et al., 1991). When introduced to a *SMN2*:$Smn^{-/-}$ mouse, the A2G transgene delays the onset of motor neuron loss, resulting in a mild SMA phenotype by delaying the onset of motor neuron loss. These mice exhibit many of the pathalogical characteristics of type III (mild) mice.

1.3.3 Conditional Knockout of Murine *Smn* Gene Using the Cre-loxP system

A different approach using the Cre-loxP system to specifically delete *Smn* was employed to create tissue-specific *Smn*-null mouse models (Frugier et al., 2000). A mouse line carrying two loxP sequences flanking *Smn* exon 7 (*SmnF7*) has been established through homologous recombination. Cre-mediated deletion of *SmnF7* directed to neurons has been

achieved by crossing the *SmnF7* mice with a transgenic mouse line expressing Cre recombinase, expressed under the control of a neuron-specific enolase (NSE) promoter, in neurons. These neuronal mutant mice displayed severe motor defects associated with tremors from two weeks of age, leading to complete paralysis and death at a mean age of four weeks. Morphological analysis of skeletal muscle revealed a severe muscle denervation process. Surprisingly, although pronounced morphological changes of motor neurons were observed in mutant mice, no significant loss of motor neurons of the anterior horn was reported. This approach was therefore able to produce mice with a motor defect related to a muscle denervation process of neurogenic origin, a constant feature found in human SMA (Byers and Banker, 1961). These data demonstrated that a *Smn* gene defect directed to neurons but not to skeletal muscle leads to an SMA phenotype indicating that motor neurons are a primary target of the *Smn* gene defect in SMA. However, unlike SMA in humans, morphological changes of motor neurons were observed in the mutant mice but no significant loss of motor neurons of the anterior horn were reported. The same group also directed Cre-mediated deletion of *SmnF7* to skeletal muscle that lead to a dystrophic phenotype leading to muscle paralysis and death (Cifuentes-Diaz et al., 2001).

1.3.4 The $Smn^{-/+}$ Mouse as a Model for Mild SMA

The $Smn^{-/+}$ mouse created by homologous recombination (Schrank et al., 1997) displays 50% reduction of Smn protein levels in the spinal cord, a marked loss of the cytoplasmic Smn pool and motor neuron degeneration resembling SMA type III (Jablonka et al., 2000). At birth $Smn^{-/+}$ and $Smn^{+/+}$ mice have the same number of motor neurons. At 6 months of age, the $Smn^{-/+}$ mice have lost approximately half their motor neurons in the lumbar region. A mild mouse model at an early time point is potentially useful for determining mechanisms

leading up to the degeneration of motor neurons in SMA. For this reason, preliminary experiments in this study were performed using 5-week-old *Smn*$^{-/+}$ mice.

1.4 Hypothesis and Principal Objectives

Previous studies have shown that large amounts of SMN protein are specifically required for transcription, pre-mRNA splicing, mRNA transport or another unidentified process in motor neurons but the SMA-causative function of SMN depletion is still unknown. This study attempted to use high-throughput gene and protein profiling techniques to reveal molecular pathways that are sensitive to an SMN deficit in spinal cord tissue in hopes of elucidating the mechanism(s) linking the SMN defect to SMA pathogenesis. The two principal objectives were (1) to create a detailed profile of changes at the mRNA and protein levels caused by SMN depletion in spinal cords and (2) to identify the mechanisms affected by SMN depletion leading up to the degeneration of motor neurons. Experiments were performed using preclinical, 5-week-old *Smn*$^{+/-}$ mice and wildtype littermates and the following three profiling techniques: (1) Representational Difference Analysis, (2) Microarray Analysis and (3) Apoptosis and Kinase Protein Screens.

Genomic profiling results showed subtle changes in the transcriptome of SMA mice, especially in genes coding for protein involved in apoptosis, RNA binding and transcription factors. Interestingly, microarray results showed a decreased expression of genes coding for calcium-activated proteins in SMA mice indicating a disruption of cellular homeostasis. Several promising candidate genes were further investigated: Gelsolin, an actin-cytoskeleton regulator, showed increased levels of mRNA but not protein in the SMA mice.

The pro-apoptotic Bid gene and protein levels were increased but anti-apoptotic N-Bak showed a decreased expression at the transcript level that did not translate to the protein level. Protein profiling and immunoblotting show signaling pathways and apoptotic protein levels do not seem to be significantly altered in the SMA mouse spinal cord at the 5-week preclinical stage suggesting that the cells are presenting the first signs of the apoptotic process in response to the stress of Smn depletion.

Materials and Methods

2.1 Animal Protocol

2.1.1 Breeding of *Smn* Knockout C57/Bl6 Mice

We obtained the heterozygote knockout of the survival of motor neuron gene ($Smn^{-/+}$) mouse line from Dr. Michael Sendtner (University of Würzburg, Germany) and have maintained it on a C57/Bl6 background. The mice were transferred to the University of Ottawa Animal Care and Veterinary Services Facility and housed and bred in accordance with the Institutional Animal Care and Use Committee guidelines.

2.1.2 Genotyping of *Smn* Knockout Mice Litters

C57/Bl6 mice heterozygous for mouse *Smn* were mated to wildtype C57/Bl6 mice (Charles River, QC). The offspring were weaned at three weeks of age, their ears tagged and their tails clipped for DNA isolation. Total genomic DNA was extracted from the tail clipping as follows: in an Eppendorf tube containing a tail clipping, 300 µl of STD buffer (1 mM Tris-Hcl pH 8.0, 0.5 mM EDTA pH 8.0, and 5 mM NaCl), 200 µl of 2 X lysis buffer (Applied Biosystem Inc., Mississauga, ON), 40 µl of 10 mg/ml proteinase K (Boehringer Manheim, Montreal, QC), and 1.25 µl of 0.5 µg/µl RNAse (Boehringer Manheim, Montreal, QC) were added. Eppendorf tubes were incubated overnight at 50°C in a water bath and then were centrifuged at 14 000 X g for 5 minutes. The supernatant was transferred to new tubes and 400 µl of phenol:chloroform:water (1:1:1) (Applied Biosystems Inc., Mississauga, ON) was added. The samples were centrifuged at 14 000 X g for 5 minutes and the supernatant was transferred to new tubes. The phenol:chloroform:water step was repeated. The supernatant was transferred to new tubes and the DNA was precipitated with 50 µl of

sodium acetate pH 5.5 and 500 µl of 100% isopropanol (Applied Biosystems Inc., Mississauga, ON). The samples were centrifuged at 14 000 X g for 15 minutes. The supernatant was discarded and the pelleted DNA was washed in 70% ethanol. The samples were centrifuged at 14 000 X g for 5 minutes, the supernatant was removed and the DNA pellet air-dried. The DNA was resuspended in 50 µl of filter-sterilized water.

Polymerase chain reaction (PCR) was performed on isolated DNA to detect the *lacZ* gene encoding ß-galactosidase indicating a knockout of the mouse *Smn* gene. Forward and reverse primers (4192 and 4193 respectively) were used to amplify *lacZ*. Mouse *CFTR* primers of DNA quality were used as an internal control. *lacZ* and *CFTR* specific primers were designed in house. *LacZ* and *CFTR* primer sequences are listed in Table 1. For the duplex PCR amplifying both *lacZ* and *CFTR*: 2.0 µl of a 10 mM deoxynucleotide solution (Gibco-BRL, Rockville, MD), 2.5 µl of 10 X PCR buffer (Perkin-Elmer, Norwalk, CT), 0.8 µl of 50 mM $MgCl_2$ (Perkin-Elmer, Norwalk, CT), 2.0 µl of forward and reverse primers for *lacZ* (0.05 µg/µl 4192 and 0.05 µg/µl 4193, respectively), 1.2 µl of forward and reverse primers for *CFTR* (0.05 µg/µl mus CFTR-F and 0.05 µg/µl mus CFTR-R, respectively), 0.2 µl Thermus aquaticus (Taq) DNA polymerase enzyme (Gibco-BRL, Rockville, MD), and 11.2 µl of sterile water was added to 2.0 µl of sample DNA for a total sample volume of 25.0 µl. Aliquots of wildtype mouse genomic DNA was used as negative control for the *lacZ* amplification and aliquots containing sterile water were used as a negative control for the PCR procedure. The PCR products were electrophoresed in a 1% agarose gel containing ethidium bromide (EtBr). The DNA was visualized under ultra violet light and an animal was considered a heterozygote for *Smn* when both sets of primers yielded a band of DNA the correct size (200bp for *CFTR* and 300bp for *lacZ*).

Primer Name	Strand	Sequence
4192	Forward	5' CCC ATT ACG GTC AAT CCG CCG TTT GTT C
4193	Reverse	5' CAT CCG CCA CAT ATC CTG ATC TTC CAG
mus CFTR-F	Forward	5' TAT TTT TGG CCT TCA TCG CAT
mus CFTR-R	Reverse	5' CAG GTA GAA TAC CTG AGA CTG TGC AG

Table 1: Sequence and strand location of lacZ and CFTR specific primers used in genotyping of *Smn* knockout, *Smn* heterozygote and wildtype mice.

2.2 ***Motor Neuron Counts***

Motor neuron counts were conducted on paraffin embedded sections (10 μm thick) of the lumbar region (L1-L6) of the spinal column. Sections were stained using the Kluver Barrera stain, a combination of luxol fast blue and methyl green pyronine (Kluver & Barrera, 1953). Images of the sections are captured under the microscope so that the anterior horn motor neurons could be counted. Motor neurons were identified and counted using the following criteria: large soma (>30 μm), a clear nucleus with an intact nuclear membrane, and one clump of nucleolar material to prevent counting the same neuron twice (Clarke & Oppenheim, 1995). Counting was performed on every fifth section of each lumbar region of the spinal cord.

2.3 RNA and Protein Sources and Extraction

2.3.1 Spinal Cord Dissection

5-week, 3-month and 6-month-old $Smn^{-/+}$ and $Smn^{+/+}$ littermates were euthanized by intraperitonal (i.p.) sodium pentobarbital (MTC Pharmaceuticals, Cambridge, ON) injection and the cranium was separated from the spine above the first cervical region (C1) using a scalpel. Two parallel longitudinal incisions were made on each side of the vertebral column from the lumbar to the sacral level. The column was then transected at the most distal position. The cranial end was held directly over a Petri dish. Forceps were inserted at the

sacral end and used to hold the vertebral column; a blunt 21-gauge needle attached to a 10 ml syringe filled with 1 X phosphate buffered saline (PBS) (Sigma-Aldrich, St.Louis, MO) was introduced about 5 mm into the caudal end of the vertebral canal through the cranial end. Pressure was applied to the syringe plunger with the thumb until the spinal cord was ejected from the vertebral canal (DeSousa & Horricks, 1979). The cord was washed with 1 X PBS, snap frozen in liquid nitrogen and stored at -80°C until required for experiments.

2.3.2 Sciatic Nerve Dissection

5 week, 3 month and 6 month-old *Smn*$^{-/+}$ and *Smn*$^{+/+}$ littermates were euthanized by i.p. sodium pentobarbital injection and underwent cervical dislocation. Mice were laid upon a clean paper towel and had all 4 extremities pinned to a thin Styrofoam board. The sciatic nerve was removed from L4 to the ankle (Martin et al., 1999), snap frozen in liquid nitrogen and stored at -80°C until required for experiments.

2.3.3 Muscle Dissection

3-month wildtype mice were euthanized by i.p. sodium pentobarbital injection. Skeletal muscle tissue was removed by cutting out the biceps femoris from the thigh bone. Tissues were stored in a freezer (-80°C) until required for experiments.

2.3.4 RNA Isolation

Spinal cords from 35-day-old *Smn*$^{-/+}$ (n = 24, balanced for gender) and *Smn*$^{+/+}$ (n = 24, balanced for gender) mice were collected as described above and homogenized using a Model PRO 200 homogenizer (PRO Scientific Inc, Monroe, CT) in Trizol Reagent (Invitrogen Corporation, Carlsbad, CA). Dissected tissue from spinal cord, sciatic nerves or muscle was handled on dry ice to avoid thawing before processing. All RNA was prepared

using RNase-free reagents. Total RNA was isolated using the RNeasy maxi kit (Qiagen Sciences, Germantown, MD) or polyA$^+$ mRNA with the Oligotex polyA$^+$ kit (Qiagen Sciences, Germantown MD), according to the manufacturer's instructions. RNA was resuspended in RNase free water (Sigma-Aldrich, St.Louis, MO) and its concentration determined by spectrophotometry at 260 nm. RNA was stored at –80°C until required for experiments.

2.3.5 Protein Extraction

Spinal cords collected from 35-day-old *Smn*$^{-/+}$ (n = 6, balanced for gender) and *Smn*$^{+/+}$ (n = 6, balanced for gender) mice were weighed and homogenized with the Model PRO 200 homogenizer (PRO Scientific Inc, Monroe, CT) at 4 °C in homogenization buffer containing [20 mM 3-(*N*-morpholino) propane sulfonic acid (MOPS) (Fisher Scientific International, Hampton NH), 2 mM EGTA (Sigma-Aldrich, St.Louis, MO), 5 mM EDTA (VWR International, West Chester PA), 30 mM sodium fluoride (Sigma-Aldrich, St.Louis, MO), 40 mM ß-glycerophosphate (Sigma-Aldrich, St.Louis, MO), 20 mM sodium pyrophosphate (Sigma-Aldrich, St.Louis MO), 1 mM sodium orthovanadate (Sigma-Aldrich, St.Louis, MO), 1 mM phenylmethylsulfonylfluoride (PMSF) (Sigma-Aldrich, St.Louis, MO), 3 mM benzamidine (Sigma-Aldrich, St.Louis, MO), 5 µM pepstatin A (Sigma-Aldrich, St.Louis, MO), and 10 µM leupeptin (Sigma-Aldrich, St.Louis, MO), pH 7.2] (4 mL homogenization buffer/1 g tissue). The homogenates were then ultracentrifuged (100 000 X *g*, 30 min, 4°C). The supernatant (cytosolic fraction) and particulate pellets were conserved and stored at -80°C.

2.4 Affymetrix Gene Expression Profiling

2.4.1 Affymetrix GeneChip® Expression Profiling

Freshly isolated total RNA samples were diluted to 1 μg/μl with RNase free water and pooled to form total RNA stock solutions. The total RNA stock solutions were further diluted to 0.05 μg/μl with RNase free water to a final volume of 5.0 μl. The samples were transferred to the Ottawa Genome Centre for quality assessment analysis of the RNA using the Agilent 2100 bioanalyzer (Agilent Technologies Inc., Palo Alto, CA). The Agilent 2100 bioanalyzer uses fluorescent labelling combined with chromatographic techniques and quantification to determine the concentration and purity/integrity of RNA samples. RNA degradation was identified by a shift in the RNA size distribution toward smaller fragments and a decrease in fluorescence signal.

Once the quality of the RNA was confirmed, an additional 5.0 μl of 0.05 μg/μl total RNA was sent to the Ottawa Genome Centre (Ottawa, ON) to perform the GeneChip Eukaryotic Small Sample Target Labelling protocol developed by Affymetrix (Santa Clara, CA). This protocol generated labelled target through two successive rounds of cDNA synthesis and *in vitro* transcription. Affymetrix GeneChip® technology for gene expression profiling was performed by hybridizing each pool of mouse spinal cords with a single MOE430a GeneChip® (Affymetrix, Santa Clara, CA).

2.4.2 Microarray Quality Control and Normalization

The scanned images were analysed using Affymetrix GeneChip v3.1 software. Each gene chip of the series underwent a stringent quality control regime. The following

parameters were considered: housekeeping genes, internal probe set controls, scaling factor, comparison of hybridization intensity between scans and comparison of distribution of hybridization intensity between gene chips from animals of the same experimental group (R^2), percentage of Present calls. Values for these parameters are reported in results (expression profiling data generation section).

Two normalization processes were used for the microarrays: one for chip-chip comparisons (scaling factors) and one for temporal analysis normalization to the average of the naïve average difference (difference between control and raw signal) values for each gene. The scaling factor determinations were conducted using default Affymetrix algorithms with a target intensity of chip sector fluorescence to 1500. Experiment normalization was performed by normalizing individual gene chips from both $Smn^{-/+}$ and $Smn^{+/+}$ animals to the mean of the four chips from $Smn^{+/+}$ animals. This mean was set as a basal gene expression level for each of the probe sets.

2.4.3 Expression Profiling Data Analysis

Three statistical analyses were used. First the default Affymetrix interpretations of probe set hybridization patterns (8 perfect match and 8 mismatch 25mer oligonucleotides for each gene) was used to provide assessment of signal/noise ratios (Absent or Present calls).

Second, to maintain all potentially important probe sets (genes/ESTs), a probe set was not excluded unless less than 25% of the scanned gene chips showed a Present call for that particular gene. This "data scrubbing" maintained approximately 50% of probe sets on the chips (11365 probe sets from the 22690 genes and ESTs represented on the mouse MOE430a expression array).

The third level of data analysis was the comparison of differential gene expression. Genes that showed both a greater than 1.2 fold change and Welch ANOVA *t* test *p*-value of less than 0.05 between $Smn^{-/+}$ and $Smn^{+/+}$ groups were considered significant. Although a *p*-value of less than 0.05 alone would give many false-positives, the combination of fold change threshold and *p*-values is expected to eliminate most of the false-positives (Bakay et al., 2002).

Each gene discussed in the text is cross-referenced by its accession number (eg, BB821035 for the *Smn* gene).

2.5 ***Representational Difference Analysis***

Representational difference analysis (RDA) is a combination of subtraction and kinetic enrichment coupled to subsequent amplification, originally developed for genomic DNA to isolate differences between two complex genomes (Lisitsyn et al., 1993). It was later adapted for the detection of differentially expressed genes between two mRNA pools (Gress et al., 1997). The latter application of RDA was used to detect differential expression of genes using spinal cords isolated from 5-week-old $Smn^{-/+}$ and $Smn^{+/+}$ mouse spinal cords (Figure 1).

2.5.1 Generation of probes for differential hybridizations

$PolyA^+$ mRNA was made with the Oligotex Direct mRNA Midi/Maxi Kit (Qiagen Sciences, Germantown, MD), using spinal cords isolated from 5-week-old $Smn^{-/+}$ and $Smn^{+/+}$ mouse spinal cords as described previously. Direct isolation of mRNA from animal tissue with the Oligotex Direct mRNA Midi/Maxi Kit utilized denaturing lysis conditions to generate an immediate RNase-free environment for the isolation of intact mRNA.

Figure 1: Graphical schematic of Representational Difference Analysis followed by Spot Blot to determine differentially expressed genes in total spinal cords of 5-week-old *Smn*$^{-/+}$ and *Smn*$^{+/+}$ mice. Subtraction and kinetic enrichment and amplification is used to isolate genes that are specifically expressed or upregulated in *Smn*$^{-/+}$ mice. PCR amplified cDNA representing genes that are upregulated in the heterozygote are cloned into plasmid vectors and stored. As a secondary screening a reverse northern dot blot is performed by purifying and amplifying the inserts and spotting them onto duplicate nylon membranes. The duplicate membranes are probed with labeled *Smn*$^{-/+}$ and *Smn*$^{+/+}$ mouse cDNA. A Clone is deemed to be differentially expressed if the normalized signal intensity of the *Smn*$^{-/+}$ blot is greater than the normalized signal intensitiy of the *Smn*$^{+/+}$ blot.

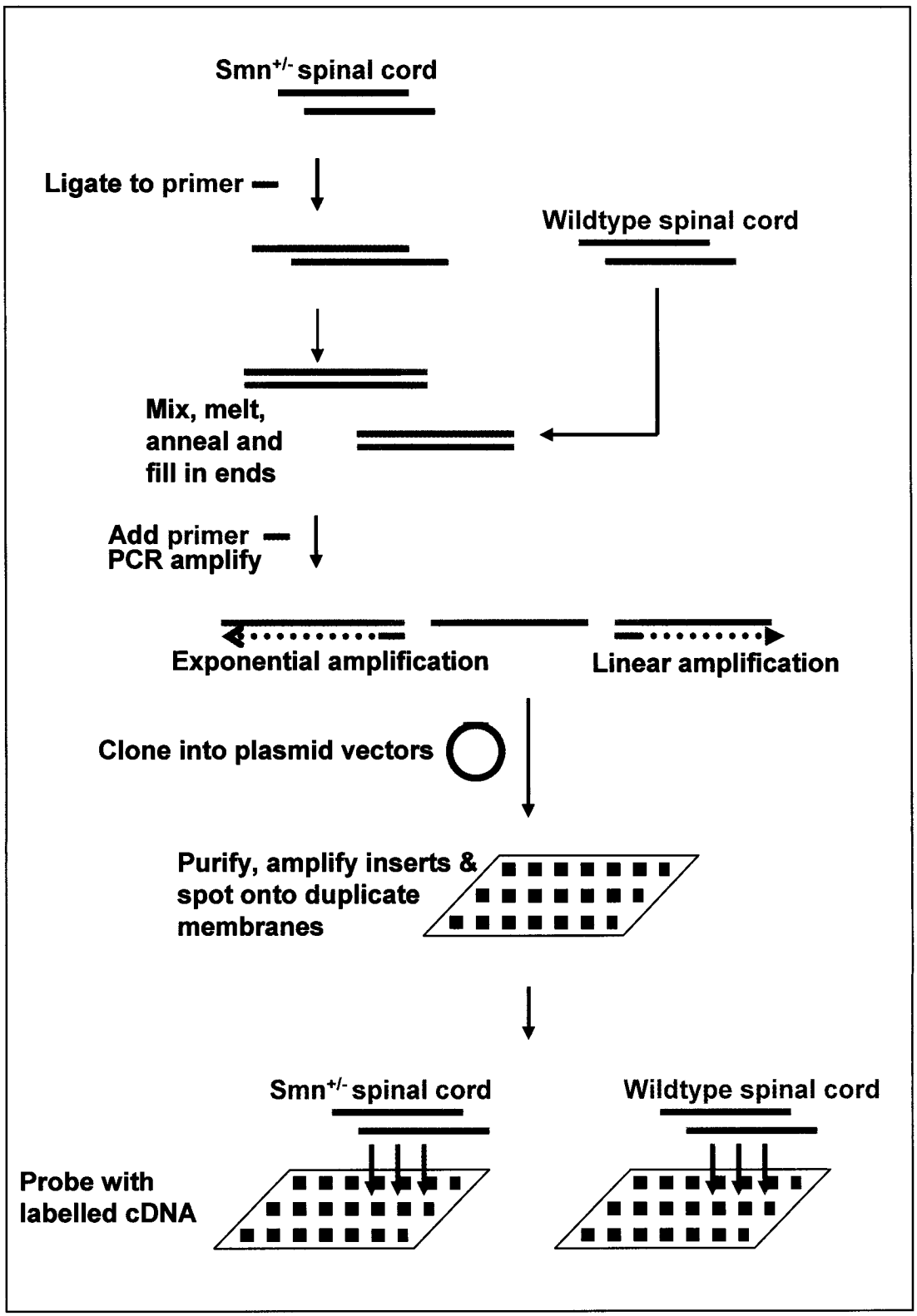
Smn+/- spinal cord
Ligate to primer
Wildtype spinal cord
Mix, melt, anneal and fill in ends
Add primer
PCR amplify
Exponential amplification
Linear amplification
Clone into plasmid vectors
Purify, amplify inserts & spot onto duplicate membranes
Smn+/- spinal cord
Wildtype spinal cord
Probe with labelled cDNA

RNA-protecting lysis and hybridization conditions resulted in efficient purification (greater than 90% recovery) of ready to use polyA$^+$ mRNA. RNA was resuspended in RNase free water (Sigma-Aldrich, St.Louis, MO) and its concentration determined by spectrophotometry at 260 nm. RNA was stored at -80°C. Total RNA and polyA$^+$ mRNA were run on a 1.5% agarose gel to visualize the isolation products. First strand and second strand cDNA were synthesized according to the instructions provided with the PCR-Select cDNA subtraction system (CloneTech, Palo Alto, CA). Double-stranded cDNA products were eventually used for labelling as described below.

2.5.2 Generation of RDA-probes

A subtracted cDNA library was created using the PCR-Select cDNA subtraction system (CloneTech, Palo Alto, CA). Subtractions were performed only in the forward direction, enriching for differentially expressed sequences present in polyA+ RNA from *Smn*$^{-/+}$ mice (cDNA1, tester) but not polyA+ RNA from *Smn*$^{+/+}$ mice (cDNA2, driver) (Figure X). The result was a subtracted cDNA population containing sequences upregulated in *Smn*$^{-/+}$ mice that was used for differential screening.

Pooled polyA$^+$ cDNA of spinal cords from 5-week-old *Smn*$^{+/+}$ mice formed the driver; tester was isolated from the pooled *Smn*$^{-/+}$ samples. A positive control polyA+ RNA (1μg/μl; from skeletal muscle) was performed alongside the *Smn*$^{-/+}$ and *Smn*$^{+/+}$ RNA throughout the differential screening. Each cDNA was restriction digested with *Rsa* I to obtain shorter, blunt ended molecules. Different adaptors were ligated to the tester population but not the driver cDNA. In the first hybridization procedure an excess of driver

cDNA was added to each tester cDNA, and the samples were heat denatured and allowed to anneal. The remaining ss cDNAs (available for the second hybridization) were dramatically enriched for differentially expressed sequences. Templates for PCR amplification were generated from differentially expressed sequences. After denaturation and re-annealing at 67°C for 48 h, suppression PCR was preformed with the tester-specific primers. This method allowed differentially expressed sequences to be amplified exponentially. A second round of PCR in this manner reduced background and further enriched for differentially expressed sequences. Subsequent to PCR-amplification, the driver amplicon was again digested with *Rsa*I for the removal of the adapter cassette. A 1.5% agarose EtBr gel electrophoresis was used to visualize the primary and secondary PCR products. To ensure the validity of the products a PCR was performed to attempt to amplify *Smn* through various steps in the RDA: 2 µl of a 10 mM deoxynucleotide solution (Gibco-BRL, Rockville, MD), 2.5 µl of 10 X PCR buffer (Perkin-Elmer, Norwalk, CT), 0.75 µl of 50 mM $MgCl_2$ (Perkin-Elmer, Norwalk, CT), 2 µl of forward and reverse primers (0.05 µg/µl 4192 and 0.05 µg/µl 4193, respectively), 1.2 µl of forward and reverse primers (0.05 µg/µl 4192 and 0.05 µg/µl mus 4193, respectively), 0.2 µl Thermus aquaticus (Taq) DNA polymerase enzyme (Gibco-BRL, Rockville, MD), and 14.15 µl of sterile water was added to 1 µl of sample DNA. *Smn* sequences are listed in Table 2. DNA from the following RDA products were used as templates: *Rsa* I digested $Smn^{+/+}$, $Smn^{-/+}$, control cDNAs, forward/reverse/control subtraction hybridization products, forward/reverse/control, subtracted and unsubtracted hybridization products following the first and second rounds of hybridization. The PCR products were electrophoresed in a 1% agarose gel containing EtBr. The DNA was visualized under an ultraviolet light and the presence of a band at 258 base pairs indicated the presence of *Smn* cDNA in the sample.

Primer Name	Strand	Sequence
mSmnF	Forward	5' TCCTCCAGATCGCTCAGAAG
mSmnR	Reverse	5' ATCAGTGTCATCCAGACAGT

Table 2: Sequence and strand location of *Smn* specific primers used in the analysis of RDA results.

2.5.3 T/A Cloning of RDA Products

The amplified fragments of the forward and reverse tester populations were then ligated into the pCR2.1 vector using the TOPO-TA cloning kit (Invitrogen, Carlsbad, CA). The kit utilizes a modified form of the TA cloning method by covalently linking an enzyme (Topoisomerase I) to the T-overhangs of the pCR2.1 vector that catalyzes the ligation of the PCR product into the vector. The cDNA library was prepared in *Escherichia coli* TOP10F'cells. The protocol was followed as described in the TOPO-TA cloning manual. Clones were selected on LB-agar (containing Xgal and Kanamycin) for the forward-subtracted population. These plates were sealed with Parafilm and stored at 4°C in an inverted position until required for further experiments.

2.5.4 Reverse Northern Dot Blots

Several clones were randomly selected and purified using the Plasmid Mini Kit (Qiagen Sciences, Germantown, MD). Purified inserts of the cDNA clones obtained in the first and second rounds of RDA were screened using the reverse northern dot blot approach. The plasmidic DNA was extracted from 300 clones and cDNA inserts were isolated from each of them. Insert DNA was spotted onto a nylon membrane using a 96 well minifold II microsample filtration system manifold (Schleicher and Schuell, Hahnstrabe, Denmark) with controls for each

membrane. One μg RNA was suspended in a solution of 153 μl water, 33 μl 12 X SSC and 13 ml of 0.2 M NaOH and incubated at 37°C for 15 minutes. The denatured samples were loaded onto nitrocellulose filters (Schleicher and Schuell, Hahnstrabe, Denmark) that were made in duplicate and pre-soaked in 2 X SSC for 1 minute. After vacuuming the membranes were dried and ultraviolet (UV) cross-linked to the membranes. Radioactive probes made from spinal cord cDNA from $Smn^{-/+}$ (HET) or $Smn^{+/+}$ (WT) mice were prepared using the Rediprime™ II (Amersham Pharmacia Biotech Inc, Piscataway, NJ) random prime labelling system, and filters were hybridized for 48 hours at 55°C in a hybridization solution containing 30 ml 1 M sodium phosphate (pH 7.2), 116 μl 0.5 M EDTA (VWR International, West Chester PA), 9 g sodium dodecyl sulphate (Fisher Scientific International, Hampton, NH), 12 ml 50X Denharts and 0.6 ml 250μg/ml denatured salmon sperm DNA. After probing, exposure to a film allowed us to assess upregulated cDNAs in the spinal cord of $Smn^{-/+}$ mice.

2.6 Multi-kinase and Apoptosis Protein Analysis

2.6.1 Protein Extract Preparation for Kinexus Screening

The supernatant (cytosolic fraction) of the total spinal cord protein homogenate stored at -80°C was thawed in a 37°C water bath. Protein concentration was determined by the Bradford assay (Bradford, 1976) using the Bio-Rad Protein Assay reagent (Bio-Rad Laboratories, Hercules, CA). Bovine serum albumin was used as a protein standard (New England Biolabs, Mississauga, ON). Protein extracts were prepared at a final protein concentration of 1 mg/ml. and boiled in sodium dodecylsulphate-polyacrylamide gel electrophoresis (SDS-PAGE) sample buffer (Laemmli, 1970). Samples were stored at room temperature until use. The samples were shipped to Kinexus Inc. (Vancouver, BC) for the

proteins to be screened using KAPS-1.0, the Kinetworks Apoptosis Protein Screen (see Appendix A) and KPKS-1.2, the Kinetworks Protein Kinase Screen (see Appendix B).

2.7 Polymerase Chain Reaction Analysis of Genes and Proteins Showing Differential Expression

2.7.1 Quantitative Real Time Reverse Transcription Polymerase Chain Reaction

Several experimental genes were chosen for validation through quantitative real-time (QRT) RT-PCR using the QuantiTect® SYBR® Green RT-PCR Kit (Qiagen Sciences, Germantown MD) according to the manufacturer's instructions. The sequence of the primers designed for the experimental and control genes are in Table 4. The RT-PCR Master-Mix contained the following components: 15 µl of 2x QuantiTect SYBR Green RT-PCR Mix, 2.5 µl each of a 0.05 µg/µl solution of forward and reverse primers for the gene being assayed, 1 µl uracil-N-glycosylase (Qiagen Sciences, Germantown MD), 0.12, 0.06 and 0.03 ng template DNA and water to make up to 25 µl. Aliquots containing sterile water in the place of template DNA were used as a negative template control for each primer set used in the PCR procedure. The samples were placed in the ABI PRISM® 7700 real-time cycler (Applied Biosystems, Foster City, CA) and the PCR products were analysed with the ABI 7000 SDS Software (Applied Biosystems, Foster City, CA). A dilution series of RNA served as a standard curve, to ensure that results were within the standard curve range. All PCR reactions exhibited single melting point peaks, indicating a single amplified product.

Table 4: Sequence of the primers designed for gene validation using QRT RT-PCR

Primer Name	Strand	Sequence
CSIAH-F	Forward	5' TGAATAGTGACTGCCTAGTG
CSIAH-R	Reverse	5' CAGCAGCACTATGTGTTGAC
GAPDH-F	Forward	5' TGCACCACCAACTGCTTAG
GAPDH-R	Reverse	5' GGATGCAGGGATGATGTTC
CGEL-F	Forward	5' TACCGCTCTTCACTGCTCTG
CGEL-R	Reverse	5' AGTTGCACAGTAAAGATGGC
CGEL-R2	Reverse	5' CCTCAGACACCCGACTTTGG
CFXR1H-F	Forward	5' GAGGACTGATGAAGATGCTG
CFXR1H-R	Reverse	5' GGAAAGGCTTCCTCCATTAT
CUBE2D2-F	Forward	5' CCAACACTTCACATCTCCCT
CUBE2D2-R	Reverse	5' AGAGGGACACAGGGTCTTAA
CAMPPK-F	Forward	5' CCCATTTTTAGCCACAGCTG
CAMPPK-R	Reverse	5' CAGCAATACCCATAAGCCAC
CCLCN-F	Forward	5' CTGACTATCTTTCCAGGGAC
CCLCN-R	Reverse	5' CTCCTGTGGCGTGTAGATTAGCA
CAIAR-F	Forward	5' AGACACTTCGGACTGAGGTT
CAIAR-R	Reverse	5' GCCTCAAAGTGGTGTTCCTT
CCC1-F	Forward	5' GCTATCCCCATGAATCAGTG
CCC1-R	Reverse	5' ACGTGCCATTTTATTGAGCT
CP162-F	Forward	5' AAGCCAACTGATCTGACAGC
CP162-R	Reverse	5' ACAGAAAACCCCATTACAACC
CRAB6-F	Forward	5' GAAAAGCCTCAGGAGCAACC
CRAB6-R	Reverse	5' TGAAGGGAAAAGGTTCAAGC
CUNRL-F	Forward	5' GAGGACTGGGAAACCTATTGC
CUNRL-R	Reverse	5' CTCCCTGTTGGACTCTGACC
SMN-F	Forward	5' GGGTGAAAGGTTATGTGCTG
SMN-R	Reverse	5' GTCGGATTCGTGAATGAGCC
CCOX-F	Forward	5' AACCGAGTCGTTCTGCCAAT
CCOX-R	Reverse	5' CCTGGTCGGTTTGATGTTAC
CNED4-F	Forward	5' AATAGCATGAGCCATGTCCC
CNED4-R	Reverse	5' AACCCCTTTCAAACAGCCAG
CCDK2-F	Forward	5' TACCACCAATGAGCCAGGTT
CCDK2-R	Reverse	5' GGTCAAAGCCTTACAAAAGC
CCDC7-F	Forward	5' ATCTTGGTCAGAGGGAATGG
CCDC7-R	Reverse	5' GGAAGCCTGGTATGCTATCT
CCNTF GAMMA-F	Forward	5' GACCCCGGTTTCTATTTTGC
CCNTF GAMMA-R	Reverse	5' TCCTCTCTGGATGGAAAGGA

Prss2-Fa	Forward	5' TCTGATCCTAGCCCTTGTGG
Prss2-Ra	Reverse	5' TGGCAGAATCAACAAACTGC
Prss2-Fb	Forward	5' CCAAGTGAGACTGGGAGAG
Prss2-Rb	Reverse	5' TGTTCACACCATTGCTGAG
Neurogenin2-Fa	Forward	5' AAGAGGACTCTGGCGTGTGG
Neurogenin2-Ra	Reverse	5' AGATCACAGGGACCAGTTGC
Neurogenin2-Fb	Forward	5' GTGTGCAGAGCAGACTGAC
Neurogenin2-Rb	Reverse	5' ACAGGTGAAATTCCCACAG
NBAK1-F	Forward	5' CAGAGGAGGTCTTTCGAAGC
NBAK1-R	Reverse	5' AAATAGGCTGTGCATGTTGC
Kif20a-F	Forward	5' GCAGGAAAACTTCGTCAAGC
Kif20a-R	Reverse	5' GTTGAGCTTTGGCAGGTAGG
GPR91-F	Forward	5' CTGTCTGGGCCTTAGTGACC
GPR91-R	Reverse	5' TCAGGGTTTCCAGAACTTGC
ALS2-F	Forward	5' GCATTTCTGACTCGGAGACC
ALS2-R	Reverse	5' AGGTGTTCCACCTTCTGTGG
BAK1-F	Forward	5' CCTCCAGCCTATTTAAGAGTGGC
BAK1-R	Reverse	5' GTCAGGATGGGGTCTCTACG
Tbx21-F	Forward	5' CAGGATGTTTGTGGATGTGG
Tbx21-R	Reverse	5' CATCTGGGTCACATTGTTGG
ELAV-F	Forward	5' CTCGATCAGGGATGCTAACC
ELAV-R	Reverse	5' CCTTTGATGGCTTCTTCTGC
SIVA-F	Forward	5' ATCGTGCATGAGATCTGTGG
SIVA-R	Reverse	5' AGGCTTCAAACATAGCACAGC
Vax2-F	Forward	5' CATTCGGGAAATTGTCTTGC
Vax2-R	Reverse	5' CTGGTCCTTCTTCTGCTTGG
Foxc2-F	Forward	5' GGCTAGGACTGGACAACTCG
Foxc2-R	Reverse	5' GCTCCTGGTTCTGAGAGAGG
Snrp70-F	Forward	5' GGAAGGGCTAGGTAGTGATGG
Snrp70-R	Reverse	5' GGTGGAAAAGGCTAGGAAGG
Tbx4-F	Forward	5' CCAGCCTGTTCTACCACTGC
Tbx4-R	Reverse	5' CGACGTCCACATGTTACAGC
Tcfap2a-F	Forward	5' GTTTGGCTCACTCCAGAAGG
Tcfap2a-R	Reverse	5' TCCTCCGGTTTGTATGAAGC
Zfp316-F	Forward	5' TAGGCTGTGCATCTCAGTGG
Zfp316-R	Reverse	5' CTGTAAAGCCCACCTTCAGC
Sfrs10-F	Forward	5' CCAGATCAACCTCCAAGTCC
Sfrs10-R	Reverse	5' AGACTTGGACTCTCGCTTCG
Brca1-F	Forward	5' ATTGTTGTGAGCCCTTCACC
Brca1-R	Reverse	5' CAGTCCCACATCACAAGACG
Fbl-F	Forward	5' CTTTATCTGTCGCGGAAAGG
Fbl-R	Reverse	5' GGCCGACAATATCAGAGACG
Tfap2d-F	Forward	5' TAAGTGGGTACGAGGCAAGG
Tfap2d-R	Reverse	5' ATCCGTCGTGACGTATCTCC
Api5-F	Forward	5' GTTTCCTCTTTGCGTGAAGG

Api5-R	Reverse	5' GAAGGAAGCAAAGGATGAGG

2.8 *Immunoblot and Immunohistochemical Analysis of Candidates Showing Differential Expression*

2.8.1 Western Blot Analysis of Genes and Proteins Showing Differential Expression

Differences of the candidate gene products gelsolin, Bid and N-Bak levels in between the cytosolic protein fractions of $Smn^{+/+}$and $Smn^{-/+}$ spinal cords at the 5-week, 3-month and 6-month time points were determined using standard western blotting techniques and antibodies specific to these proteins. Protein samples (extracted as previously described) of a known amount were electrophoresed on a 4 - 20% polyacrylamide gradient gel (Bio Rad Laboratories, Hercules, CA) and transferred to a PVDF membrane (Millipore Corporation, Bedford, MA). The membranes were rinsed thoroughly with 1 X PBS (Sigma-Aldrich, St.Louis, MO) blocked overnight in Licor Blocking Buffer (LI-COR Biotechnology, Lincoln, NB) which was diluted 1:1 with 1 X PBS. The membranes were incubated for 1 hour at room temperature in a solution of Licor blocking buffer diluted 1:1 with 1 X PBS, containing 0.1% tween (VWR International, Mississauga, ON) and the primary antibody at a dilution recommended by the manufacturer. Primary antibodies used are: polyclonal rabbit anti-mouse gelsolin antisera stock (a generous gift from Dr. Hisakazu Fujita, Hokkaido University, Japan), polyclonal rabbit anti-Bak antibody (BD Biosciences PharMingen, Palo Alto, CA), polyclonal rabbit anti-Bid antibody (Santa Cruz Biotechnology Inc., Santa Cruz, CA), polyclonal rabbit anti-Lamin A/C antibody (Cell Signaling Technology, Beverly, MA), polyclonal rabbit anti-PARP antibody (Cell Signaling Technology, Beverly, MA), polyclonal rat anti-myelin basic protein antibody (Research Diagnostics, Inc., Flanders, NJ),

polyclonal rabbit anti-Raf-B antibody (Santa Cruz Biotechnology Inc., Santa Cruz, CA), polyclonal rabbit anti-cleaved caspase-3 antibody (Cell Signaling Technology, Beverly, MA), monoclonal rabbit anti-active caspase-3 antibody (BD Biosciences PharMingen, Palo Alto, CA), monoclonal mouse anti-glyceraldehyde-3-phosphate dehydrogenase antibody (GAPDH) (Advanced ImmunoChemical, Inc., Long Beach, CA), monoclonal mouse anti-β-actin antibody (Sigma-Aldrich, St.Louis, MO) and monoclonal rabbit anti-SMN antibody (BD Biosciences PharMingen, Palo Alto, CA). The membranes were then washed with 1 X PBS containing 0.1% tween 4 times for 1 minute. The membranes were then incubated for 1 hour at room temperature in a solution of Licor blocking buffer diluted 1:1 with 1 X PBS, containing 0.1% tween and the secondary antibody at a dilution recommended by the manufacturer. The secondary antibody used for all primary antibodies except anti-GAPDH was Alexa Fluor 680 goat anti-rabbit IgG (Molecular Probes, Eugene, OR). For the GAPDH westerns Alexa Fluor 680 goat anti-mouse IgG (Molecular Probes, Eugene, OR) was used as the secondary antibody. After the incubation the membranes were rinsed with 1 X PBS for 5 minutes to minimize non-specific signals and air-dried. The membranes were scanned and quantified using the Odyssey Infrared Imaging System (LI-COR Biotechnology, Lincoln, NB) and Odyssey Software Release 1.1 (LI-COR Biotechnology, Lincoln, NB). Stripping and reprobing of the blots was done according to the manufacturer's instructions.

2.8.2 Immunohistochemical Analysis of Genes and Proteins Showing Differential Expression

Several experimental proteins were identified in the lumbar region of 5-week, 3-month and 6-month $Smn^{+/+}$ and $Smn^{-/+}$ vertebral columns using an immunoperoxidase stain procedure with primary antibodies specific to the corresponding protein. Slides were deparaffinized in three successive containers of toluene (Sigma-Aldrich, St.Louis, MO) for 5 minutes each and then rinsed with 2 successive 1-minute washes with absolute alcohol and a 5-minute rinse in cold running tap water. To reduce background staining by removing endogenous peroxidases slides were treated with 3% hydrogen peroxide (Sigma-Aldrich, St.Louis, MO) in 1 X TBS (pH 7.6) [83 mL of 1.5 M Tris (Roche, Switzerland), 42 g sodium chloride (VWR International, West Chester PA), 4875 mL distilled water] for 10 minutes and rinsed in 1 X TBS for 5 minutes. To block non-specific binding of proteins that create undesired background the slides were blocked with a general suppressor [(4.0 g BSA (bovine serum albumin) (Sigma-Aldrich, St.Louis, MO), 10.0 g sucrose (Fisher Scientific International, Hampton, NH), 1.0 mL NSS (normal swine serum) (The Jackson Laboratory, Bar Harbor, MA) and 100.0 mL TBS (pH 7.6), for 20 minutes at room temperature in a humid chamber (Anchor Hocking, Lancaster, OH). The excess suppressor was decanted and the slides were incubated with primary antibodies diluted with primary antibody diluent [10.0 g sucrose, 1.0 g BSA, 100.0 g, 100.0 mL 1 X TBS, 0.01% of NaN (sodium azide) (VWR International, West Chester PA)] for 1 hour at room temperature in the humid chamber. A 1:500 dilution was used for the polyclonal rabbit anti-Bak antibody (BD Biosciences PharMingen, Palo Alto, CA) and a 1:100 dilution was used for the polyclonal rabbit anti-Bid antibody (Santa Cruz Biotechnology Inc., Santa Cruz, CA). The slides were rinsed twice with 1 X TBS using a squeeze bottle and then left in 1 X TBS for 5 minutes and then the secondary polymere antibody, DAKO EnVision Labelled Polymere Peroxidase (DAKO Corporation, Carpinteria, CA) was applied for 30 minutes at room temperature in

the humid chamber. The sections were rinsed well with 1 X TBS twice for 5 minutes and developed by incubating with a working solution of DAB [(2.0 mL DAB (Sigma-Aldrich, St.Louis, MO) dissolved in 250 mL 1 X TBS (pH 7.6) and 50 uL hydrogen peroxide 30% (VWR International, West Chester PA)] for 10 minutes in the dark with constant agitation, rinsing with the last 1 X TBS and washing for 5 minutes under running water. The slides were counterstained in filtered Harris' Hematoxylin (Sigma-Aldrich, St.Louis, MO) for 1 minute, washed in running water, differentiated with 0.2% acid alcohol [0.2% HCl (Fisher Scientific International, Hampton, NH) in 70% ethanol (Commercial Alcohols Inc., Brampton, ON)] for 10 dips, washed in running water for 1 minute, blued in saturated lithium carbonate (Fisher Scientific International, Hampton, NH) for 1 dip, washed in running water for 5 minutes, rinsed in absolute ethanol in three successive containers for 20 dips each and cleared in toluene in 2 successive containers for 20 dips each. All sections were mounted with Permount (Fisher Scientific International, Hampton, NH). Sections were viewed with an Axiophot light microscope (Carl Zeiss, Germany) using Northern Eclipse Software (Empix, Mississauga, ON).

2.9 Statistical Analysis

All data represent the mean +/- standard deviation of measurements from 2-12 mice from each experimental group. The differences between experimental groups were analysed using one-way analysis of variance (ANOVA) and Student's t-test (unpaired, significance level P < 0.05). Values of $p < 0.05$ were considered to be significant.

Results

3.1 Characterization of Smn$^{-/+}$ Mice

3.1.1 Analysis of Smn Protein Content in the Spinal Cords of 5-week-old *Smn*$^{-/+}$ Mice

To confirm that there is an alteration in Smn protein content in the spinal cord of *Smn*$^{-/+}$ mice at the 5-week time point western blot analysis was performed. Comparison of Smn protein content between wildtype and *Smn*$^{-/+}$ mice showed a reduction of 61 ± 9% in Smn protein levels (Figure 2). This is comparable to the 46.0 ± 9.8% reduction of Smn protein levels observed between spinal cords of 6-month-old wildtype and *Smn*$^{-/+}$ mice (Jablonka et al., 2000).

3.1.2 Quantification of Motor Neuron Loss in *Smn*$^{-/+}$ Mice

Newborn *Smn*$^{-/+}$ mice have a normal number of motor neurons in the lumbar spinal cord. However in 6-month-old animals 40% of the motor neurons are lost in comparison to wild-type mice (Jablonka et al., 2000). An analysis was performed to study the effect of inactivation of one *Smn* allele on motor neurons in 5-week and 3-month-old *Smn*$^{-/+}$ mice. To determine whether the *Smn*$^{-/+}$ mice exhibited loss of motor neurons in the spinal cord at these time points a histological analysis of the number of motor neurons was conducted. Motor neuron counts were performed on every fifth section of the lumbar spinal cord (L1-L6) in both *Smn*$^{-/+}$ and *Smn*$^{+/+}$ mice. Strikingly, 28% of the motor neurons were already lost in 5-week-old animals in comparison with wildtype mice (Table 5, Figure 3). Spinal motor neuron loss in 3-month-old mice was 30% (Table 5). The loss of spinal motor neurons between 5 weeks and 3 months of age was not statistically significant ($P > 0.05$). Analysis of the cell bodies at 5 weeks and 3 months of age did not show differences in diameter

between *Smn*$^{-/+}$ and *Smn*$^{+/+}$ mice or differences between age groups (Table 6). A loss in diameter length suggests a reduction in cell body size, which is observed when cell bodies atrophy (Ferri et al., 2004). The results indicate that although degeneration of motor neurons has occurred by 5 weeks of age in *Smn*$^{-/+}$ mice it likely does not progress between 5 weeks and 3 months of age. By profiling the gene and protein expression in 5-week-old *Smn*$^{-/+}$ mice the changes observed may be the result of motor neuron atrophy that has already occurred or due to changes occurring in the motor neurons preceding degeneration.

Table 5: Number of motor neurons in the lumbar regions (L1 - L6) of 10 μm section of control and *Smn* $^{-/+}$ spinal cords during the time course of the disease. Values are the mean of the sum of motors neurons observed in sections of the lumbar regions L1 – L6 ± standard deviation. Two animals and 600 cells were examined for each group.

Age	*Smn*$^{+/+}$	*Smn*$^{-/+}$	Reduction
5 weeks	36 ± 3 (n=3)	26 ± 3 (n=3)	28% (P<0.02)
3 months	40 ± 5 (n=3)	28 ± 5 (n=3)	30% (P<0.05)

Figure 2: Smn protein levels detected using a western blot, in 5-week-old *Smn*$^{-/+}$ and *Smn*$^{+/+}$ mouse spinal cord. A monoclonal anti-mouse Smn antibody detects a single band at 38 kDa. Equal protein content in the individual lanes was controlled by stripping off the first antibody and reprobing with anti-β-actin antibody (42 kDa) (bottom). Analysis performed in triplicate with n = 4 mice / group.

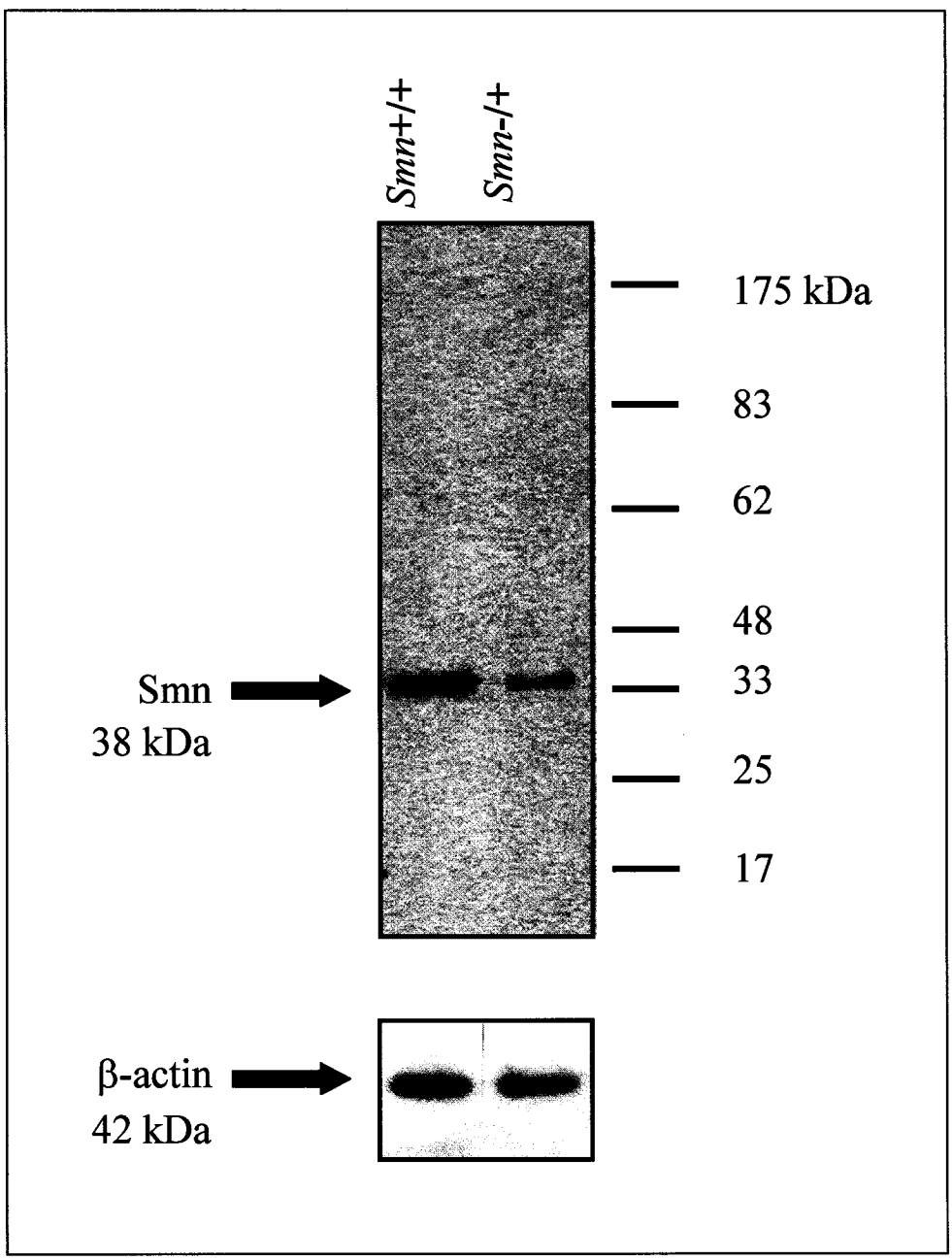
Smn+/+
Smn-/+
175 kDa
83
62
48
33
25
17
Smn
38 kDa
β-actin
42 kDa

Figure 3: Morphology of spinal cord motor neurons in 5-week-old *Smn*$^{+/+}$ (A) and *Smn*$^{-/+}$ (B) mice. Motor neurons in the lumbar region of *Smn*$^{+/+}$and *Smn*$^{-/+}$ mice spinal cords stained with Harris' Hematoxylin and visualized with a light microscope appear the same in size and staining. The position of the ventrolateral motor neuron pool is indicated by arrows. Bar in (A) 100μm.

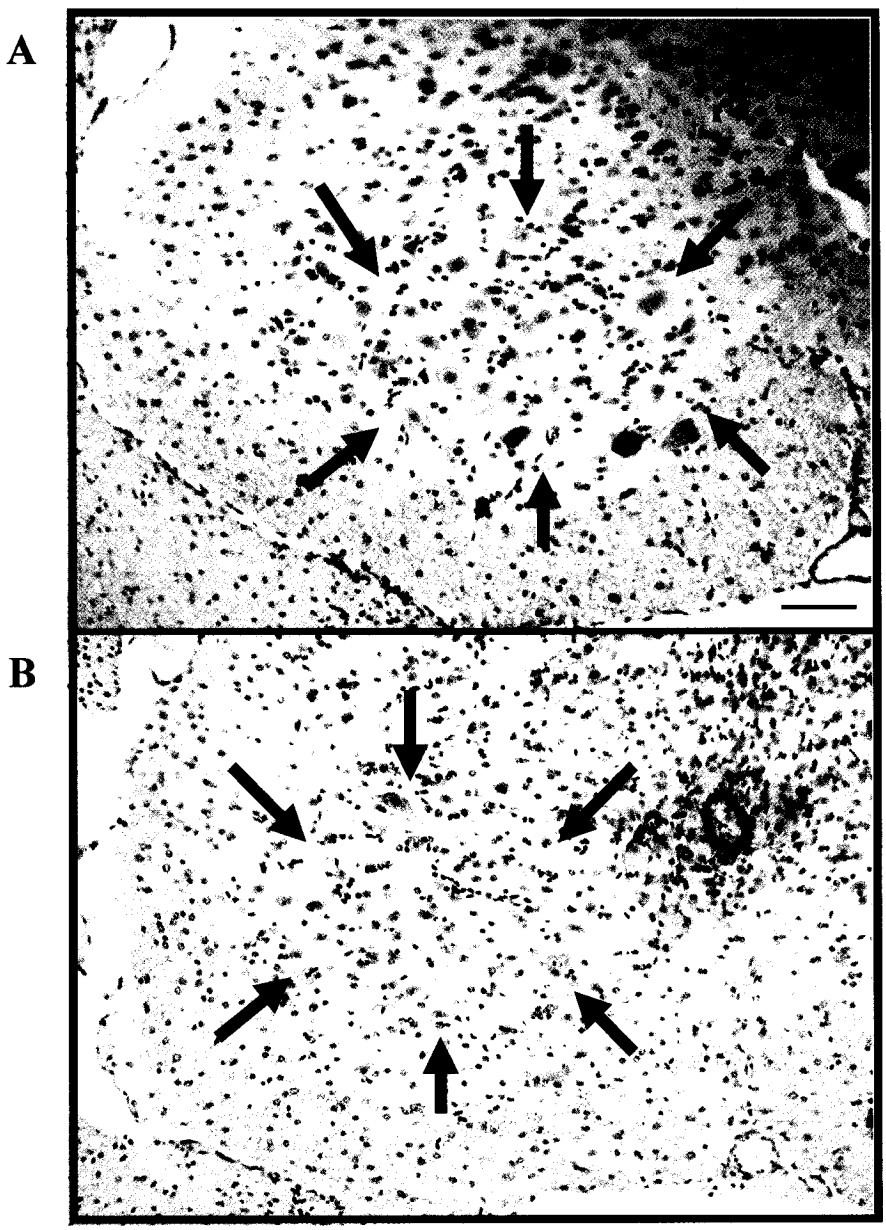
A
B

Figure 4: *Smn* is subtracted from the tester ($Smn^{-/+}$) population. PCR was performed using mouse *Smn*-specific primers to amplify *Smn* mRNA from unsubtracted cDNA isolated from $Smn^{-/+}$ spinal cord tissue and the RDA subtracted spinal cord cDNA. CDNA was made using mRNA from 3 male and 3 female mice from each genotype. RDA subtraction was performed by using heterozygote cDNA as "tester" cDNA and using the wildtype littermate cDNA as "driver".

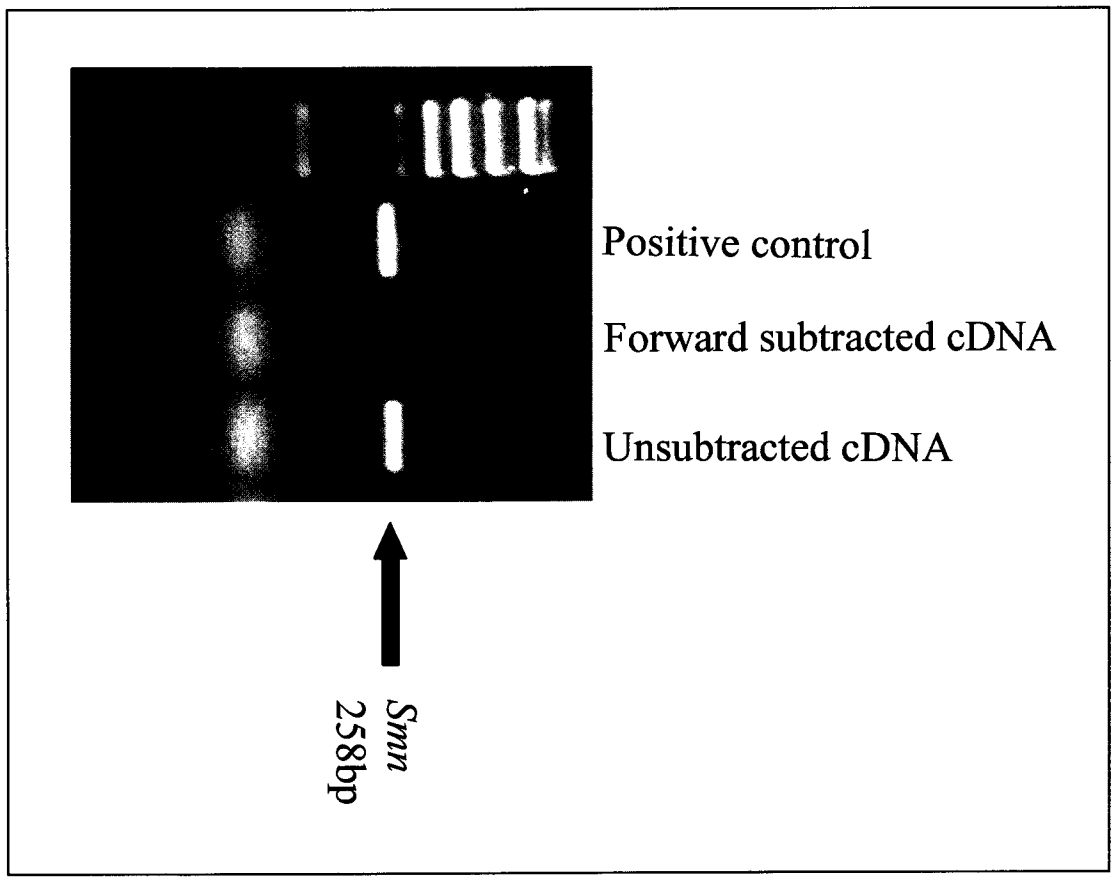
Positive control
Forward subtracted cDNA
Unsubtracted cDNA
Smn
258bp

Table 6: Mean diameter of motor neurons (μm) in control and *Smn* $^{-/+}$ lumbar spinal cords during the time course of the disease. Values are the mean of the diameter of motors neurons observed in sections of the lumbar regions L1 – L6 ± standard deviation. Two animals and 600 cells were examined for each group. (n.s. = not significant).

Age	*Smn*$^{+/+}$	*Smn*$^{-/+}$	% loss
5 weeks	37.8 ± 3.3 (n=3)	37.6 ± 5.2 (n=3)	n.s.
3 months	37.9 ± 5.1 (n=3)	36.9 ± 4.4 (n=3)	n.s.

3.2 Representational Differential Analysis of 5-week-old Smn$^{-/+}$ Mouse Spinal Cords

3.2.1 Products of the RDA Procedure

Gene expression is specifically regulated in *Smn*$^{-/+}$ spinal cords compared to *Smn*$^{+/+}$ spinal cords. Representational Differential Analysis (RDA) can be used to identify the changes in the pattern of gene expression caused by SMN depletion. RDA is a combination of subtraction and kinetic enrichment coupled to subsequent amplification and has previously been used to detect genes specifically expressed in several disease models (Gress et al., 1997, Seale et al, 2000, Bates et al, 2001, Graveel et al, 2001). To clone genes whose expression is dramatically upregulated in the *Smn*$^{-/+}$ mouse, RDA with ds-cDNA from 5-week-old *Smn*$^{-/+}$ spinal cord tissue was used as a tester and ds-cDNA from 5-week-old *Smn*$^{+/+}$ spinal cord tissue was used as a driver. To confirm a successful forward subtraction the polymerase chain reaction (PCR) amplification of *Smn* mRNA was attempted using unsubtracted cDNA isolated from *Smn*$^{-/+}$ spinal cord tissue and forward subtracted RNA as templates. As expected a band appeared at 258 base pairs for the manufacturer-provided positive control and the unsubtracted *Smn*$^{-/+}$ spinal cord cDNA (Figure 4) and no band appeared for the reaction using forward subtracted RNA as a template. The lack of *Smn*

amplification in the *Smn*$^{-/+}$ specific enriched cDNA library indicated that the RDA reaction successfully removed *Smn* which was initially deficient in the *Smn*$^{-/+}$ mRNA.

3.2.2 Analysis of the *Smn*$^{-/+}$ Specific Enriched Library

RDA was performed twice to yield two hundred and fifty clones. Sixty-four clones were picked from the library and subjected to DNA sequencing analysis. The sequences were compared with the GenBank database by Blast search (Altschul et al., 1997). The identified clones included genes involved in cell death processes such as Gelsolin and Cox-2, structural genes (β-actin, Myelin basic protein, Myelin proteolipid protin, C-type lectin and Radixin), metabolic genes (Androgen-inducible aldehyde reductase, Osmotic shock protein 94, Seven in absentia homolog and Enolase-1α). A complete listing of sequenced RDA clones is given in Table 7.

3.2.3 Spot Blot Results Confirm RDA Results

To analyze the expression pattern of the cloned genes, an RNA slot blot analysis was performed with 10μg total RNA from 5-week-old *Smn*$^{-/+}$ and *Smn*$^{-/+}$ spinal cord tissues (Figure 5). All clones displayed either an equal or stronger signal when probed by cDNA from 5-week-old *Smn*$^{-/+}$ spinal cord tissue than from *Smn*$^{+/+}$ spinal cord tissue (confirming the low-frequency of false-positive clones). Many of spots representing clones showed only a slight elevation of intensity relative to the background. Included in the collection were genes whose basal expression in the mouse spinal cord were relatively high (β-Actin, Myelin basic protein, RIKEN cDNA 5730525G14 and KIAA0847 protein) and much lower (Supressor of actin mutations 1, Enolase 1, Protein phosphatases 3α and Rab11 interacting

Table 7: Clones identified by RDA to be upregulated in 5-week-old *Smn*$^{-/+}$ mouse spinal cords compared to wildtype mice. The subtracted library was cloned, sequenced, and subjected to Blast analysis for gene identification (name and accession number) twice, independently. Shown for each clone are the closest homolog found in the GenBank database, the accession number of the homolog, the number of times each clone was isolated in the course of sequencing the two subtracted libraries and the function(s) of the gene product.

Gene homology	Accession	Frequency
Apoptosis		
Aflatoxin aldehyde-reductase (Akr7a5)	NM_025337	3
AMP deaminase 3 (AMPD3)	D88984	2
Cytochrome c oxidase subunit II (CoxII)	AF378830	1
Enolase 1 (Eno1)	NM_023119	2
Gelsolin	BC023143	1
Glial cell line derived neurotropic factor gene (rattus norvegicus) homolog (GDNF)	AJ011432	1
Iduronate 2-sulfatase (IDS)	NM_010498	1
Member of ras oncogene family (Rab27b)	NM_030554	1
Member of ras oncogene family (Rab6)	NM_024287	1
Metabolism		
Mouse RNA polII large subunit (RPB-1)	U37500	1
Mouse tumour differentially expressed 1 like protein (Tde1l)	NM_019760	
Mouse Ubiquitin conjugating enzyme E2D2 (Ubc 2d2)	NM_019912	1
Osmotic stress protein (Osp)	BC012712	1
Rat UDP-Gal:β-GlcNAC B 1,4-galactosyltransferase, polypeptide 6 (B4galt6)	NM_031740	1
Seven in absentia splice 1A (Siah1a)	NM_009172	1
Tyrosinase (Homo sapiens) homolog (Tyr)	XM_133679	1
Upstream of N-RAS (Homo sapiens) homolog (Unr)	XM_032696	1
Zinc-finger protein 216 (Znf216)	NM_009551	1
Protein Binding		
Mouse ubiquitin conjugating enzyme E2D2 (Ubc 2d2)	NM_019912	1
Nedd4 WW domain - interacting protein 5	AF220209	1

Seven in absentia splice 1A (Siah1a)	NM_009172	1
Translation initiation factor p162	U14172	2
RNA binding		
Mouse fragile X-related protein (Fxr1h)	AF124393	1
Mouse splicing factor 3b subunit 1 (Sf3b1 / SAP155), a subunit of U2 snRNP	NM_031179	1
Nuclear autoantigen (Homo sapiens) homolog (SG2NA)	XM_030180	1
Purα extended 3'UTR (Homo sapiens) homolog	X91648	2
Signal transduction		
Chinese hamster cAMP-dependent protein kinase	M63312	2
G protein pathway suppressor 2 (Homo sapiens) homolog, (GPS2)	CR541723	1
Map kinase phosphatase - homologous region present in A1, A2, B1, B2, MKP-7	A1-AF345951 A2- AF345952 B1- AF345952 B2- AF345954 MKP-7- AB052157	1
Protein phosphatases 3α (PPP3R1)	NM_000945	1
Rat Per1 interacting protein (Pips)	NM_134386	2
SH3 domain protein 2A	BC018385	1
Transmembrane protein with EGF-like and two follistatin-like domains 1(Homo sapiens) homolog	BC021991	1
Structural		
β Actin, cytoplasmic (Actb)	NM_007393	2
β-amyloid binding protein precursor	NM_032027	1
C-type lectin protein MT75	AF311699	1
Gelsolin	BC023143	1
Mayven	NM_007246	1
Mouse radixin	NM_009041	1
Myelin basic protein (Mbp)	NM_010777	3
Myelin proteolipid protein (Plp)	BC027010	1
Supressor of actin mutations 1 (S. cerevisiae) homolog (Sacm1l)	NM_030692	3
Uncharacterized genes		
Genomic DNA sequence from chromosome 1	AL606536	1

Genomic DNA sequence from chromosome 11	AL596084	1
Genomic DNA sequence from chromosome 11	AL606466	1
Genomic DNA sequence from chromosome 11	AL669979	1
Genomic DNA sequence from chromosome 15	AL513346	1
Human BAC clone RP11-49F1	ACO84010	1
KIAA0847 protein (Homo sapiens) homolog	AB020654	1
RIKEN cDNA 0610011L14	BC019988	2
RIKEN cDNA 2010008E23	AK008158	1
RIKEN cDNA 5730525G14	AK017787	1
SDS stable vimentin-bound DNA fragment	AJ297014	1

Figure 5: Typical hybridization patterns obtained with a spot blot of purified RDA clones using unsubtracted cDNA probes isolated from spinal cord tissue obtained from 5-week-old *Smn*$^{-/+}$ mice (A) and spinal cord tissue from wildtype littermate controls (B). Clones were classified as differentially expressed by subtracting signal intensities corrected for background of B from those in A. The positions of a selection of clones spotted as controls are highlighted on all autoradiographies by arrows. PCR-amplified segment of the *GAPDH* gene was used as a positive control and a purified vector-only clone was used as a negative control. Please note that none of the vector-only clones gave a specific signal in any of the hybridizations.

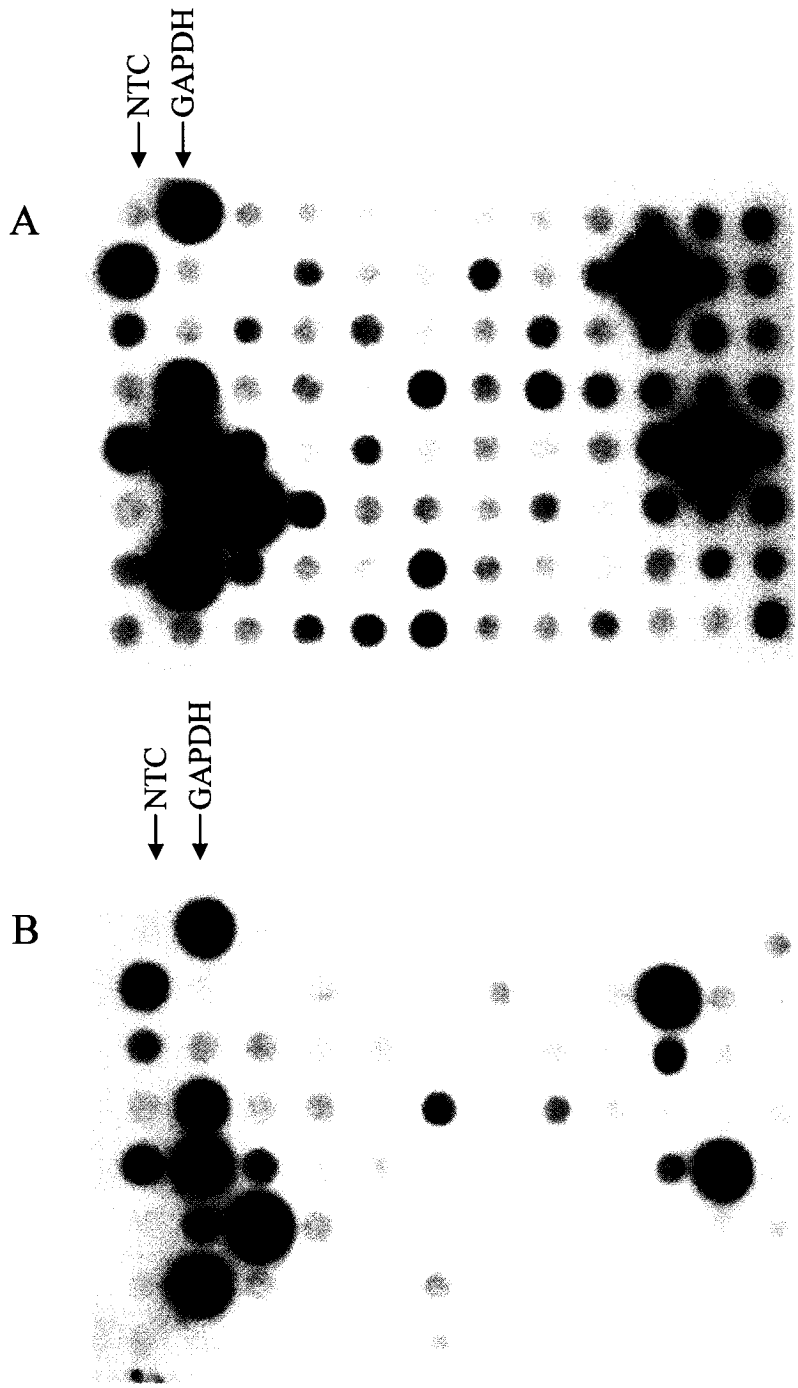
A
NTC
GAPDH
B
NTC
GAPDH

protein Rip11). In all cases, results show only subtle differences between the screens probed with $Smn^{-/+}$ cDNA and $Smn^{+/+}$ cDNA. To determine true positives, the expression of four genes was quantified using RT-PCR analysis with primers designed according to the sequence of the genes (Figure 6). Genes were chosen for validation with RT-PCR based on three factors: 1) differential hybridization intensities on the slot blot, 2) a possible relevance to mechanisms associated with SMA pathology based on the literature and 3) the absence of non-specific amplification in the PCR reaction using primers designed to amplify the specific gene. The target RNA was amplified in serial dilutions of $Smn^{-/+}$ and $Smn^{+/+}$ spinal cord total RNA, and detected using the SYBR Green dye. The fold change was calculated based on the slopes of amplification curves. Three of the four genes showed upregulation in 5-week $Smn^{-/+}$ mouse spinal cords: Gelsolin (173 ± 10%), Nedd4-interacting protein (147 ± 40%), UbiquitinE2D2 (210 ± 60%). The fourth gene, androgen-inducible aldehyde-reductase, was not differentially expressed in the $Smn^{-/+}$ mouse spinal cords (97 ± 16%). Thus the combination of RDA to create an $Smn^{-/+}$ specific enriched library followed by the slot blot hybridization was an effective method for identifying differentially expressed genes in 5-week-old $Smn^{-/+}$ mouse spinal cord tissue.

To determine if changes at the transcript level translated to the protein level, Gelsolin, the most interesting and significantly upregulated gene identified in the RDA was chosen for western blot analysis. Although there was a 1.7 ± 0.1 fold increase of gelsolin mRNA in the $Smn^{-/+}$ mouse spinal cord based on three replicates of Quantitect SYBR Green RT-PCR there

Figure 6: Quantitect SYBR Green RT-PCR verification of candidate genes from spot blot shows a slightly increased expression of Gelsolin, Nedd4-interacting protein 5 and Ubiquitin-conjugating enzyme 2D2 in 5-week-old *Smn*$^{-/+}$ mice. ABI PRISM 7000 was used for PCR amplifications of four RDA candidates (Aiar, Gelsolin, Nedd4-interacting protein 5 and Ubiquitin-conjugating enzyme 2D2). PCR was performed in triplicate for each gene with total RNA template from 5-week-old *Smn*$^{-/+}$ mice (six male and six female) and control *Smn*$^{+/+}$ mice (six male and six female mice). Data was normalized using the housekeeping gene, *Gapdh*. As expected, the control gene, *Smn*, was downregulated by 50% in *Smn*$^{-/+}$ mice. Error bars show standard deviation based on at least three independent replicates. Statistically significant fold change values with a p value < 0.05 are indicated by an asterix.

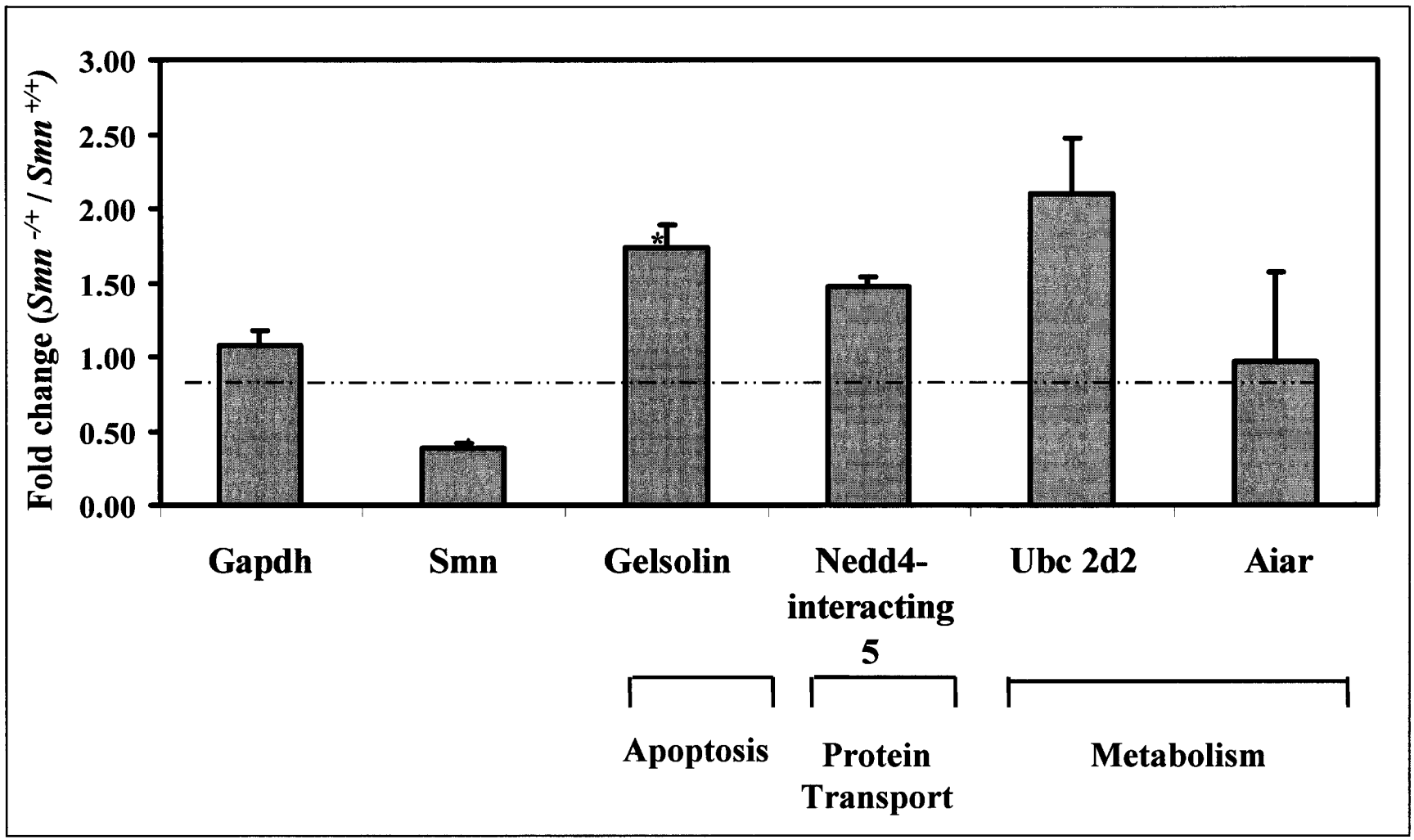
Fold change (Smn -/+ / Smn +/+)
3.00
2.50
2.00
1.50
1.00
0.50
0.00
*
Gapdh
Smn
Gelsolin
Nedd4-interacting 5
Ubc 2d2
Aiar
Apoptosis
Protein Transport
Metabolism

was no differences in gelsolin protein level between $Smn^{-/+}$ and $Smn^{+/+}$ spinal cord tissue (Figure 7).

3.3 Affymetrix Gene Expression Profiling of 5-week-old $Smn^{-/+}$ Mouse Spinal Cords

A disadvantage of RDA profiling is that the analysis is optimised to detect genes whose expression is dramatically upregulated in the *$Smn^{-/+}$* mouse. There are also many steps in the protocol, risking a loss of clones in the process. In order to study more subtle differences a more complex and thorough complementary method, Affymetrix Gene Expression Profiling, was used. For gene expression analysis total RNA was extracted from 5-week-old *$Smn^{+/-}$* and control spinal cords used to make labelled cDNA targets which were hybridized to nucleic acid probes attached to the solid support. By monitoring the amount of label associated with each DNA location it was possible to infer the abundance of each gene represented. Each sample consisted of six female and six male spinal cords in order to prevent sex bias. Affymetrix GeneChip® analysis was performed in quadruplicate on *$Smn^{+/+}$* and *$Smn^{-/+}$* samples using the mouse MOE430A GeneChip® arrays, representing approximately 22 690 mouse genes.

Expression profiles fulfilled the following quality control measures: cRNA fold changes greater than 1.2 and at least 25% of "present" (P) call. Comparison of average difference values defined by a scatterplot between gene chips from different pooled samples of the same experimental group showed tight correlation coefficients (R^2) from 0.955 to 0.996 (Figure 8).

Figure 7: Gelsolin protein levels are unaffected in spinal cords of *Smn+/-* mice. Western blot analysis was performed using mouse Gelsolin and GAPDH specific antibodies and cytosolic protein lysate isolated from $Smn^{-/+}$ and $Smn^{+/+}$ mouse spinal cord tissue. Increasing cycles were performed. Shown below are fold changes in expression in 5-week-old $Smn^{-/+}$ mouse spinal cord tissue relative to $Smn^{+/+}$ tissue (n=8) averaged between three trials.

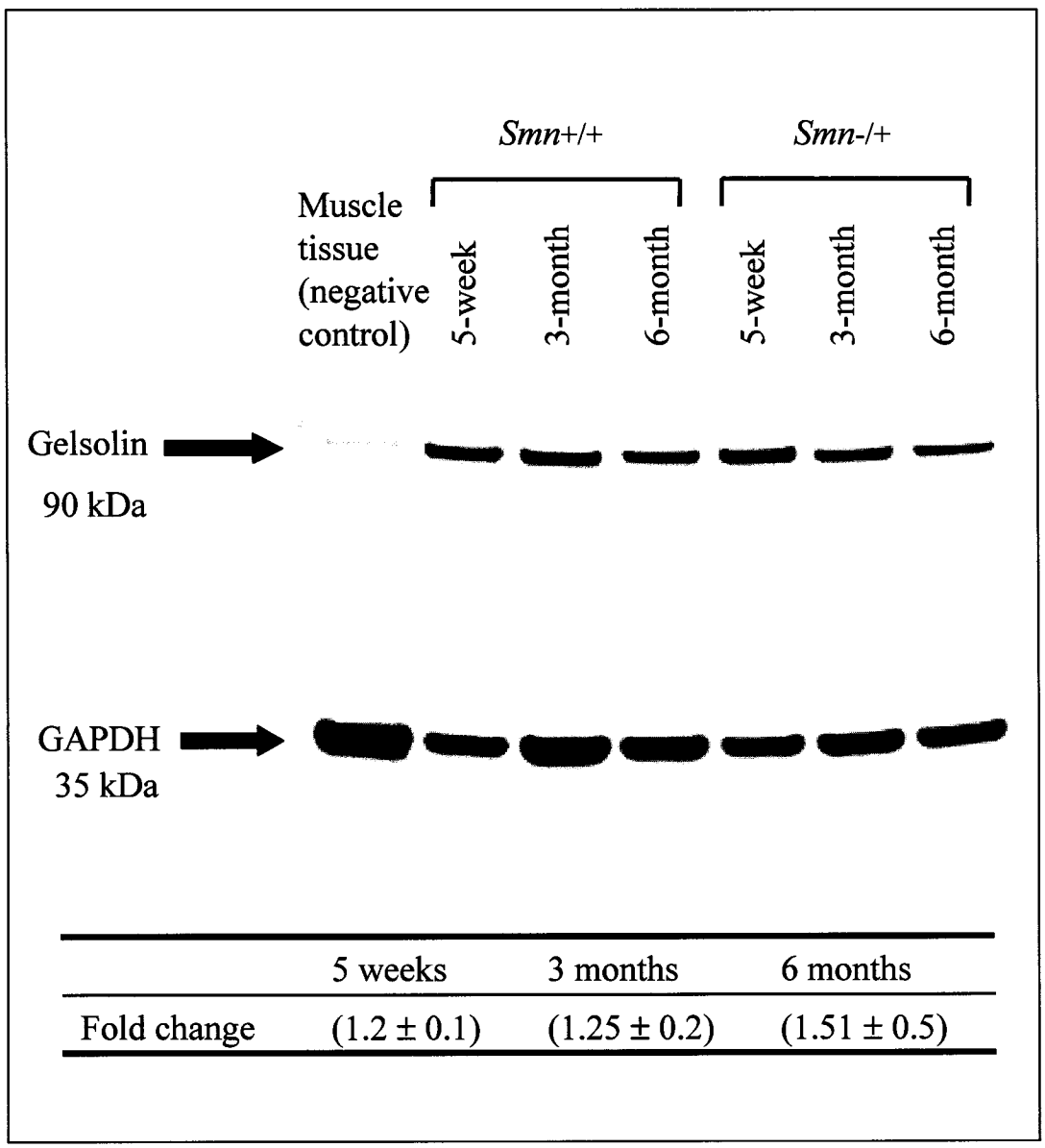

	5 weeks	3 months	6 months
Fold change	(1.2 ± 0.1)	(1.25 ± 0.2)	(1.51 ± 0.5)

Figure 8: Examples of scatterplots of probe set hybridization intensities (average difference values) between GeneChips® from pooled samples of different or similar experimental groups. These represent the highest (R^2 = 0.996) (A) and the lowest (R^2 = 0.955) (B) correlation coefficients from the series consisting of 8 Affymetrix chips. Average difference values were calculated by averaging the raw and control signals for each probe set. All 22690 probe sets were plotted.

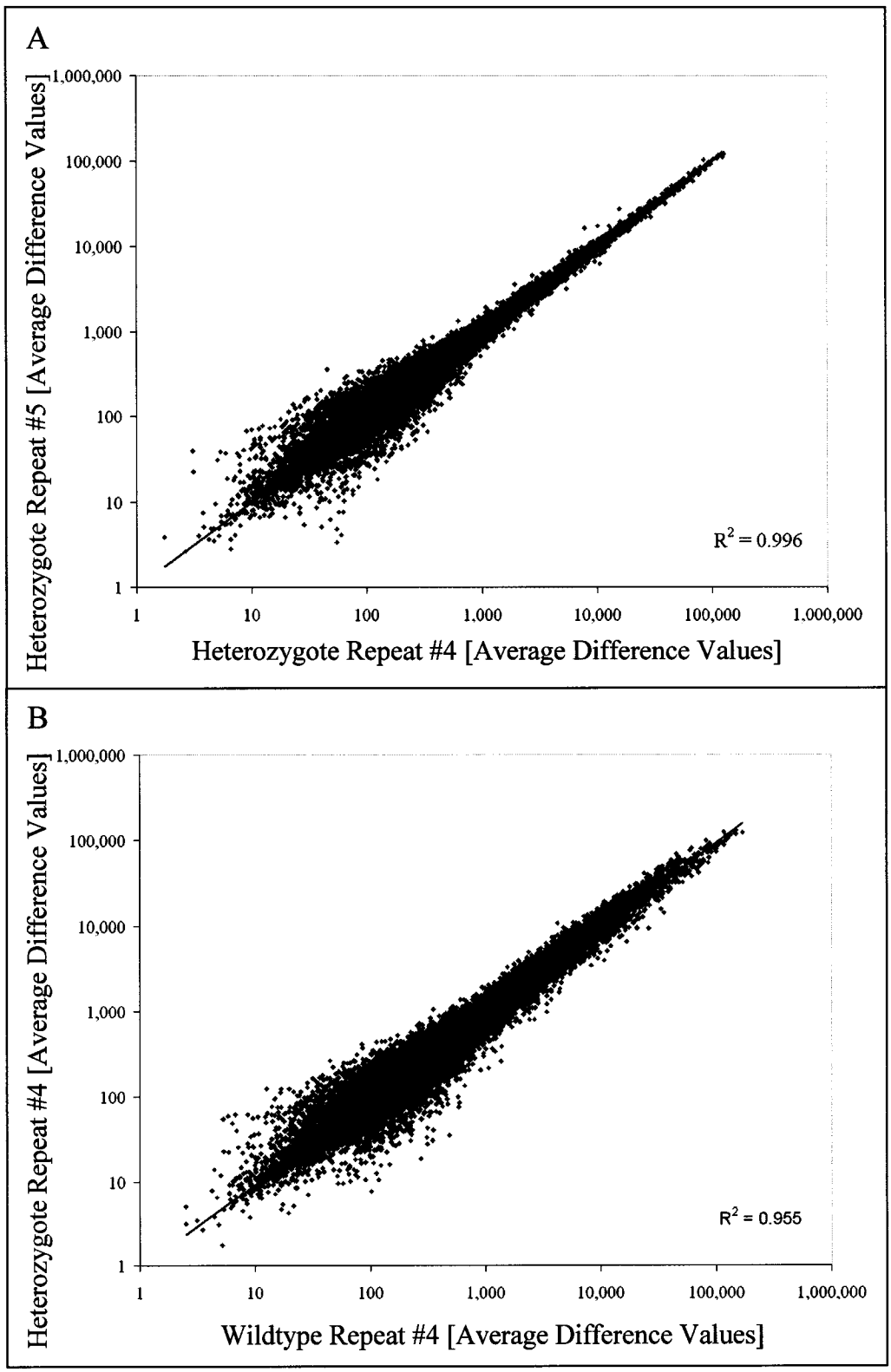
A
Heterozygote Repeat #5 [Average Difference Values]
1,000,000
100,000
10,000
1,000
100
10
1
1
10
100
1,000
10,000
100,000
1,000,000
Heterozygote Repeat #4 [Average Difference Values]
R2 = 0.996
B
Heterozygote Repeat #4 [Average Difference Values]
1,000,000
100,000
10,000
1,000
100
10
1
1
10
100
1,000
10,000
100,000
1,000,000
Wildtype Repeat #4 [Average Difference Values]
R2 = 0.955

3.3.1 **Analysis of Gene Expression in 5-week-old *Smn*$^{-/+}$ Mice**

In light of the tight correlation coefficient values between the profiles of the two experimental groups the threshold of differential expression was set to 1.2 fold to identify the most relevant genes. One hundred and twenty genes showed more that 1.2 fold differential expression from the baseline with a *p*-value equal to or less than 0.05 (Table 8). Most of the observed genes had well-characterized full-length sequences reported in databases, but six genes were expressed sequence tags (ESTs). ESTs are short sequences obtained by analysis of cDNA extracted from a tissue sample. They are a rapid means of gaining access to sequences of unknown genes or polymorphs. Five of these ESTs were RIKEN clones, which are a library of full-length cDNAs collected from different stages, called the iMouse Gene Encyclopedia (constructed by the RIKEN group and international FANTOM consortium). Seventy-nine of the 120 genes were downregulated and only 41 were upregulated. Genes for the extracellular matrix and cytoskeleton constitute the largest group of differentially expressed genes (n = 37). Other gene families included those coding for proteins involved in signaling pathways, protein transport and RNA binding. Interestingly 17 of the 18 calcium-dependent receptor signaling genes observed were downregulated, possibly due to a decrease in intracellular calcium levels in *Smn*$^{-/+}$ mouse spinal cords.

To independently validate the microarray data, a quantitative RT-PCR method was used to analyse a subset of genes that were either down- or upregulated. Genes chosen for RT-PCR analysis satisfied one or more of the following criteria: 1) high fold change; 2) low *p*-value 3) have a possible relevance to mechanisms associated with SMA pathology based on

Table 8: SMA-related changes in gene expression in spinal cord as determined by microarray profiling.

Gene	Accession number	Fold change	*p* value
Actin-related			
Solute carrier family 13 (sodium-dependent dicarboxylate transporter), member 3 (Slc13a3)	BB497755	4.2	0.02
Telomeric repeat binding factor 2, interacting protein (Terf2ip)	BC017641	2.7	0.02
Axin	BG072066	2.6	0.01
Prolactin receptor (Prlr)	BC005555	2.4	0.04
BH3 interacting domain death agonist (Bid)	BC002031	2.0	0.03
TNFAIP3 interacting protein 2 (Tnip2)	NM_139064	1.9	0.04
Vav 3 oncogene	NM_020505	1.7	0.05
CasL interacting molecule	BB209438	1.6	0.02
Rap1 guanine-nucleotide-exchange factor	BC020532	1.5	0.04
ARP1 actin-related protein 1 homolog B (Actr1b)	BG228102	1.5	0.01
Proteasome 26S subunit, non-ATPase, 4 (Psmd4)	AB029145	1.5	0.04
RuvB-like protein 2 (Ruvbl2)	NM_011304	-1.5	0.003
RIKEN cDNA 4921517D21 gene	NM_026338	-1.5	0.04
Nebulin-related anchoring protein (Nrap)	NM_008733	-1.5	0.03
Signal transducing adaptor molecule (SH3 domain and ITAM motif) 2	NM_019667	-1.5	0.03
Villin (Vil)	NM_009509	-1.6	0.01
DnaJ (Hsp40) homolog, subfamily A, member 3 (Dnaja3)	AK007852	-1.6	0.04
Arachidonate lipoxygenase, epidermal (Alox12e)	U39200	-1.7	0.03
Immunoglobulin kappa chain variable 8 (Igk-V8)	M35669	-1.8	0.03
Syndecan binding protein 2 (Sdcbp2)	BC005556	-2.1	0.01
Tropomyosin 2β (Tpm2)	BC024358	-2.4	0.05
Immunoglobulin heavy chain 4 (Igh-4)	X88902	-2.8	0.04
Parvin γ (Parvγ)	BC011200	-3.1	0.03
Ubqln1	NM_019509	-3.3	0.03
Actinin α1 (Actn1)	BC003232	-4.9	0.04
RIKEN cDNA 2310047B08 gene	AK005411	-5.7	0.02
Down syndrome critical region gene 1-like 2 (Dscr1l2)	AF237888	-7.3	0.03
Kinesin family member 20A (Kif20a)	NM_009004	-7.6	0.002
Apoptosis-related			
BH3 interacting domain death agonist (Bid)	BC002031	2.0	0.03
Apoptosis inhibitor 5 (Api5)	BB813983	1.9	0.04

Cd27 binding protein (Hindu God of destruction) (Siva)	AF033112	1.4	0.02
Glutathione peroxidase 1 (Gpx1)	BI219063	1.3	0.05
Peroxiredoxin 2 (Prdx2)	NM_011563	-1.2	0.02
Hepatoma-derived growth factor, related protein 1 (Hdgfrp1)	AF180109	-1.3	0.02
Fas-ligand (FasL)	NM_010177	-1.3	0.05
Scotin gene	BC010238	-1.4	0.009
BCL2-antagonist/killer 1	NM_007523	-1.5	0.01
Neuronal Bak1, alternatively spliced (Nbak1)	AF402617	-2.5	0.00004
Breast cancer 1 (Brca1)	U31625	-2.9	0.0004
Calcium dependent signaling			
Guanine nucleotide binding protein, α15 (Gnα15)	NM_010304	2.0	0.05
Spectrin α1 (Spnα1)	U87455	-1.4	0.05
Bone morphogenetic protein 7 (Bmp7)	BM055476	-1.5	0.04
Synaptojanin 2 (Synj2)	AK019694	-1.6	0.04
Nucleobindin 2 (Nucb2)	NM_016773	-1.7	0.04
Crumbs (Drosophila) homolog 1 (Crb1)	NM_133239	-1.7	0.04
Calbindin-D9K (Calb3)	NM_009789	-1.8	0.04
Purinergic receptor P2X, ligand-gated ion channel 4 (P2rx4)	AJ251462	-1.9	0.04
Calcium binding protein 5 (Cabp5)	NM_013877	-2.0	0.04
Naked cuticle 1 (Drosophila) homolog (Nkd1)	NM_027280	-2.0	0.03
ADAM-like decysin 1 (Adamdec1)	NM_021475	-2.1	0.03
Immunoglobulin κ chain variable 8 (Igκ-V8)	AV057155	-2.2	0.01
Annexin A6 (Anxa6, Anx6, Cabm, Camb, AnxVI)	AK013026	-3.1	0.008
Ribosomal protein L3-like (Rpl3l)	NM_025425	-3.1	0.04
Triadin (Trdn)	AF223417	-3.2	0.0005
RAN binding protein 17 (Ranbp17)	NM_023146	-3.3	0.0006
Serine protease 21 (Prss21)	NM_020487	-3.3	0.0006
Actinin α1 (Actn1)	BC003232	-4.9	0.0005
Cytoskeletal			
Protein tyrosine phosphatase, non-receptor type 4 (Ptpn4)	NM_019933	1.9	0.02
Kinesin family member 5B (Kif5b)	BF099632	1.4	0.04
Kinesin family member 3C (Kif3c)	NM_008445	1.1	0.02
Kinesin family member 12 (Kif12)	BC022225	-1.5	0.03
Tropomyosin 2β (Tpm2)	BC024358	-2.4	0.05
Parvin γ (Parvγ)	BC011200	-3.1	0.03
Keratin complex 2 gene 10 (Krt2-10)	X99143	-3.8	0.002
Actinin α1 (Actn1)	BC003232	-4.9	0.04
Kinesin family member 20A (Kif20a)	NM_009004	-7.6	0.002

Protein Transport			
Fatty acid binding protein 1 (Fabp1)	NM_017399	-3.0	0.03
RAN binding protein 17 (Ranbp17)	NM_023146	-3.3	0.0006
Ras and Rab interactor 1 (Rin1)	BC011277	-3.3	0.001
Rab17, member RAS oncogene family	NM_008998	-7.6	0.03
Kinesin family member 20A (Kif20a)	NM_009004	-7.6	0.002
Intermediate Filament-Related			
Meiosis-specific nuclear structural protein 1 (Mns1)	NM_008613	4.9	0.05
Lamin B2 (Lmnb2)	D13455	1.9	0.04
Pericentrin 2 (Pcnt2)	BB320388	1.4	0.04
Keratin complex 2 gene 10 (Krt2-10)	X99143	-3.8	0.002
Microtubule/Kinesin Motor-Related			
Kinesin family member 5B (Kif5b)	BF099632	1.4	0.04
Pericentrin 2 (Pcnt2)	BB320388	1.4	0.04
Cytoskeleton-associated protein 1 (Ckap1)	NM_025548	1.3	0.04
Kinesin family member 3C (Kif3c)	NM_008445	1.1	0.02
Kinesin family member 12 (Kif12)	BC022225	-1.5	0.03
Kinesin family member 20A (Kif20a)	NM_009004	-7.6	0.002
Myosin			
Immunoglobulin κ chain variable 8 (Igκ-V8)	M35669	-1.8	0.03
Tropomyosin 2β (Tpm2)	BC024358	-2.4	0.05
NF-κ Cascade			
Killer cell lectin-like receptor subfamily A, member 12 (Klra12)	AF307947	4.2	0.005
Oxidized low density lipoprotein receptor 1 (Olr1)	NM_138648	3.8	0.04
Kit oncogene	BB333334	3.3	0.04
Protein C receptor (Procr)	NM_011171	2.5	0.008
Blocked early in transport 1 (S. cerevisiae) homolog (Bet1)	NM_009748	2.3	0.03
Guanine nucleotide binding protein, α15 (Gnα15)	NM_010304	2.0	0.05
ADAM-like decysin 1 (Adamdec1)	NM_021475	-2.1	0.04
Guanylate cyclase 2e (Gucy2e)	NM_008192	-2.1	0.02
Aldo-keto reductase family 1, member C18 (Akr1c18)	NM_134066	-2.2	0.03
Immunoglobulin κ chain variable 8 (Igκ-V8)	AV057155	-2.2	0.05
Odorant receptor 16 (Ors16)	NM_021368	-2.3	0.03
Glial cell line derived neurotrophic factor family receptor α1 (Gfrα)	AI196411	-2.3	0.05
Granzyme E (Gzme)	NM_010373	-2.3	0.02
Olfactory receptor 7b (Olfr7b)	NM_030553	-2.3	0.03

Collagenase-like B (Mcolb)	NM_032007	-2.4	0.04
Tropomyosin 2β (Tpm2)	BC024358	-2.4	0.05
Transition protein 1(Tnp1)	AV206780	-2.7	0.04
Homer (Drosophila) homolog 1 (Homer1)	AF093257	-2.8	0.04
Ribosomal protein L3-like (Rpl3l)	NM_025425	-3.1	0.04
Triadin (Trdn)	AF223417	-3.2	0.0005
RAN binding protein 17 (Ranbp17)	NM_023146	-3.3	0.0006
Olfactory receptor 78 (Olfr78)	BB132229	-5.4	0.05
Protein Kinase Cascade			
Killer cell lectin-like receptor subfamily A, member 12 (Klra12)	AF307947	4.2	0.005
Guanine nucleotide binding protein, β1 (Gnβ1)	NM_008142	1.3	0.01
cDNA sequence AJ430384	NM_130880	-1.3	0.02
EBNA1 binding protein 2 (Ebna1bp2)	AV151335	-1.5	0.01
Glutathione transferase ζ1 (Gstζ1)	AB041613	-1.5	0.0003
Adaptor-related protein complex 3, σ2 subunit (Ap3σ2)	NM_009682	-1.6	0.04
Killer cell lectin-like receptor subfamily G, member 1 (Klrg1)	NM_016970	-1.7	0.04
Testis expressed gene 14 (Text14)	NM_031386	-1.7	0.01
Purinergic receptor P2X, ligand-gated ion channel 4 (P2rx4)	AJ251462	-1.9	0.04
ADAM-like decysin 1 (Adamdec1)	NM_021475	-2.1	0.04
Immunoglobulin κ chain variable 8 (Igκ-V8)	AV057155	-2.2	0.05
Ribosomal protein L3-like (Rpl3l)	NM_025425	-3.1	0.04
Triadin (Trdn)	AF223417	-3.2	0.0005
RAN binding protein 17 (Ranbp17)	NM_023146	-3.3	0.0006
RNA Binding			
RIKEN cDNA A230070D14 gene	BB731282	1.5	0.02
Poly(rC) binding protein 2 (Pcbp2)	AV309800	1.5	0.008
U1 small nuclear ribonucleoprotein polypeptide A (Snrp70)	BC002169	1.5	0.02
Embryonic lethal, abnormal vision, Drosophila-like 4 (Elavl4)	NM_010488	1.5	0.003
CGI-74-like SR-rich	BG075618	1.4	0.04
Mitochondrial ribosomal protein L11 (Mrpl11)	NM_025553	1.3	0.05
Fibrillarin (Fbl)	NM_007991	1.3	0.03
Fragile X mental retardation syndrome 1 homolog (Fmr1)	AF170530	1.3	0.03
Pumilio 1 (Drosophila) (Pum1)	BB823786	1.3	0.006
RIKEN cDNA 2810477H02 gene	AK013413	-1.8	0.03
Splicing factor, arginine/serine-rich 10 (Sfrs10)	U14648	-1.9	0.04
Survival motor neuron (Smn)	BB821035	-2.7	0.008
Breast cancer 1 (Brca1)	U31625	-2.9	0.0004

STAT Cascade			
Killer cell lectin-like receptor subfamily A, member 12 (Klra12)	AF307947	4.2	0.005
Oxidized low density lipoprotein receptor 1(Olr1)	NM_138648	3.8	0.04
Kit oncogene	BB333334	3.3	0.04
Protein C receptor (Procr)	NM_011171	2.5	0.008
Blocked early in transport 1 (S. cerevisiae) homolog (Bet1)	NM_009748	2.3	0.03
Guanine nucleotide binding protein, α15 (Gnα15)	NM_010304	2.0	0.05
ADAM-like decysin 1 (Adamdec1)	NM_021475	-2.1	0.04
Guanylate cyclase 2e (Gucy2e)	NM_008192	-2.1	0.02
Aldo-keto reductase family 1, member C18 (Akr1c18)	NM_134066	-2.2	0.03
Odorant receptor 16 (Ors16)	NM_021368	-2.3	0.03
Glial cell line derived neurotrophic factor family receptor α1 (Gfrα1)	AI196411	-2.3	0.05
Granzyme E (Gzme)	NM_010373	-2.3	0.02
Olfactory receptor 7b (Olf7b)	NM_030553	-2.3	0.03
Collagenase-like B (Mcolb)	NM_032007	-2.4	0.04
Tropomyosin 2β (Tpm2)	BC024358	-2.4	0.05
Transition protein 1 (Tnp1)	AV206780	-2.7	0.04
Homer (Drosophila) homolog 1 (Homer1)	AF093257	-2.8	0.04
Ribosomal protein L3-like (Rpl3l)	NM_025425	-3.1	0.04
RAN binding protein 17 (Ranbp17)	NM_023146	-3.3	0.0006
Olfactory receptor 78 (Olfr78)	BB132229	-5.4	0.05
Transcription Factors			
T-box 21 (Tbx21)	NM_019507	2.8	0.02
T-box 4 (Tbx4)	AY075134	2.7	0.002
Est2 repressor factor (Erf)	NM_010155	2.0	0.02
RIKEN cDNA 4930404I05 gene	BM235038	1.9	0.0001
SRY-box containing gene 5 (sox5)	AJ010604	-1.7	0.01
Prostate specific ets transcription factor (Pse)	NM_013891	-1.7	0.02
Transcription factor AP-2α (Tcfap2α)	NM_011547	-1.8	0.002
Zinc finger protein 316 (Zfp316)	AF082568	-1.8	0.03
ESTs	AI451482	-1.8	0.05
Tyrosine kinase-associated leucine zipper protein LAZipII	BI903744	-1.9	0.01
Splicing factor, arginine/serine-rich 10 (Sfrs10)	U14648	-1.9	0.04
GLI-Kruppel family member (Gli3)	NM_008130	-1.9	0.03
Atonal homolog 7 (Drosophila) (Atoh7)	NM_016864	-1.9	0.03
Ventral anterior homeobox containing gene 2 (Vax2)	NM_011912	-2.2	0.02
Cone-rod homeobox containing gene (Crx)	BC016502	-3.0	0.05
Transcription factor AP-2δ (Tfap2δ)	AF421891	-3.0	0.02

Neurogenin 2 (Neurog2)	NM_009718	-3.7	0.03
Kruppel-like factor 5 (Klf5)	BG069607	-4.7	0.04
Forkhead box C2 (Foxc2)	NM_013519	-4.8	0.003

the literature, and 4) appeared in one of the other gene or protein profiling experiments. In most cases the PCR results confirmed that the genes were expressed differentially, as detected by the microarrays (Figure 9).

Thus, being semiquantitative in nature, the microarray technique allowed the identification of differentially expressed genes with validity (9/14) 64% of the time in this study. Two of the most relevant genes found in the Affymetrix gene expression profiling study, *Bid* and *N-Bak*, were further characterized by western blot and immunohistochemistry.

3.4 ***Multi-immunoblotting of Protein Kinases and Apoptosis Proteins***

3.4.1 **Multi-Kinase/Apoptosis Protein Analysis**

To evaluate the expression of a large number of protein kinases and apoptosis proteins in the mouse spinal cord, Kinetworks™ (Kinexus Inc., BC) protein profiling was performed, employing multi-immunoblotting with prevalidated antibodies against 78 protein kinases and 25 apoptosis proteins. Cytosolic fractions of spinal cord tissue were pooled from 2 $Smn^{-/+}$ mice and from 2 $Smn^{+/+}$ mice as the control. Figure 10 shows examples of immunoblots of protein kinases (A and B) and apoptosis proteins (C) in the cytosolic fraction of homogenized spinal cord tissue from wildtype mice. Each lane of these immunoblots is probed with cocktails of one to three different, validated antibodies for protein kinases or apoptotic proteins. The multiple bands in each lane reflect the expression of each of these target proteins and some unidentified cross-reactive proteins in the samples. Many of the target proteins for these screens were clearly evident in the immunoblots of control spinal cord. Target proteins that were not detected included the protein kinases: CDK1, CDK2,

Figure 9: Comparative ratio analysis by Moe430a microarrays and ABI PRISM 7000 PCR amplifications of 14 candidate genes differentially expressed in the spinal cord of *Smn*$^{-/+}$ mice. White and black columns show fold changes as a ratio of disease mRNA levels compared over control mRNA levels as determined by PCR and microarrays respectively. Measurements of RNA with SYBR Green quantitative RT-PCR were obtained from a separate group of animals than the Affymetrix study. PCR amplifications were performed in triplicate, n = 12 and four microarrays were screened for each sample group. Statistically significant fold change values with a p value are indicated as follows: * $p < 0.05$, ** $p<0.01$ and *** $p<0.0005$.

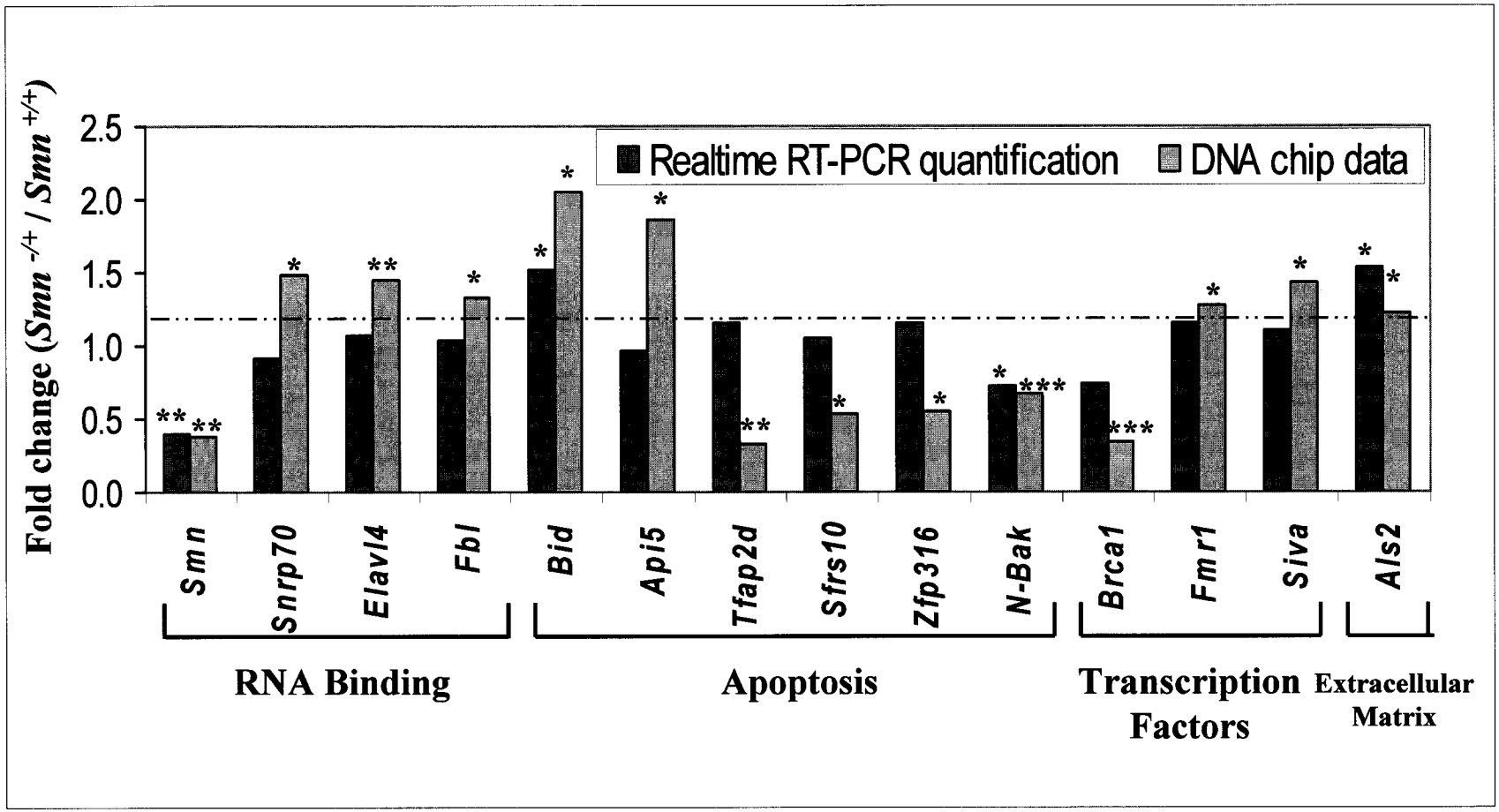
Fold change (Smn -/+ / Smn +/+)
2.5
2.0
1.5
1.0
0.5
0.0
Realtime RT-PCR quantification
DNA chip data
Smn
Snrp70
Elavl4
Fbl
Bid
Api5
Tfap2d
Sfrs10
Zfp316
N-Bak
Brca1
Fmr1
Siva
Als2
RNA Binding
Apoptosis
Transcription Factors
Extracellular Matrix

Figure 10: Kinetworks™ KPKS 1.0 protein kinases (a and b) and KAPS 1.0 apoptosis proteins (c) analyses of mouse wild-type spinal cord. The corresponding number of each protein target that can be identified is labeled on the blot. Cytosolic fractions pooled from two mouse spinal cords for each sample were screened in duplicate and assessed for expression levels of 78 protein kinases and 25 apoptotic proteins.

(a) Protein kinases tracked:

1.	Aurora2	20.	ERK2'''	40.	PKCe
2.	CDK1	21.	ERK3	41.	PKCe'
3.	CDK2	22.	ERK3'	42.	PKCg
4.	CDK4	23.	GSK3a	43.	PKCl
5.	CDK5	24.	GSK3b	44.	PKCm
6.	CDK6	25.	IKKbeta	45.	PKCm'
7.	CDK7	26.	MEK1	46.	PKCt
8.	CDK9	27.	MEK2	47.	PKCz
9.	CK2	28.	MEK4	48.	PKCz'
10.	CK2'	29.	MEK6	49.	PKR
11.	CK2''	30.	MOS1	50.	RAFB
12.	COT	31.	p38 MAPK	51.	ROKa
13.	DNAPK	32.	PAK1	52.	RSK
14.	eEF2k	33.	PAK3	53.	RSK1
15.	ERK1	34.	PDK1	54.	RSK2
16.	ERK1'	35.	PKBa	55.	S6K p70
17.	ERK2	36.	PKBa'	56.	S6K p70'
18.	ERK2'	37.	PKCa	57.	S6K p70''
19.	ERK2''	38.	PKCb	58.	SAPKb
		39.	PKCd		

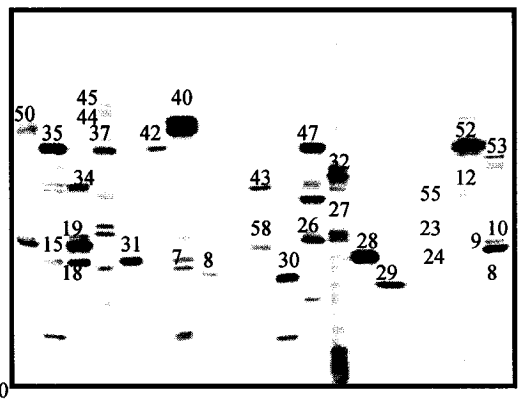

(b) Protein kinases tracked:

1.	BMX (Etk)	10.	FYN	22.	MST1
2.	BTK	11.	FYN'	23.	PKA
3.	CaMK1	12.	GCK	24.	PKG1
4.	CaMK4	13.	GRK2	25.	PYK2
5.	CaMKK	14.	HPK1	26.	RAF1
6.	CK1d	15.	IKKa	27.	RAF1'
7.	CK1e	16.	JAK1	28.	SRC
8.	CSK	17.	JAK2	29.	SYK
9.	DAPK	18.	KSR1	30.	YES1
10.	ERK6	19.	LCK	31.	ZAP70
11.	FAK	20.	LYN	32.	ZIP
		21.	MNK2	33.	'ZIP

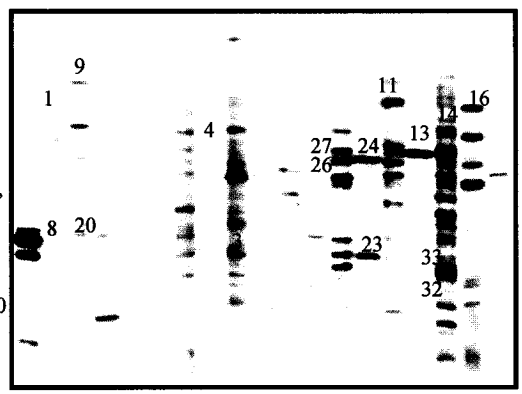

(c) Apoptosis proteins tracked:

1.	PARP	14.	CASP9
2.	AIF	15.	CAS
3.	XIAP	16.	CytoC
4.	SODD	17.	DAXX
5.	CASP1	18.	DFF45
6.	CASP12	19.	MSH2
7.	CASP2	20.	PERP
8.	CASP3	21.	SOD (Cu/Zn)
9.	CASP4	22.	SOCS-4
10.	CASP5	23.	TRADD
11.	CASP6	24.	FAS
12.	CASP7	25.	FasL
13.	CASP8		

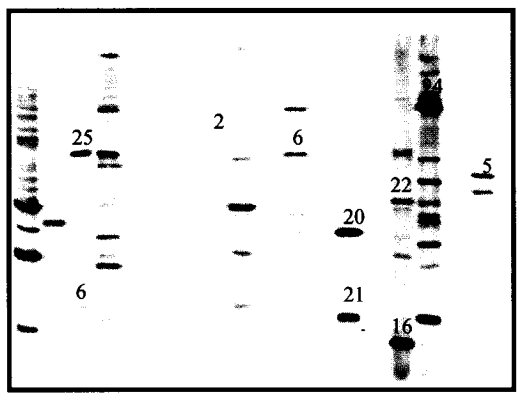

CDK4, CDK6, DNAPK, ERK3, FYN, KSR1, LCK, MEK7, MST1, MNK2, NEK2, PAC3, PKCθ, PYK2, ROKA, SRC, SYK and Zap70 and apoptosis proteins: CAS, DAXX, MSH2, PARP, proCASP2, proCASP3, proCASP6, proCASP7, proCASP8, proCASP9, proCASP12 prodomain, TRADD and XIAP.

Figure 11 provides quantitative information regarding the levels of protein kinases (Figure 11a and b) and apoptotic proteins (Figure 11c) in pooled samples of cytosolic fractions from spinal cords obtained from 5-week-old *Smn*$^{-/+}$ mice and controls. For instance, the following proteins kinases are highly expressed in the cytosolic fraction: ERK1, MEK4, PKCβ and PKCε. The patterns of expression of protein kinases can differ profoundly between mammalian tissues, but the spinal cord results observed in this study were generally similar to what was previously observed in human spinal cord (Hu et al., 2003b) as well as in mouse brain and spinal cord (Hu et al., 2003a).

3.4.2 Expression of Specific Protein Kinases and Apoptosis Proteins

The Kinetworks™ study was used to select those specific protein kinases and apoptosis protein that demonstrated differences in expression between *Smn*$^{-/+}$ and *Smn*$^{+/+}$ mice. While small differences were observed, many of the detected proteins were not appreciably altered between *Smn*$^{-/+}$ and *Smn*$^{+/+}$ mice (Figure 11). From the results of the Kinetworks™ analysis, the expression of Raf B, a protein kinase, was chosen for re-analysis in the cytosolic fraction of total spinal cord tissue from 2 *Smn*$^{-/+}$ mice and 2 *Smn*$^{+/+}$ mice, by western blot analysis.

Figure 11: Kinetworks^{TM} profiles of protein kinases (a and b) and apoptosis proteins (c) in pooled samples of cytosolic fractions from spinal cord tissue obtained from 5-week-old *Smn*$^{-/+}$ mice (solid bars) and controls (open bars). Screens were performed in duplicate using n = 2 for each sample in each replicate. Bars represent the mean average of two screens with error bars indicating the standard deviation. For the full names of the proteins screened in the Kinetworks Apoptosis Protein Screen and Protein Kinase Screens, please refer to appendices A and B, respectively.

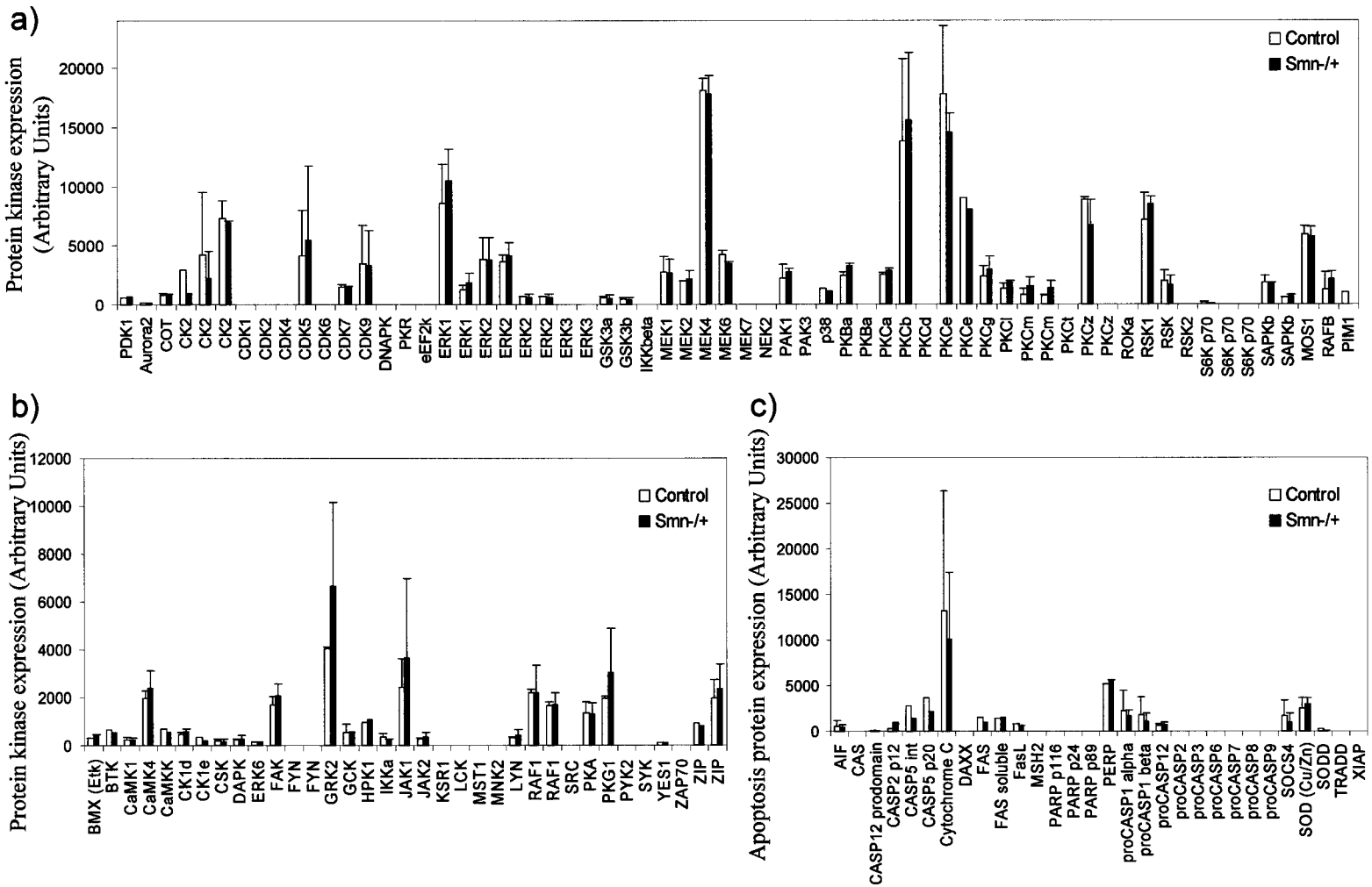
a)
Protein kinase expression (Arbitrary Units)
Control
Smn-/+
PDK1
Aurora2
COT
CK2
CK2
CK2
CDK1
CDK2
CDK4
CDK5
CDK6
CDK7
CDK9
DNAPK
PKR
eEF2k
ERK1
ERK1
ERK2
ERK2
ERK2
ERK2
ERK3
ERK3
GSK3a
GSK3b
IKKbeta
MEK1
MEK2
MEK4
MEK6
MEK7
NEK2
PAK1
PAK3
p38
PKBa
PKBa
PKCa
PKCb
PKCd
PKCe
PKCe
PKCg
PKCl
PKCm
PKCm
PKCt
PKCz
PKCz
ROKa
RSK1
RSK
RSK2
S6K p70
S6K p70
S6K p70
SAPKb
SAPKb
MOS1
RAFB
PIM1
b)
Protein kinase expression (Arbitrary Units)
Control
Smn-/+
BMX (Etk)
BTK
CaMK1
CaMK4
CaMKK
CK1d
CK1e
CSK
DAPK
ERK6
FAK
FYN
FYN
GRK2
GCK
HPK1
IKKa
JAK1
JAK2
KSR1
LCK
MST1
MNK2
LYN
RAF1
RAF1
SRC
PKA
PKG1
PYK2
SYK
YES1
ZAP70
ZIP
ZIP
c)
Apoptosis protein expression (Arbitrary Units)
Control
Smn-/+
AIF
CAS
CASP12 prodomain
CASP2 p12
CASP5 int
CASP5 p20
Cytochrome C
DAXX
FAS
FAS soluble
FasL
MSH2
PARP p116
PARP p24
PARP p89
PERP
proCASP1 alpha
proCASP1 beta
proCASP12
proCASP2
proCASP3
proCASP6
proCASP7
proCASP8
proCASP9
SOCS4
SOD (Cu/Zn)
SODD
TRADD
XIAP

In the initial Kinetworks kinase screen, the kinase, B-Raf, appeared to be substantially upregulated in *Smn*$^{-/+}$ mice. This finding along with the results of a study in embryonic motor neurons, where it was discovered that B-Raf is required as a signalling intermediate in the survival responses of the embryo to CNTF (Wiese et al., 2001) suggested the pertinence of B-Raf in SMA pathogenesis. For these reasons B-Raf was chosen for re-examination (Figure 12). Immunoblots performed to validate this result using the same anti-B-Raf antibody as the Kinexus screen and the same pooled 5-week-old *Smn*$^{-/+}$ and control mouse spinal cord samples revealed that B-Raf protein expression was not altered in *Smn*$^{-/+}$ mice. The next set of kinase screens supported this finding.

Examination of these results show that the expression levels of protein kinases and apoptosis proteins do not reveal a general upregulation or downregulation of expression nor are the proteins significantly altered in *Smn*$^{-/+}$ mouse spinal cords. Kinetworks screens measure the expression levels but not activity of the proteins, but for approximately 25% of the kinase screen proteins, phosphorylation can be observed by band shifts, indicating kinase activation. In this study no such bands shifts worthy of following up were observed.

3.5 *Protein Level Studies of Candidate Genes in 5-week-old Smn*$^{-/+}$ *Mouse Spinal Cords*

3.5.1 Immunoblot Analysis of Candidate Genes in 5-week-old *Smn*$^{-/+}$ Mouse Spinal Cords

Neuronal-Bak (N-Bak) (Figure 13a) and Bid (Figure 13b) proteins were studied by triplicate western blots comparing *Smn*$^{-/+}$ and *Smn*$^{+/+}$ mouse spinal cords at the 5-week, 3-month and 6-month time points. The *Bid* gene showed increased mRNA and protein

Figure 12: Equivalent expression levels of B Raf in total spinal cord tissue lysates from 5-week old *Smn*$^{-/+}$ and *Smn*$^{+/+}$ mice. Western blotting was performed using mouse B-Raf and Gapdh specific antibodies and cytosolic 20 μg of protein lysate isolated from *Smn*$^{-/+}$ (n=4) and *Smn*$^{+/+}$ (n=4) mouse spinal cord tissue. Analysis in duplicate did not show any differences.

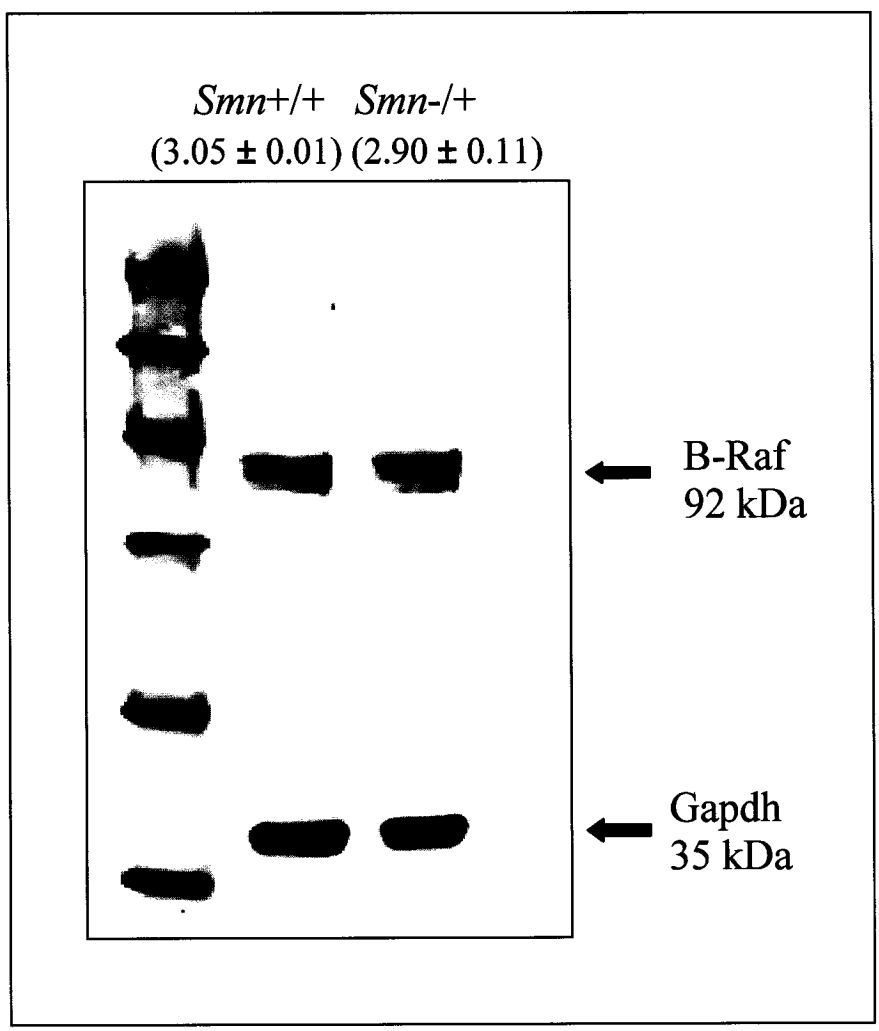
Smn+/+ *Smn*-/+
(3.05 ± 0.01) (2.90 ± 0.11)
B-Raf
92 kDa
Gapdh
35 kDa

Figure 13: Immunoblot shows unchanged levels (A) Neuronal-Bak (N-Bak) and increased levels of (B) Bid in spinal cords of *Smn*$^{+/-}$ mice compared to controls at either 5 weeks, 3 months or 6 months of age. Western was performed using mouse N-Bak, Bid and GAPDH specific antibodies and cytosolic protein lysate isolated from *Smn*$^{-/+}$ and *Smn*$^{+/+}$ mouse spinal cord tissue. Shown underneath are fold changes in expression in *Smn*$^{-/+}$ spinal cord tissue relative to *Smn*$^{+/+}$ mouse spinal cord tissue averaged between three trials and normalized to GAPDH levels.

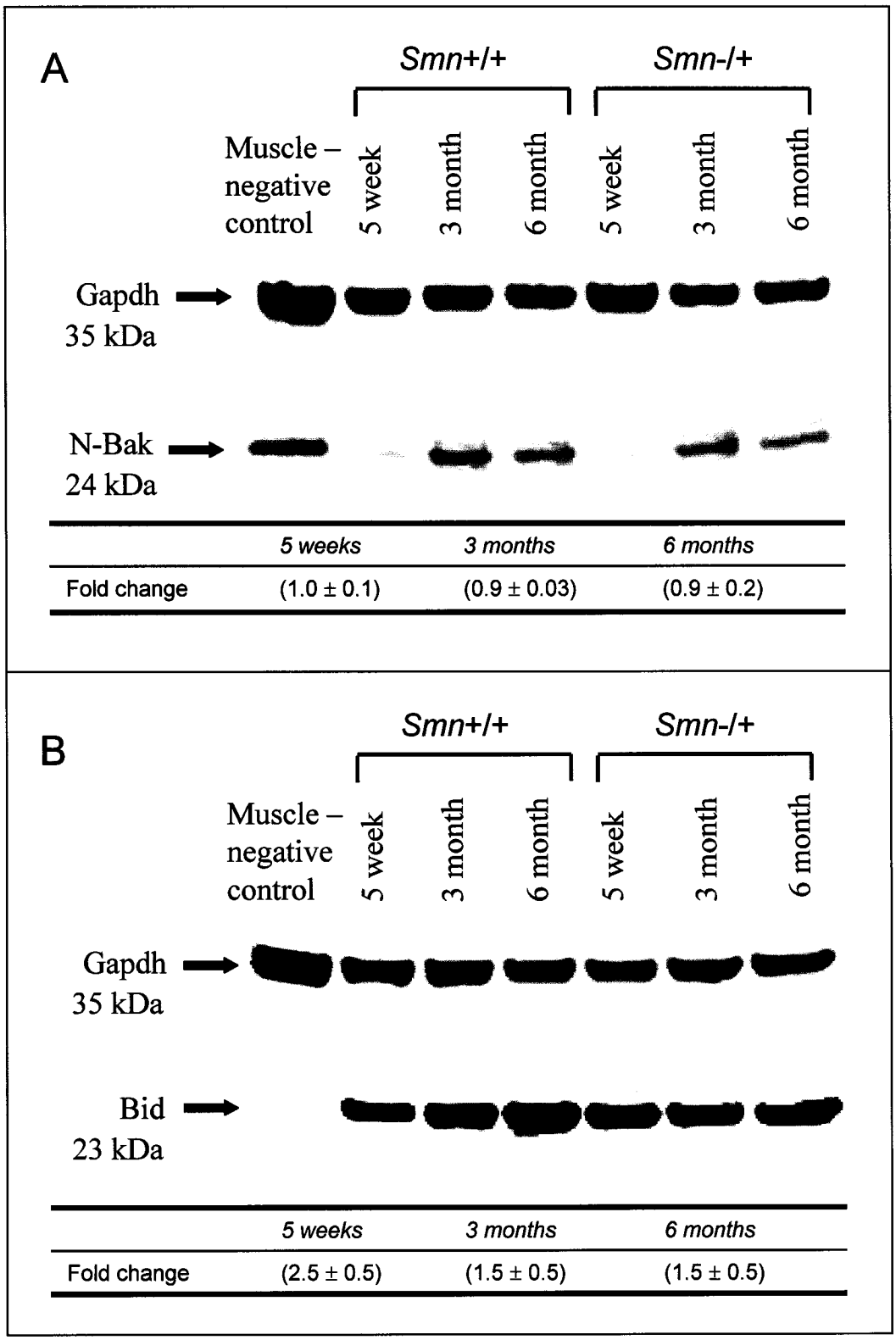

	5 weeks	*3 months*	*6 months*
Fold change	(1.0 ± 0.1)	(0.9 ± 0.03)	(0.9 ± 0.2)

	5 weeks	*3 months*	*6 months*
Fold change	(2.5 ± 0.5)	(1.5 ± 0.5)	(1.5 ± 0.5)

expression at the 5-week (2.5 ± 0.5), 3-month (1.5 ± 0.5) and 6-month (1.5 ± 0.5) time points. Moreover, the extent of the mRNA change (2.0 ± 0.03) at 5-weeks of age was very similar to the protein expression change at that time point. The *N-Bak* gene showed decreased mRNA expression but did not show a significant decrease in protein expression at any time point. There are two possible explanations for the lack of correlation between *N-Bak* mRNA and protein expression levels. The first explanation is that translational and posttranslational modifications of many gene products and protein turnover are able to compensate for the decreased mRNA expression seen in $Smn^{-/+}$ mice. The second, more likely explanation is that since the is no N-Bak specific antibody commercially available, the peptide sequence used to generate the anti-Bak antibodies (BD Biosciences PharMingen, Palo Alto, CA) is present in both Bak and N-Bak (Krajewski et al., 1996). Since N-Bak is expressed in neurons, but not in other cells, whereas Bak is expressed everywhere except neurons, any changes in N-Bak protein levels within the spinal cord would be overshadowed by the abundant Bak expressed in non-neuronal cells (Yun-Fu et al., 2001).

3.5.2 Immunohistochemical Analysis of Candidate Genes in 5 -week-old $Smn^{-/+}$ Mouse Spinal Cords

To observe the cell-specificity mouse lumbar spinal cord sections were stained with polyclonal rabbit anti-Bak antibody and polyclonal rabbit anti-Bid antibody. Immunoreactions of anti-Bak antibody in the ventral horn were distributed throughout the extracellular processes and the nucleus of the neuron cells, including motor neuron (Figure 14). Immunoreactivity for Bid, on the other hand, was only observed in the extracellular processes (Figure 15). There were no apparent changes in staining patterns in the spinal

cord sections from different genotypes ($Smn^{-/+}$ and $Smn^{+/+}$) or at different time points (5 weeks and 3 months of age.)

Figure 14: The lumbar spinal cord immunostained with 1:500 dilution of polyclonal rabbit anti-Bak antibody does not show motor neuron specific staining in *Smn*$^{-/+}$ and *Smn*$^{+/+}$ mice at 5 weeks or 3 months of age. Spinal motor neurons in 5-week-old (a) *Smn*$^{+/+}$ and (b) *Smn*$^{-/+}$mice, and 3-month-old (c) *Smn*$^{+/+}$ and (d) *Smn*$^{-/+}$mice. Motor neurons in *Smn*$^{+/+}$ and *Smn*$^{-/+}$: mice appear the same in size and staining. Testis tissue was used as a positive control for anti-Bak staining (e). Bar in (a) 200μm.

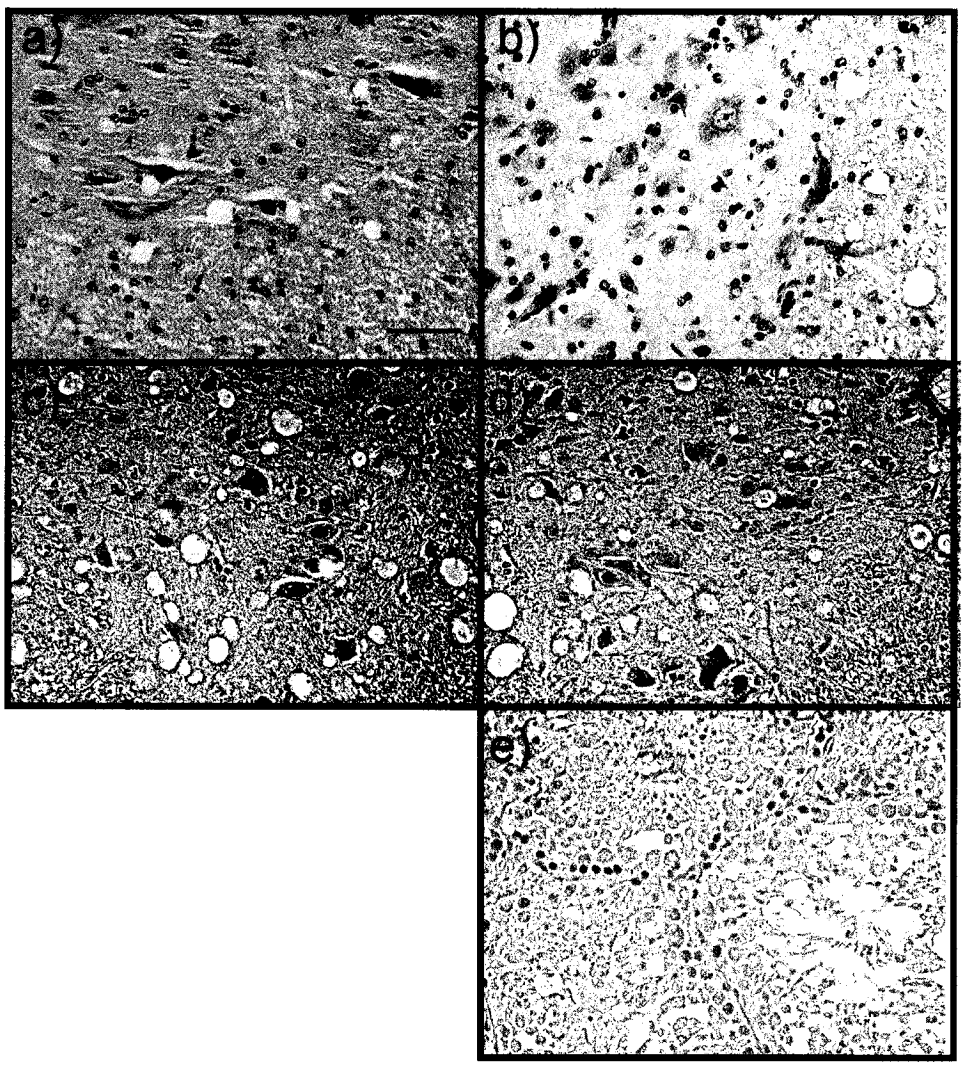
a)
b)
c)
d)
e)

Figure 15: The spinal cord of the lumbar level immunostained with 1:100 dilution of polyclonal rabbit anti-Bid antibody does not show motor neuron specific staining in *Smn*$^{-/+}$ and *Smn*$^{+/+}$ mice at 5 weeks or 3 months of age. Spinal motor neurons in 5-week-old (a) *Smn*$^{+/+}$ and (b) *Smn*$^{-/+}$mice, and 3-month-old (c) *Smn*$^{+/+}$ and (d) *Smn*$^{-/+}$mice. Motor neurons in *Smn*$^{+/+}$ and *Smn*$^{-/+}$. Testis tissue was used as a positive control for anti-Bid staining (e). Bar in (a) 200μm.

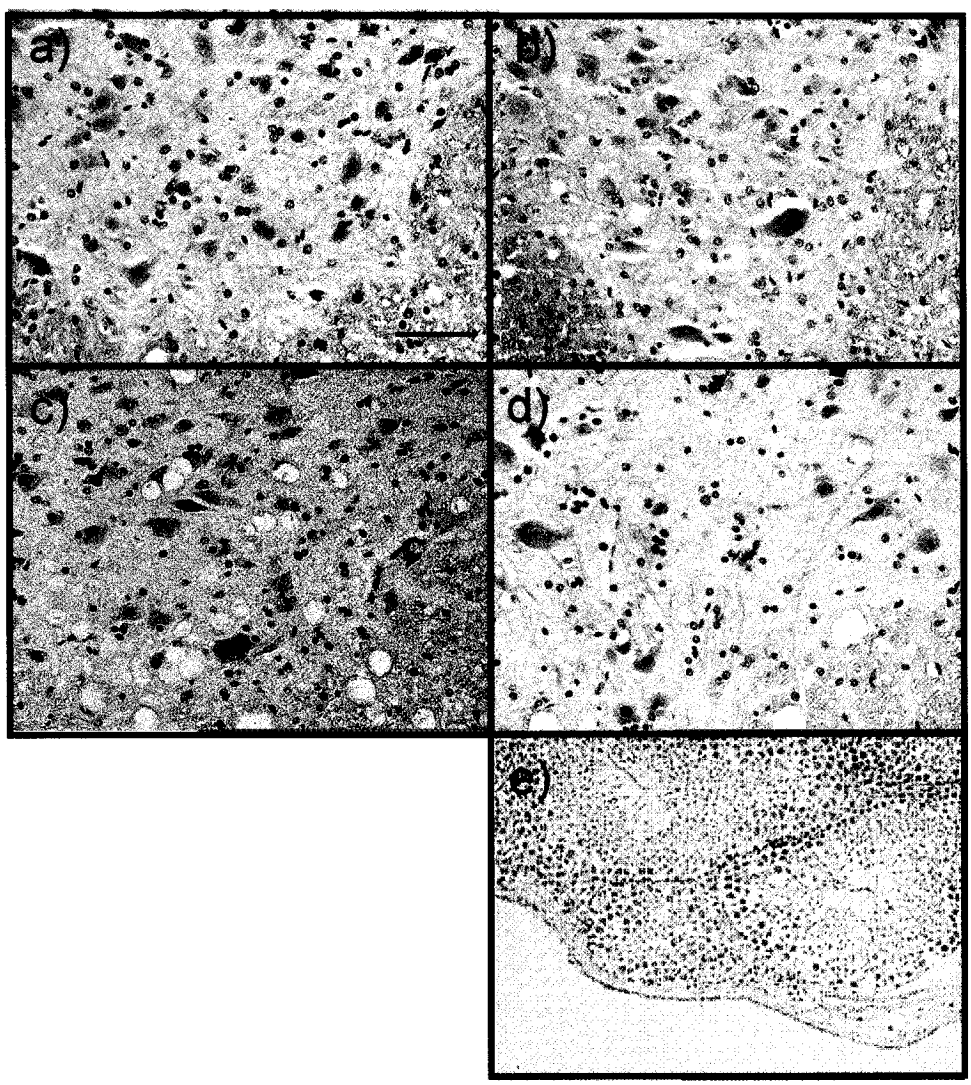
a)
b)
c)
d)
e)

Discussion

4.1 Selection of 5-week-old Smn$^{-/+}$ Mice for Expression Studies

The aim of this study was to capture gene and protein profiles of *Smn*$^{-/+}$ mice at a timepoint preceding motor neuron degeneration. Based on a previous study, enriching for motor neurons in primary spinal cord cultures (Camu and Henderson, 1992) from 15-day embryonic mice did not yield enough motor neurons to provide a sufficient amount of RNA for the Representational Difference Analysis protocol (data not shown). Profiling was therefore chosen to be done on whole spinal cords that consist of interneurons and motor neurons and their processes, sensory neuron processes, oligodendrocytes, astroglia and microglia. Given the difficulty of harvesting spinal cords from younger mice the 5-week-old mice were chosen as a starting point for profiling (data not shown). Given that this is the first time point at which motor neuron loss is reported, it is hypothesized that 5 weeks is a pre-clinical time point.

4.2 *Motor Neuron Loss at 5 Weeks and 3 Months of Age in Smn$^{-/+}$ Mice*

The characteristic histopathological changes associated with Spinal Muscular Atrophy (SMA) include degeneration and loss of large motor neurons. A study done on the lumbar spinal cord of newborn *Smn*$^{-/+}$ mice showed as many motor neurons as were present in their wildtype counterparts (Jablonka et al., 2000). The same study showed that by 6 months of age 40% or the motor neurons were lost in comparison with wildtype mice, and spinal motor neuron loss in 1-year-old mice was 54%. On the basis of a correlation between motor unit number and motor unit potential areas, it has been assumed that a loss of about 50% motor neurons can be compensated for by reinnervation and collateral sprouting (Sharrad, 1955, Wohlfart, 1957; Hansen and Ballatyne et al., 1978). This mouse model is in accordance

with SMA type III patients who develop normally during the first months of life, gain the capability to stand and walk and then develop typical SMA motor deficits before an age of 3 to 6 years. The degeneration of motor neurons in *Smn*$^{-/+}$ mice spinal cord is rapid between birth and 6 months and significantly slows down between 6 and 12 months of age. The degree of motor neuron loss in *Smn*$^{-/+}$ mice spinal cords between birth and 6 months of age was previously unknown. This study shows that by 5 weeks of age the *Smn*$^{-/+}$ mice has already lost 28% of its motor neurons in the anterior horn of the lumbar spinal cord compared to wildtype mice (Table 5). However the number of motor neurons lost in *Smn*$^{-/+}$ mice between 5 weeks and 3 months of age does not reach statistical significance and is substantially lower than the neurons lost between birth and 5 weeks of age . This study supports previous findings suggesting that motor neuron loss in SMA patients occurs in a stepwise fashion and occurs early in life (Crawford & Pardo, 1996). The gene and protein profiles done on 5-week-old mice capture a time where approximately half of the motor neurons in the *Smn*$^{-/+}$ mouse that will be lost by 1 year of age have already degenerated. Genes found to be differentially regulated in this model are therefore either directly or indirectly contributing to create an environment for motor neuron loss or are the direct or indirect result of motor neuron degeneration.

4.3 ***Protein Kinase and Apoptotic Protein Expression in 5 -week-old Smn$^{-/+}$ Mouse Spinal Cords***

In this work the expression of 78 distinct protein kinases (PKs) and 25 apoptotic proteins (APs) were analysed in the spinal cords of 5-week-old Smn$^{-/+}$ mice and unaffected littermates that expressed normal levels of *Smn* mRNA and protein. The Kinetworks KPKS 1.0 and KAPS 1.1 protein screens allowed a rapid approach for screening 5-week-old *Smn*$^{-/+}$

and *Smn*$^{+/+}$ mouse spinal cord samples in duplicate. Comparison of 103 proteins in spinal cord tissue from *Smn*$^{-/+}$ mice did not reveal any statistically significant differences in expression. As was evident from Figure 11, standard deviations of PKs and APs were large not only for *Smn*$^{-/+}$ mice having a similar phenotype, but also for the controls. Data variability was expected to occur when expression levels are small. The variability of proteins such as cytochrome c, Protein kinase C β (PKC β) and Janus kinase 1 (Jak 1) in the face of reasonable expression levels was particularly surprising. This variability may reflect animal-to-animal variability or limitations of the protein screening technique. Variability appeared to be similar in *Smn*$^{-/+}$ and *Smn*$^{+/+}$ mice.

Preliminary findings show possible elevated expression of protein kinase Cλ (PKCλ) (56% increase), protein kinase Cμ (PKCμ) (112% increase), bone marrow X kinase (BMX) (37% increase) and PERP (8% increase) and reduced expression of MAP kinase kinase 6 (MEK6) (19% decrease) and FasL (22% decrease) (Figure 11a,b). The robustness of the data is confirmed by the patterns of expression of protein kinases in the Smn$^{-/+}$ and Smn$^{-/+}$ mouse spinal cords which were similar to what was formerly observed in human spinal cord tissue of Amyotrophic Lateral Sclerosis (ALS) patients (Hu et al., 2003b) as well as in mouse brain and spinal cord of an ALS mouse model (Hu et al., 2003a).

Further replicates of the Kinetworks screens would have to be performed in order to validate the consistency and statistical significance of these findings.

4.3.1 Protein Kinase Expression in *Smn*$^{-/+}$ Mice

Only a few studies have examined the expression of protein kinases in the rodent central nervous system. A study of phosphatidyl-inositol 3-kinase (PI3-K), protein kinase B (PKB), p70 S6K and ERK expression in the spinal cords of mice having the progressive neuropathy mutation (pmn) and control mice revealed that these four kinases were highly expressed in spinal cords and that p70 S6K was reduced in pmn mice (Wagey et al., 2001b). The profiling in the current study does show high levels of ERK1 but not PKB or p70 S6K. Furthermore, S6K is slightly reduced in the *Smn*$^{-/+}$ mice but the difference is not significant. Another study showed that PI3-K and PKB protein expressions are markedly declined at an early presymptomatic stage in the anterior horn neurons of G93A mutant superoxide dismutase 1 (SOD1) transgenic mice (Warita et al., 2001). PI3-K and PKB have been shown to play a central role in neuronal survival against apoptosis supported by nerve growth factor (NGF) (Dudek et al., 1997) or insulin-like growth factor-1 (IGF-1). PKB is not significantly upregulated in the *Smn*$^{-/+}$ mice.

Two previous studies have used Kinetworks PK screens on total spinal cords from G93A transgenic (mSOD) mouse models of ALS (Hu et al., 2003a) and thoracic spinal cord tissue from patients with ALS at *post mortem* (Hu et al., 2003b). PKs expressed in the central nervous system of the mSOD mouse compared with control mice were dissimilar to those between ALS patients and controls. It was observed that ALS is associated with the differential expression of many PKs, whereas in mSOD mouse spinal cord tissue there were relatively few differences in the expression levels of PKs compared to controls (increased expression of CK1d, ERK3, p38 MAP kinase, PKCd, PKCm and Raf1). In addition, neither of the PK screens revealed any strikingly similar expression patterns to those observed for

Smn$^{-/+}$ mice. The above information indicates that the activation of PKs in neuron death may different for all three of the neurodegenerative models.

A similarity that all three studies shared was the elevated expression of different isoforms of PKC. PKCs appear in spinal cord tissue of *Smn*$^{-/+}$ mice (PKCλ and PKCμ), mSOD mice (PKCδ and PKCμ), and thoracic spinal cord of ALS patients (PKCα, PKCβ and PKCζ). There is controversy about whether PKC is neuroprotective or neuroapoptotic (Mather, 2001; Noh et al., 2000; Wagey et al., 2001a). It is possible that the increased PKC expression found in spinal cord tissue from *Smn*$^{-/+}$ mice is involved in the disease. There is evidence that riluzole, a neuroprotectant compound that appears to modify the clinical course of SMA (Haddad et al., 2003; Russman et al., 2003), has antagonistic actions on the activation of PKC (Noh et al., 2000). In this study, increased expression was observed for an atypical PKC (aPKC) and a novel protein kinase. PKCλ is an aPKC that requires neither diacylglycerol (DAG) nor calcium for its activation. aPKCs have been shown to modulate NF-kB, which promotes neuronal survival (Wooten, 1999). PKCμ is a 'novel' PKC isoform that requires DAG for activation. The significance of the elevated level of 'novel' PKCs is unknown and it is not clear whether different isoforms of PKCs play similar or different roles in neuron survival. Furthermore, it is not established which cell type or types have increased expression of PKC. The elevated PKC expression could occur in the motor neurons that are affected in SMA, but also could occur in interneurons or non-neuronal cells. The elevated PKC could also be a consequence of regenerative activity from non-neuronal cells, or a manifestation of inflammation within the central nervous system which has been claimed to occur in ALS (McGeer and McGeer, 1998). An immunocytochemical study of

PKC in spinal cord tissue from ALS and control patients at autopsy has demonstrated that in control spinal cord intense PKC immunoreactivity is seen in certain large motor neurons, but that this immunoreactivity is decreased in spinal motor neurons from ALS patients (Nagao et al., 1998). If that study is correct, this indicates that the elevated PKC expression arises in interneurons or in non-neuronal cells.

4.3.2 Apoptotic Protein Expression in *Smn*$^{-/+}$ Mice

The analysis of 25 apoptotic proteins in the spinal cord of *Smn*$^{-/+}$ mice and unaffected littermates provides interesting normative data on the expression of these proteins in the rodent CNS. The activation of caspases (as seen by the generation of cleaved subunits and cleavage of specific substrates) is of particular interest. Since pro-caspase 6 but not pro-caspase 3 expression is increased in 5-week-old *Smn*$^{-/+}$ spinal cords (data not shown) it would be expected to observe increased levels of these pro-forms over time, as well as activation of caspases, corresponding to the cell death process of degenerating motor neurons (Stennicke and Salvesen, 2000) . Contrary to the results from the western blots performed by our group neither pro-caspase 6 nor pro-caspase 3 were detected by the KAPS 1.1 screen. Out of a full set of pro-caspases only pro-caspase 1 and pro-caspase 5 were detected (Figure 11c). Since western blots done in our lab confirm the presence of several APs that are on the KAPS screen (pro-caspase 3, procaspase 6, PARP) it can be assumed that these proteins are not present at high enough concentrations to be detected by the corresponding antibodies in the screen.

4.3.3 Evaluation of Protein Kinase and Apoptotic Protein Expression in *Smn*$^{-/+}$ Mice

The presence of specific alterations in PKs and APs in *Smn*$^{-/+}$ mice implicates a role for some of these aberrant proteins in the neurodegeneration in *Smn*$^{-/+}$ mice. However, given the substantial degree of screen-to-screen variations for the screens performed in this study as well as previous screens for Amylotrophic Lateral Sclerosis (Hu et al., 2003a; Hu et al., 2003b) it appears that Kinetworks screens are not sensitive enough to observe subtle, cell-specific changes in tissue. To overcome this challenge, motor neurons, the cells of interest to this study, would have to be purified from the spinal cord into a homogeneous cell population before performing the kinase and apoptosis screens. By decreasing the tissue complexity it might become easier to identify cell-specfic differences in protein levels using the Kinetworks sceens (Wurmbach et al., 2002).

4.4 *Candidates Identified by RDA*

The representational difference analysis (RDA) method is a combination of subtraction and kinetic enrichment coupled to subsequent amplification. Originally developed to isolate differences between two complex genomes (Lisitsyn et al., 1993), it was later adapted for use with cDNA to study differential gene expression between two mRNA populations (Hubank et al., 1994). It has been used to detect genes specifically expressed in pancreatic cancer (Gress et al., 1997), in hepatocellular carcinomas (Graveel et al., 2001) following ischemic stroke in the rat (Bates et al., 2001) and in myoblast regeneration (Seale et al., 2000). In this case we assessed gene expression as it is specifically regulated in *Smn*$^{-/+}$ vs. *Smn*$^{+/+}$ spinal cords. RDA was performed twice to yield two hundred and fifty clones of which sixty-four were sequenced (Table 7). In order to independently confirm the RDA results a slot blot hybridization using purified inserts from the clones was also performed in

duplicate (Figure 5). Despite the sensitivity of the spot blot screen, the differences in transcript levels between *Smn*$^{-/+}$ and Smn$^{+/+}$ spinal cords were very subtle indicating either that the diseased and control tissue samples are almost indistinguishable or that the RDA was not successful in yielding differentially expressed genes. Since the RDA results were also confirmed in 3 out of 4 candidate genes tested using RT-PCR amplification it can be concluded that the RDA experiment was successful in the identification of subtly upregulation mRNAs but the gene expression profiles of *Smn*$^{-/+}$ and *Smn*$^{+/+}$ spinal cords are very similar at the 5-week time point. Some functional groups emerged from the identified genes, the most prominent groups being structural genes and metabolic genes.

4.4.1 Upregulated Structural Genes Discovered by RDA

RDA results showed an upregulation of several β-actin-related genes such as: β-actin (NM_007393), supressor of actin mutations 1 (Sac1, NM_030692), Gelsolin (BC023143), Mayven (NM_007246) and the exocyst subunit SEC15 (BC030428). Recent evidence shows that Smn with its binding partner hnRNP R associates with the 3' UTR of β-actin mRNA and that this association is important for its transport to distal parts of the axon and growth cones (Rossoll et al., 2003), where its gene product is required for the proper function of the cytoskeleton (Bassell et al., 1998; Zhang et al., 1999, 2001). The gene products of identified clones such as Mayven (Soltysik-Espanola et al., 1999) and Sac1 (Novick et al., 1989) interact with actin presumably as components or controllers of the assembly or stability of the actin cytoskeleton. Actin-binding proteins such as radixin (Castelo & Jay, 1999) and gelsolin (Sobue, 1993; Furnish et al., 2001) have been shown to play roles in growth cone motility and neurite outgrowth. Since the actin cytoskeleton plays

an important role in axon initiation, growth, guidance, retraction, synapse formation and stability (Luo, 2002) it is easy to imagine the decrease in actin levels having a generalized affect on transcription of β-actin and other proteins involved in the cytoskeleton.

4.4.2 Upregulated Metabolic Genes Discovered by RDA

Several metabolic genes were found to be upregulated in *Smn*$^{-/+}$ mice, likely due to a general disruption in homeostasis. These genes included: Enolase 1 (NM_023119), AMP deaminase 3 (D8898), Aldo-keto reductase 7a5 (NM_025337), Osmotic stress protein (BC012712), Seven in absentia (NM_009172), Tyrosinase (XM_133679), Iduronate 2-sulfatase (NM_010498), Glia-derived neurotrophic factor (AJ011432), Galactosyltransferase (NM_031740) and Cyclooxygenase-2 (Cox-2) (AF378830). Cox-2 which is an enzyme implicated in mediating both excitotoxic and inflammatory processes via its prostanoid products, was found to be upregulated in the *Smn*$^{-/+}$ spinal cord. Interestingly Cox-2 also appeared in a transciption profiling study using spinal cords of SOD1-G93A mice (Olsen et al., 2001). Recent studies have demonstrated that Cox-2 is elevated in the ALS transgenic models and in sporadic ALS spinal cord samples (Almer et al., 2001), whereas Cox-2 inhibitors rescue motor neurons in models of ALS (Drachman et al., 2000; Drachman et al., 2002). ALS is another progressive motorneuron disease which is thought to have common or similar pathological mechanisms as SMA, and therefore the Cox-2 elevation may also be implicated in SMA.

Although the RDA experiment successfully identified several upregulated genes, the expression profiles of *Smn*$^{-/+}$ and *Smn*$^{+/+}$ spinal cords are very similar at the 5-week time point suggesting that a more sensitive highthroughput transcript level detection system might

be of use. For this reason, we turned our efforts next to microarray profiling using Affymetrix GeneChips®.

4.5 Changes in the Transcription Factor Profile of 5 -week-old Smn$^{-/+}$ Mouse Spinal Cords

The GeneChip Mouse Expression Array 430A represents approximately 22000 full-length mouse genes and EST clusters, including all murine RefSeq database sequences. Spinal muscular atrophy may induce a complex cellular response through the activation and/or suppression of one or more transcriptional pathways in motor neurons and/or other cell types. Traditional analysis of mRNA expression for single genes using RT-PCR has so far only demonstrated the differential expression of SIP1 variants in SMA and ALS in muscle tissue (Aerbajinai et al., 2002). In contrast, using the Affymetrix MOE430A high-density oligonucleotides, the changes of 23,000 genes and ESTs in the heterozygote SMA model were examined. In some cases, genes with common biological functions or in the same metabolic pathway showed co-ordinated expression. For this reason, some genes implicated by microarray analysis will be discussed by emphasizing functional clusters of co-regulated genes and pathways. Generally, similarities in temporal expression patterns may point to the existence of common regulatory structures and pathways.

As in the RDA analysis, using the gene chip to study the transcriptome of the spinal cord in the *Smn*$^{-/+}$ mouse is particularly demanding due to the heterogenous nature of these cells. The spinal cord contains a large variety of cell populations that are closely intermingled. The expression of any specific gene may be restricted to motor neurons or another

subpopulation of cells, and changes in gene expression may occur in only a small fraction of the cells expressing that transcript. Due to this dilution effect, many genes of interest are expected to have relatively low levels of expression in the spinal cord homogenates. Furthermore, biologically significant changes in expression may result in only small fold-changes, such as the *Smn* gene, whose expression, when cut in half results in the SMA phenotype. For this reason we chose to go with a low cut off value of 1.2 fold when observing the gene profiles. Although this increases the rate of false-positive genes, it also increases the chance of identifying a biologically significant gene. Using RT-PCR to idependently validate the candidate genes we found a true-positive rate of 64% based on the validation of 14 genes.

4.5.1 Intracellular Signaling

Apoptosis Regulators: Apoptosis is a form of programmed cell death that primarily occurs physiologically during development and in the adult, guiding the fate of individual cells or organs (Brill et al., 1999). Nevertheless, it is thought that the dysregulation of apoptosis contributes to neuronal loss during neurodegenerative diseases such as SMA (Iwahashi et al., 1997; Lefebvre et al., 1998) and amylotrophic lateral sclerosis (ALS) (Vukosavic et al, 1999; Honig and Rosenberg, 2000). Apoptosis is an active cell death characterized by classical morphological and biochemical changes (McConkey, 1998) operated by the caspase family of enzymes. Bid, which is shown to mediate neuronal cell death after cerebral ischemic insult (Plesnila et al., 2001), is cleaved by caspase-8 to tBid after death receptor stimulation and moves to mitochondria, where it interacts with and induces oligomerization of members of the Bcl-2 family, Bax and Bak (Eskes et al., 2000; Perez et al., 2000; Wei et al., 2000) to affect the mitochondrial apoptotic pathway and thereby initiate a caspase cascade (Wei et al.,

2001). These findings indicate that the increase of pro-apoptotic *Bid* mRNA and protein levels and decrease in anti-apoptotic *N-Bak* mRNA levels may contribute to the demise of motor neurons in $Smn^{-/+}$ mice. However, further immunohistochemical analyses show that differential expression of both Bak and Bid are not motor neuron specific. The N-Bak antibody used cross-reacted with ubiquitously expressed Bak, showing non cell-specific cytosolic staining (Figures 13). Bid expression was found mainly in the nuclei and the axonal processes (Figure 15). The mRNA coding for the pro-apoptotic protein Fas-ligand (FasL) is decreased the same extent as the protein, as determined by the Kinetworks kinase screen. Other genes to show increased expression in 5-week-old $Smn^{-/+}$ mouse spinal cords were the genes coding for pro-apoptotic proteins Cd27 binding protein (Siva) and glutathione peroxidase 1 (Gpx1) and the anti-apoptotic Apoptosis Inhibitor 5 (Api5). Decreased expression was evident in the genes coding for pro-apoptotic proteins hepatoma-derived growth factor related protein 1 (Hdgfrp1) and the Scotin gene and anti-apoptotic protein Peroxiredoxin 2 (Prdx2). The expression profile shows a disruption in apopotic protein expression involved in either survival or death signalling pathways. This is likely due to the fact that at the 5-week timepoint already 30% of the motor neurons have died (Table 5). At this timepoint some motor neurons are dying while some are trying to survive. There may also be stress-induced effects on cells other than motor neurons, emphasizing the need to perform profiling on isolated motor neuron cultures.

Transcription Factors: Among transcription factors found to be significantly altered in expression are two T-box family members, Tbx4 and Tbx21. Members of the T-box family of transcription factors share an evolutionarily conserved DNA-binding domain and play significant roles in various processes of embryonic development (Herrmann et al., 1990).

There was also a decreased expression of two AP-2 transcription factors: α and δ which play an important role in regulating gene expression during development and differentiation of multiple organs and tissues. One study showed that an AP-2 isoform other than α is critical for the promoter activity of Cox-2 (Kirtikara et al., 2000), which was shown upregulated in our RDA analysis.

4.5.2 Calcium Dependent Signalling

The execution of cell death relies on mitochondria, the organelles that integrate death signals mediated by proteins belonging to the Bcl-2/Bax family and kill cells by releasing critical factors such as cytochrome c that activate executioner caspase proteases (Green and Reed, 1998; Martinou and Green, 2001). Mitochondria eventually decide whether Ca^{2+} signals, the cellular messengers that control every aspect of cell and tissue physiology, are decoded as life or death signals (Szalai et al., 1999). Spinal cord injury evokes an increase in intracellular free Ca^{2+} levels which in turn activate calpain and mediate mitochondrial damage leading to neuronal death following injury (Wingrave et al., 2003). This study shows mostly decreased expression of calcium dependent signaling (Table 8). Several studies indicate that the Ca^{2+} content of the endoplasmic reticulum (ER) determines the cell's sensitivity to apoptotic stress. Procedures that decrease the Ca^{2+} concentration in the ER protect cells from apoptosis (Nakamura et al., 2000; Pinton et al., 2001). Decreased calcium dependent signalling activity suggests a general decrease in free calcium levels possibly as an attempt to protect cells at risk of undergoing apoptotic death.

4.5.3 Extracellular Matrix and Cytoskeleton:

Actin-Related: As in the RDA analysis several actin-interacting proteins showed differential expression presumably due to the defective actin-cytoskeleton found in motor axons of SMA patients. These include BH3 interacting domain death agonist (100% increase), ARP1 actin-related protein 1B (50% increase), Nebulin-related anchoring protein (50% decrease), Villin (60% decrease), Tropomyosin 2β (140% decease) and Parvin γ (210% decrease). These results taken together strongly suggest a disregulation of actin pathways.

Cytoskeletal: Altered expression of several kinesin family members was observed in the $Smn^{-/+}$ mice: Kinesin family member 3C (Kif3c), Kinesin family member 5B (Kif5b), Kinesin family member 12 (Kif12), Kinesin family member 20A (Kif20a). Kinesins are motor proteins responsible for transport of organelles and vesicles away from the microtubule-organizing center near the nucleus (Hirokawa et al., 1991). Studies have shown that a reduction of kinesin levels results in impaired microtubule dependent trafficking of organelles to the cell periphery, and to the eventual collapse of the intermediary filament network which contributes in the atrophy and death of affected cells (Yoshiyama et al., 2003). Another study found kinesins selectively accumulated in the large axonal swelling (spheroids), in the spinal cords of patients with motor neuron disease, causing a disturbance of the anterograde fast axonal transport machinery (Toyoshima et al., 1998). The perturbation of the balance in microtubule-dependent transport caused by aberrant kinesin

homeostasis is consistent with the observed impairment of axonal traffic in Spinal Muscular Atrophy disease neurons and their subsequent degeneration. (Rossoll et al., 2003).

4.6 ***Conclusion***

The study presented here was the first to apply mRNA and protein profiling to *Smn*$^{-/+}$ mice possessing a mild SMA phenotype. Closely-related studies have done mRNA and protein expression profiles on ALS, another motor neuron disease (Olsen et al., 2001), brain injury models (Di Giovanni et al., 2003), and one study looked at protein expression changes in the skeletal muscle of SMA type III patients (Anderson et al., 2003). We chose to use spinal cord tissue for the profiling analyses in this study since SMA pathology is neurogenic. The 5-week timepoint was chosen for *Smn*$^{-/+}$ mice because half of the motor neurons that the *Smn*$^{-/+}$ mouse will lose by 1 year of age have already degenerated while the other half are priming for cell death. Therefore we postulate that the genes and proteins found to be differentially regulated in this model are either directly or indirectly contributing to create an environment for motor neuron loss or are the direct or indirect result of motor neuron degeneration.

Three profiling analyses were carried out in order to uncover mechanisms affected by SMN depletion leading up to the degeneration of motor neurons. This study created a detailed profile of changes caused by SMN depletion in spinal cords at the mRNA level using RDA and microarray analysis and at the protein level using the Kinetworks screens.

The Kinetworks screens were used to analyse the expression of 78 distinct protein kinases and 25 apoptotic proteins in the spinal cords of 5-Week-old $Smn^{-/+}$ mice and controls. Although the comparison of 103 proteins in spinal cord tissue from *Smn*$^{-/+}$ mice did not reveal statistically significant differences in expression there were some alterations in PKs and APs in $Smn^{-/+}$ mice that may prove to be significant if the number of performed screens is increased. By comparing the protein kinase profile of our model to those of previous ALS model we were able to underline some differences and similarities in the disease mechanisms. Overall, signalling pathways and apoptotic protein levels do not seem to be significantly altered in the SMA mouse spinal cord at the 5-week preclinical stage. However, there was a high degree of variability for the screens performed in this study as well as previous screens for Amylotrophic Lateral Sclerosis using total tissue homogenates indicating that these screens may not be sensitive enough to observe subtle, cell-specific changes in tissue.

RDA results allowed the detection of subtle differences between the $Smn^{-/+}$ and $Smn^{+/+}$ screens. Several gene groups were identified including actin-cytoskeleton related genes and metabolic genes. The expression of four clones, AIAR, Nedd4, Ubc2d2 and gelsolin were validated using RT-PCR techniques. A western was performed for the most promising gene, gelsolin, revealing that the changes observed in the transcript level did not appear at the protein level at this time point.

The microarray analysis was performed to assess the relative expression of 22,600 genes in the 5-week-old $Smn^{-/+}$ mice. Several groups were identified including intracellular signaling and cytoskeletal genes. We discovered a general decrease in the expression of

calcium-dependent signalling genes, signifying a general decrease in free calcium levels and subsequent protection of the cells from undergoing apoptotic death.

Both RDA and microarray profiles show that subtle changes occur in the transcriptome of SMA mice, especially in genes involved in the actin-cytoskeleton, apoptosis and transcription factors. Western blots were used to validate Bid and N-Bak, two apoptotic gene products found to be differentially expressed in $Smn^{-/+}$ mice. Pro-apoptotic Bid protein levels were increased at the 5-week, 3-month and 6-month time-points, but no differences in anti-apoptotic N-Bak protein levels were found at any time-point. Immunohistochemical staining against Bid and Bak show that differential expression of the proteins are not motor neuron specific, suggesting that their differential expression may not be cell-specific. Considering the subtle changes of apoptotic protein at the transcript level it is probably that cells are presenting the first signs of the apoptotic process indicating that they are responding to the stress of Smn depletion.

Although the data demonstrate the utility of a cDNA-microarray system as a means of identifying mechanisms affected by Smn depletion in spinal muscular atrophy, they present just a glimpse of the complex phenomenon underlying motor neuron degeneration. It should be emphasized that the microarray provides estimates of changes in the mRNA levels that cannot be correlated with the amount and function of the gene products. Translational and posttranslational modifications of many gene products and protein turnover have dramatic effects on function, and these cannot be inferred from expression analysis alone.

To overcome the challenges of dilution effect experienced in the conducted analyses motor neurons would have to be purified from the spinal cord into a homogeneous cell population. By decreasing the tissue complexity it becomes easier to identify cell-specfic differences at both the transcript and protein levels (Wurmbach et al., 2002). Clearly, it will be of interest to profile gene expression specifically in vulnerable cells such as the motor neurons, and extend the analysis to different time points in the SMA model.

APPENDIX A

Proteins screened in the Kinetworks Apoptosis Protein Screen, KAPS-1.0

Antibody Name	full name	RefSeq
PARP	ADP-ribosyltransferase (NAD+;poly (ADP-ribose) polymerase)	NP_001609
AIF	Apoptosis Inducing Factor	NP_004199
XIAP	Baculoviral IAP repeat-containing 4	NP_001158
SODD	BCL2 associated athanogene 4	NP_004865
CASP1	Caspase 1	NP_001214
CASP12	Caspase 12	NP_033938
CASP2	Caspase 2	NP_001215
CASP3	Caspase 3	NP_004337
CASP4	Caspase 4	NP_001216
CASP5	Caspase 5	NP_004338
CASP6	Caspase 6	NP_001217
CASP7	Caspase 7	NP_01218
CASP8	Caspase 8	NP_001219
CASP9	Caspase 9	NP_01220
CAS	Cellular Apoptosis Susceptibility	NP_001307
CytoC	Cytochrome C	NP_061820
DAXX	Death associated protein 6	NP_001341
DFF45	DNA fragmentation factor alpha	NP_004392
MSH2	mutS homolog2, colon cancer, nonpolyposis type 1	NP_000242
PERP	p53-induced protein PIGPC1	NP_071404
SOD (Cu/Zn)	Superoxide dismutase 1	NP_000445
SOCS-4	Suppressor of cytokine signalling 4	NP_543143
TRADD	TNFRSF1A-associated via death domain	NP_003789
FAS	Tumor necrosis factor superfamily member 6	NP_000034
FasL	Tumor necrosis factor ligand, member 6	NP_000630

APPENDIX B

Proteins screened in the Kinetworks Protein Kinase Screen, KPKS-1.2

Abbreviation	Kinase Name	Protein Refseq
Aurora 2	Aurora 2	NM 003600.1
BMX (Etk)	Bone marrow X kinase	NP_001712
Btk	Bruton agammaglobulinemia tyrosine kinase	NP_000052
CaMK1	Calmodulin-dependent kinase 1	NP_003647
CaMKK	Calmodulin-dependent kinase kinase	NP_006540
CaMK4	Calmodulin-dependent kinase 4	NP_001735
Cdk1	Cyclin-dependent kinase 1 (cdc2)	NP_001777
Cdk2	Cyclin-dependent kinase 2	NP_001789
Cdk4	Cyclin-dependent kinase 4	NP_000066
Cdk5	Cyclin-dependent kinase 5	NP_004926
Cdk6	Cyclin-dependent kinase 6	NP_001250
Cdk7	Cyclin-dependent kinase 7	NP_001790
Cdk9	Cyclin-dependent kinase 9	NP_001252
CK1d	Casein kinase 1 delta	NP_001884
CK1e	Casein kinase 1 epsilon	NP_001885
Ck2a	Casein kinase 2 alpha	NP_001887
COT	Cancer Osaka thyroid oncogene (Tpl2)	NP_005195
Csk	c-SRC tyrosine kinase	NP_004374
DAPK	Death associated protein kinase 1	NP_004929
DNA-PK	DNA-activated protein kinase	NP_008835
EEF2K	Elongation Factor-2 Kinase	NP 037434
Erk1	Extracellular regulated kinase 1	AAA36142.1
Erk2	Extracellular regulated kinase 2	NP_002736
Erk3	Extracellular regulated kinase 3	NP_002739
Erk6	Extracellular regulated kinase 6	NP_002960
FAK	Focal adhesion kinase	NP_005598
Fyn	Fyn oncogene related to SRC	NP_002028
Gck	Germinal centre kinase	NP_004570
Grk2	G protein-coupled receptor kinase 2 (BARK2)	NP_001610
GSK3a	Glycogen synthase kinase 3 alpha	NP_063937
GSK3b	Glycogen synthase kinase 3 beta	NP_002084
Hpk1	Hematopoetic progenitor kinase 1	NP_009112

IKKa	Inhibitor NF kB kinase alpha	NP_001269
IKKb	IKBKB; Inhibitor of kappa light poypeptide gene enhancer in B-cells, kinase beta	XP 032491
JAK1	Janus kinase 1	NP_002218
JAK2	Janus kinase 2	NP_004963
Ksr1	Kinase suppressor of Ras 1	AAC50354.1
Lck	Lymphocyte-specific protein tyrosine kinase	NP_005347
Lyn	Oncogene Lyn	NP_002341
Mek1	MAP Kinase Kinase 1	NP_002746
Mek2	MAP Kinase Kinase 2	AAH00471.1
Mek4	MAP Kinase Kinase 4	NP_003001
Mek6	MAP Kinase Kinase 6	NP_002749
Mnk2	MAP kinase interacting kinase 2	NP_060042
Mos-3	v-mos Moloney murine sarcoma viral oncogene homolog 1	NP_005363
Mst1	Mammalian sterile 20-like 1	NP_006273
p38 MAPK	p38 Hog MAP kinase	NP_001306
PAKa	p21 activated kinase 1	NP_002567
PAKb	p21 activated kinase 3	NP_002569
PDK1	3-phosphoinositide dependent protein kinase 1	NP_002604
PKA	Protein kinase A (cAMP-dependent protein kinase	NP_002721
PKB	Protein kinase B	NP_005154
PKCl	Protein kinase C lambda	NP_002731
PKCa	Protein kinase C alpha	NP_002728
PKCb	Protein kinase C beta	NP_002729
PKCd	Protein kinase C delta	NP_006245
PKCe	Protein kinase C epsilon	NP_005391
PKCg	Protein kinase C gamma	NP_002730.1
PKCm	Protein kinase C mu	NP_002733
PKCt	Protein kinase C theta	NP_006248
PKCz	Protein kinase C zeta	NP_002735
PKG1	Protein kinase G1 (cGMP-dependent protein kinase)	NP_006249
PKR	dsRNA dependent protein kinase	NP_002750
PYK2	Protein tyrosine kinase 2	NP_004094
Raf1	Oncogene Raf1	NP_002871
RafB	v-raf murine sarcoma viral oncogene homolog B1	NP_004324

ROKa	RhoA kinase	NP_004841
Rsk1	Ribosomal S6 kinase 1	NP_002944
Rsk2	Ribosomal S6 kinase 2	NP_004577
S6K	S6 kinase p70	NP_003152
SAPK	Stress activated protein kinase (JNK)	NP_002744
Src	Oncogene SRC	NP_005408
Syk	Spleen tyrosine kinase	NP_003168
Yes	Yamaguchi sarcoma viral oncogene homolog 1	NP_005424
ZAP70	Zeta-chain (TCR) associated protein kinase	NP_003168.1
ZIP	ZIP kinase (death associated protein kinase 3)	NP_001339

REFERENCES

Aerbajinai, W., Ishihara, T., Arahata, K. and T. Tsukahara. 2002. Increased expression level of the splicing variant of SIP1 in motor neuron diseases. The Int. J. Biochem. & Cell Biol. **34**: 699-707.

Almer, G., Guegan, C., Teismann, P., et al. 2001. Increased expression of the pro-inflammatory enzyme cyclooxygenase-2 in amyotropic lateral sclerosis. Ann. Neurol. **49**:167-185.

Altschul S.F., Madden, T.L., Schaffer, A.A., Zhang, J., Zhang, Z., Miller, W. and D.J. Lipman. 1997. Gapped BLAST and PSI-BLAST: a new generation of protein database search programs. Nucleic Acids Res. **25**: 3389-3402.

Bakay, M., Chen, Y. W., Borup, R., et al. Sources of variability and effect of experimental approach on expression profiling data interpretation. 2002. BMC Bioinformatics **3**: 4.

Bassell, G.J., Zhang, H., Byrd, A.L., Femimo, A.M., Singer, R.H.,, Taneja, K.L., Lifshitz, L.M., Herman, I.M and K.S. Kosik. 1998. Sorting of β-actin mRNA and protein to neuritis and growth cones in culture. J. Neurosci. **18**: 251-265.

Bates, S., Read, S. J., Harrison, D. C., Topp, S., Morrow, R., Gale, D., Murdock, P., Barone, F. C., Parsons, A. A., and Gloger, I. S. 2001. Characterisation of gene expression changes following permanent MCAO in the rat using subtractive hybridisation. Brain Res Mol Brain Res **93**: 70-80.

Bertrandy, S., Burlet, P., Clermont, O., Huber, C., Fondrat, C., Thierry-Mieg, D., Munnich, A. and S. Lefebvre. 1999. The RNA-binding properties of SMN: deletion analysis of the zebrafish orthologue defines domains conserved in evolution. Hum. Mol. Genet. **8**:775-782.

Bradford, M. A rapid and sensitive method for the quantitation of microgram quantities of protein utilizing the principle of protein-dye binding. 1976. Anal. Biochem. **72**, 248-254.

Brill, A., Torchinsky, A., Carp, H. and V. Toder. 1999. The role of apoptosis in normal and abnormal embryonic development. J. Assist. Reprod. Genet. **16**: 512-519.

Brzustowicz, L. M., Lehner, T., Castilla, L. H., Penchaszadeh, G. K., Wilhelmsen, K. C., Daniels, R., Davies, K. E., Leppert, M., Ziter, F., Wood, D., et al. 1990. Genetic mapping of chronic childhood-onset spinal muscular atrophy to chromosome 5q11.2-13.3. Nature 344: 540-541.

Buhler, D., Raker, V., Luhrmann, R., U. Fischer. 1999. Essential role for the tudor domain of SMN in spliceosomal U snRNP assembly: implications for spinal muscular atrophy. Hum Mol Genet. **8**:2351-2357.

Burglen, L., Seroz, T., Miniou, P., Lefebvre, S., Burlet, P., Munnich, A., Pequignot, E. V., Egly, J. M., and Melki, J. 1997. The gene encoding p44, a subunit of the transcription factor TFIIH, is involved in large-scale deletions associated with Werdnig-Hoffmann disease. Am. J. Hum. Genet. **60**: 72-79.

Burglen, L., Spiegel, R., Ignatius, J., Cobben, J.M., Landrieu, P., Lefebvre, S., Munnich, A. and J. Melki. 1995. *SMN* gene deletion in variant of infantile spinal muscular atrophy. Lancet **346**: 316-317.

Byers, R.K. and B.Q. Banker. 1961. Infantile muscular atrophy. Arch. Neurol. **5**:140-164.

Campbell, L., Potter, A., Ignatius, J., Dubowitz, V. and K. Davies. Genomic variation and gene conversion in spinal muscular atrophy: implications for disease process and clinical phenotype. Am. J. Hum. Genet. **61**: 40-50.

Camu, W. and C.E. Henderson. 1992. Purification of embryonic rat motoneurons by panning on a monoclonal antibody to the low-affinity NGF receptor, J. of Neuroscience Methods **44**:59-70.

Castelo, L. and D.G. Jay. 1999. Radixin is involved in lamellipodial stability during cone motility. Mol. Biol. Cell **10**: 1511-1520.

Chakrabartty, A., Schellman, J.A. and R.L. Baldwin. 1991. Large differences in the helix propensitiesof alanine and glycine. Nature **351**: 586-588.

Chou, S.M. and A.V. Fakadej. 1971. Ultrastructure of chromatolytic motoneurons and anterior spinal roots in a case of Werdnig-Hoffmann disease. Brain Dev. **11**: 221-229.

Cifuentes-Diaz, C., Frugier, T., Tiziano, F.D., Lacene, E., Roblot, N., Joshi, V., Moreau, M.H. and J. Melki. 2001. Deletion of murine SMN exon 7 directed to skeletal muscle leads to severe muscular dystrophy. J. Cell Biol. **152**: 1107-1114.

Cork, L.C., Altschuller, R.J., Bruha, P.J., Morris, J.M., Lloyd, D.G., Loats, H.L., Griffen, J.W. and D.L. Price. 1989. Changes in neuronal size and neurotransmitter marker in hereditary canine spinal muscular atrophy. Lab. Invest. **61**: 69-76.

Cotran, R.S., Kumar, V. and T. Collins. 1999. Robbins Pathological Basis of Disease. 6th ed. W.B. Saunders Company, Philadelphia. pp 1271, 1281.

Crawford, T.O. and C.A. Pardo. 1996. The neurobiology of childhood spinal muscular atrophy. Neurobio. Dis. **3**: 97-110.

Crowder, R.J., Freeman, R.S. Phosphatidylinositol 3-kinase and Akt protein kinase are necessary and sufficient for the survival of nerve growth factor-dependent sympathetic neurons. J. Neurosci. **18**: 2933-2943.

DeSousa, B. N., and L.A. Horricks. 1979. Development of rat spinal cord. I. Weight and length, with a method of rapid removal. Dev. Neurosci. **2**: 115-121.

DiDonato, C.J., Chen, X.N., Noya, D., Korenberg, J.R., Nadeau, J.H. and L.R. Simard. 1997. Cloning, characterization, and copy number of the murine survival motor neuron gene: homolog of the spinal muscular atrophy-determining gene. Genome Res. **7**:339-352.

Drachman, D.B., Frank, K., Dykes-Hoberg, M, et al. 2002. Cyclooxygenase 2 inhibition protects motor neurons and prolongs survival in a transgenic mouse model of ALS. Ann. Neurol. **52**:771–778.

Drachman DB, Rothstein JD. 2000. Inhibition of cyclooxygenase-2 protects motor neurons in an organotypic model of amyotrophic lateral sclerosis. Ann. Neurol. **48**:792–795.

Dubowitz, V. 1995. *Muscle Disorders in Childhood*, 2nd ed. W.B. Saunders Co. Ltd., Philadelphia, p. 328.

Dudek, H., Datta, S.R., Franke, T.F., Birnbaum, M.J, Yao, R., Cooper, G.M., Segal, R.A., Kaplan, D.R. and Greenberg, M.E. Regulation of neuronal survival by the serine-threonine protein kinase Akt. Science **275**: 661-665.

Eskes, R., Desagher, S., Antonsson, B. and J.C. Martinou. Bid induces the oligomerization and insertion of Bax into the outer mitochondrial membrane. Mol. Cell. Biol. **20**:929-35.

Fan, L. and L.R. Simard. 2002. Survival motor neuron (SMN) protein: role in neurite outgrowth and neuromuscular maturation during neuronal differentiation and development. Hum. Mol. Genet. **11**: 1605-1614.

Ferri, A., Melki, J. and A.C. Kato. 2004. Progressive and selective degeneration of motor neurons in a mouse model of SMA. Developmental Neuroscience **15**: 275-280.

Frugier, T., Tiziano, F.D., Cifuentes-Diaz, C., Miniou, P., Roblot, N., Dierich, A., Le Meur, M. and J. Melki. 2000. Nuclear targeting defect of SMN lacking the C-terminus in a mouse model of spinal muscular atrophy. Hum. Mol. Genet. **9**: 849-858.

Furnish, E.J., Zhou, W., Cunningham, C.C., Kas, J.A. and C.E. Schmidt. 2001. Gelsolin overexpression enhances neurite outgrowth in PC12 cell. FEBS Lett. **508**:282-286.

Graveel, C. R., Jatkoe, T., Madore, S. J., Holt, A. L., and Farnham, P. J. 2001. Expression profiling and identification of novel genes in hepatocellular carcinomas. Oncogene **20**: 2704-12.

Green, D.R. and J.C. Reed. 1998. Mitochondria and apoptosis. Science **281**:1309-12.

Gress, T.M., Wallrapp, C., Frohme, M., Muller-Pillasch, F., Lacher, U., Friess, H., Buchler, M., Adler, G., and J.D. Hoheisel. 1997. Identification of genes with pancreatic cancer

specific expression by use of cDNA representational difference analysis. Genes Chromosom. Cancer, **19**: 97-103.

Grunstein, M and D. S. Hogness. 1975. Colony hybridization: A method for the isolation of cloned DNAs that contain a specific gene. *Proc.* Nat. Acad. Sci. USA. **72**: 3961-3965.

Haddad, H., Cifuentes-Diaz, C., Miroglio, A., Roblot, N, Joshi, V. and J. Melki. 2003. Riluzole attenuates spinal muscular atrophy disease progression in a mouse model. Muscle Nerve **28**: 432-437.

Hansen, S. and C.M. Ballatyne. 1978. A quantitative electro-physiological study of motor neuron disease. J Meurol Neurosurg Psychiatry **41**: 773-783.

Hausmanowa-Petrusewicz, I. 1970. Infantile and juvenile spinal muscular atrophy. In: Walton, J. N., Canal, N. and G. Scarlato. Eds, Muscle Diseases. Proceedings, International Congress, Milan, 1969. Amsterdam: Excerpta Medica, I.C.S. No. 199, pp. 558-567.

Herrmann, B.G., Labeit, S., Poustka, A., King, T.R. and H. Lehrach. 1990. Cloning of the *T* gene required in mesoderm formation in the mouse. Nature **343**:617–622.

Hirokawa N., Sato-Yoshitake, R., Kobayashi, N., Pfister, K.K., Bloom, G.S. and S.T. Brady. 1991. Kinesin associates with anterogradely transported membranous organelles in vivo. J Cell Biol **114**:295–302.

Hoffmann, J. 1900. Uber die hereditare progressive spinale muskelatrophie in kindersalter. Muenchen Med. Wschr. **47**: 1649-1651.

Honig, L.S. and R.N. Rosenberg. 2000. Apoptosis and neurologic disease. Am. J. Med. **108**: 317-330.

Hsieh-Li, H.M., Chang, J.G., Jong, Y.J., Wu, M.H., Wang, N.M., Tsai, C.H. and H. Li. 2000. A mouse model for spinal muscular atrophy. Nat. Genet. **24**:66-70.

Hu. J. H., Chernoff, K., Pelech, S. and C. Krieger. 2003a. Protein kinase and protein phosphatase expression in the central nervous system of G93A mSOD over-expressing mice. J. Neurochem. **85**: 422-431.

Hu. J. H., Zhang, H., Wagey, R., C. Krieger and S.L. Pelech. and. 2003b. Protein kinase and protein phosphatase expression in amyotrophic lateral sclerosis spinal cord. J. Neurochem. **85**: 432-442.

Iannaccone, S.T., Smith, S.A. and L.R. Simard. 2004. Spinal muscular atrophy. Curr. Neurol. Neurosci. Rep. **4**: 74-80.

Iwahashi, H., Eguchi, Y., Yasuhara, N., Hanafusa, T., Matsuzawa, Y. and Y. Tsujimoto. 1997. Synergistic anti-apoptotic activity between Bcl-2 and SMN implicated in spinal muscular atrophy. Nature **390**: 413-417.

Jablonka, S., Schrank, B., Kralewski, M., Rossoll, W. and M. Sendtner. 2000. Reduced survival motor neuron (Smn) gene dose in mice leads to motor neuron degeneration: an animal model for spinal muscular atrophy type III. Hum. Mol. Genet. **9**:341-346.

Jablonka, S., Bandilla, M., Wiese, S., Buhler, D., Wirth, B., Sendtner, M. and U. Fisher. 2001. Co-regulation of survival of motor neuron (SMN) protein and its interactor SIP1 during development and in spinal muscular atrophy. Hum. Mol. Genet. **10**: 497-505.

Kirtikara, K, Raghow, R., Laulederkind, S.J.F., Goorha, S., Kanekura, T. and L.R. Ballou. 2000. Transcriptional regulation of cyclooxygenase-2 in the human microvascular endothelial cell line, HMEC-1: Control by the combinatorial actions of AP2, NF-IL-6 and CRE elements. Mol. Cellular Biochem. **203**: 41–51.

Kluver, H. and E. Barrera. 1953. A method for the combined staining of cells and fibers in the nervous system. J. Neuropathol. Exp. Neurol. **12**:400-403.

Krajewski, S., Krajewska, M. and J.C. Reed. 1996. Immunohistochemical analysis of in vivo patterns of Bak expression, a proapoptotic member of the Bcl-2 protein family. Cancer Res. **56**:2849-55.

Kugelberg, E., and L. Welander. 1956. Heredo-familial juvenile muscular atrophy stimulating muscular atrophy. Arch. Neurol. Psychiat. **75**: 500-509.

Laemmli, U. K. Cleavage of structural proteins during the assembly of the head of bacteriophage T4. 1970. Nature **227**: 680-685.

Lefebvre, S., Burglen, L., Frezal, J., Munnich, A. and J. Melki. 1998. The role of *SMN* gene in proximal spinal muscular atrophy. Hum. Mol. Genet. **715**: 1531-1536.

Lefebvre, S., Burglen, L., Reboullet, S., Clermont, O., Burlet, P., Viollet, L., Benichou, B., Cruaud, C., Millasseau, P., Zeviani, M., and et al. 1995. Identification and characterization of a spinal muscular atrophy- determining gene. Cell **80:** 155-65.

Lisitsyn, N., Lisitsyn, N., and M. Wigler. 1993. Cloning the differences between two complpex genomes. Science **259**: 946-951.

Lorson, C.L., Hahnen, E.J., Androphy, E. and B. Wirth. 1999. A single nucleotide in the SMN gene regulates splicing and is responsible for spinal muscular atrophy. Proc. Nat. Acad. Sci. USA. **96:** 6307-6311.

Luo, L. 2002. Actin cytoskeleton regulation in neuronal morphogenesis and structural plasticity. Annu. Rev. Cell Dev. Biol. **18**: 601-635.

Lyu, P.C., Liff, M.I., Marky, L.A. and N.R. Kallenbach. 1990. Side chain contributions to the stability of a-helical structure in peptides. Science. **250**: 669-673.

Maher P. 2001. How protein kinase C activation protects nerve cells from oxidative stress-induced cell death. J. Neurosci. **30**: 135-147.

Martin, L. J., Kaiser, A., and Price, A. C. Motor neuron degeneration after sciatic nerve avulsion in adult rat evolves with oxidative stress and is apoptosis. 1999. J Neurobiol **40**: 185-201.

Martinou, J.C. and D.R. Green. 2001. Breaking the mitochondrial barrier. Net. Rev. Mol. Cell Biol. **2**:63-67.

McAndrew, P. E., Parsons, D. W., Simard, L. R., Rochette, C., Ray, P. N., Mendell, J. R., Prior, T. W., and Burghes, A. H. 1997. Identification of proximal spinal muscular atrophy carriers and patients by analysis of SMNT and SMNC gene copy number. Am J Hum. Genet. **60**: 1411-1422.

McConkey, D.J. 1998. Biochemical determinants of apoptosis and necrosis. Toxicol. Lett. **99**: 157-168.

McGeer, P.L. and E.G. McGeer. 1998. Glial cell reactions in neurodegenerative diseases: pathophisiology and therapeutic interventions. Alzheimer Dis. Assoc. Disord. **12**: S1-S6.

McWhorter, M.L., Monani, U.R., Burghes, A.H.M. and C.E. Beattie. 2003. Knowckdown of the survival motor neuron (Smn) protein in zebrafish causes defects in motor axon outgrowth and pathfinding. J. Cell Biol. **162**: 919-931.

Melki, J., Abdelhak, S., Sheth, P., Bachelot, M. F., Burlet, P., Marcadet, A., Aicardi, J., Barois, A., Carriere, J. P., Fardeau, M., and et al. 1990. Gene for chronic proximal spinal muscular atrophies maps to chromosome 5q. Nature **344**: 767-768.

Miguel-Aliaga, I., Chan, Y.B., Davies, K.E. and M. van den Heuvel. 2000. Disruption of SMN function by ectopic expression of the human SMN gene in Drosophila" FEBS Lett. **486**:99-102.

Mohaghegh, P., Rodrigues, N.R., Owen, N., Ponting, C.P., Le, T.T., Burghes, A.H. and K.E. Davies. 1999. Analysis of mutations in the tudor domain of the survival motor neuron protein SMN. Eur J Hum Genet. 7:519-525.

Monani, U.R., Lorson, C.L., Parsons, D, Prior, T.W., Androphy, E.J., Burgess, A.H.M. and J.D. McPherson. 1999. A single nucleotide difference that alters splicing patters distinguishes the SMA gene SMN1 from the copy gene SMN2. Hum. Mol. Genet. **8**: 1177-1183.

Monani, U.R., Pastore, M.T., Gavrilina, T.O., Jablonka, S., Le, T.T., Andreassi, C., DiCocco, J.M., Lorson, C., Androphy, E.J., Sendtner, M., Podell, M. and A.H.M. Burghes. 2003. A transgene carrying an A2G missense mutation in the SMN gene modulates phenotypic severity in mice with severe (type I) spinal muscular atrophy. J. Cell Biol. **160**: 41-52.

Monani, U.R., Sendtner, M., Coovert, D.D., Parsons, D.W., Andreassi, C., Le, T.T., Jablonka, S., Schrank, B., Rossol, W., Prior, T.W., Morris, G.E. and A.H. Burghes. 2000. The human centromenc survival motor neuron gene (SMN2) rescues embryonic lethality in Smn(−/−) mice and results in a mouse with spinal muscular atrophy. Hum. Mol. Genet. **9**: 333-339.

Moosa, A. and V. Duvowitz. 1976. Motor nerve conduction velocity in spinal muscular atrophy of childhood. Archives of disease in childhood. **51**: 974-977.

Mouellic, H.L., Lallemand, Y. and P. Brulet. 1990 Targeted Replacement of the Homeobox Gene Hox-3.1 by the Escherichia coli LacZ in Mouse Chimeric Embryos. PNAS. **87**: 4712-4716.

Munstat, T.L. 1991. Workshop report: international SMA collaboration. Neuromusc. Disorders. **1**: 81.

Munstat, T.L., Woods, R., Fowler, W. and C.M. Pearson. 1969. Neurogenic muscular atrophy of infancy with prolonged survival. Brain. **92**: 9-24.

Murayama, S., Bouldin, T.W. and K. Suzuki. 1991. Immunocytochmical and ultra-structural studies of Wendig-Hoffmann disease. Acta Neuropathol. **81**: 408-417.

Nagao, M., Kato, S., Oda, M. and S. Hirai. 1998. Decrease of protein kinase C in the spinal motor neurons of amyotrophic lateral sclerosis. Acta Neuropathol. **96**: 52-56.

Nakamura, K., Bossy-Wetzel, E., Burns, K., Fadel, M.P., Lozyk, M., Goping, I.S., Opas, M., Bleackley, R.C., Green, D.R. and M. Michalak. 2000. Changes in endoplasmic reticulum luminal environment affect cell sensitivity to apoptosis. J. Cell Biol. **150**: 731-740.

Nehls M, Messerle M, Sirulnik A, Smith AJ and T. Boehm. 1994. Two large insert vectors, lambda PS and lambda KO, facilitate rapid mapping and targeted disruption of mammalian genes. **17**:770-775.

Noh, K.M., Hwang, J.K., Shin, H.C. and J.Y. Koh. 2000. A novel neuroprotective mechanism of riluzole: direct inhibition of protein kinase C. Neurobiol. Dis. **7**: 375-386.

Novick, P., Osmond, B.C. and D. Botstain. 1989. Suppressors of yeast actin mutations. Genet. **121**: 659-674.

Olsen, M.K., Roberds, S.L., Ellerbrook, B.R., Fleck, T.J., McKinley, D.K. and M.E. Gurney. 2001. Disease mechanisms revealed by transcription profiling in SOD-G93A transgenic mouse spinal cord. Ann. Neurol. **50**: 730-740.

Pagliardini, S., Giavazzi, A., Setola, V., Lizier, C., Di Luca, M., DeBiasi, S. and G Battaglia. 2000. Subcellular localization and axonal transport of the survival motor neuron (SMN) protein in the developing rat spinal cord. Hum. Mol. Genet. **9**: 47-56.

Pearn, J. 1973. The gene frequency of acute Werdnig-Hoffmann disease (SMA type I). A total population survey in North-East England. J. Med. Genet. **10**: 260-265.

Pearn, J. 1978. Incidence, prevalence and gene frequency studies of chronic childhood spinal muscular atrophy. J. Med. Genet. **15**: 409-413.

Pearn, J., Hudgson, P. and J.N. Walton. 1978. A clinical and genetic study of spinal muscular atrophy of adult onset. Brain: 591-606.

Perez, D. and E. White. 2000. TNF-alpha signals apoptosis through a bid-dependent conformational change in Bax that is inhibited by E1B 19K. Mol. Cell. **6**:53-63.

Pinter, M.J., Waldeck, R.F., Wallace, N. and L.C. Cork. 1995. Motor unit behaviour in canine motor neuron disease. J. Neurosci. **15**: 3447-3457.

Pinton, P., Ferrari, D., Rapizzi, E., Di Virgilio, F., Pozzan, T. and R. Rizzuto. 2001. The Ca2+ concentration of the endoplasmic reticulum is a key determinant of ceramide-induced apoptosis: significance for the molecular mechanism of Bcl-2 action. EMBO J. **20**: 2690-2701.

Plesnila, N., Zinkel, S., Le, D.A., Amin-Hanjani, S., Wu, Y., Qiu, J., Chiarugi, A., Thomas, S.S., Kohane, D.S., Korsmeyer, S.J. and M.A. Moskowitz. 2001. BID mediates neuronal cell death after oxygen/glucose deprivation and focal cerebral ischemia. PNAS **98**: 15318–15323.

Ponting, C.P. 1997. Tudor domains in proteins that interact with RNA. Trends Biochem Sci. **22**:51-52.

Rochette, C.F., Gilbert, N. and L.R. Simard. 2001. SMN gene duplication and the emergence of the SMN2 gene occurred in distinct hominids: SMN2 is unique to Homo sapiens. Hum. Genet. **108**: 255-266.

Rossoll, W., Jablonka, S., Andreassi, C., Kroning, A.K., Karle, K., Monani, U.R. and M. Sendtner. 2003. Smn, the spinal muscular atrophy-determining gene product, modulates axon growth and localization of β-actin mRNA in growth cones of motorneurons. J. Cell Biol. **163**: 801-812.

Rossoll, W., Kroning, A.K., Ohndorf, U.M., Steegborn, C., Jablonka, S. and M. Sendtner. 2002. Specific interaction of Smn, the spinal muscular atrophy determining gene product, with hnRNP and gry-rbp/hnRNP Q: a role for Smn in RNA processing in motor axons? Hum. Mol. Genet. **11**: 93-105.

Roy, N., Mahadevan, M. S., McLean, M., Shutler, G., Yaraghi, Z., Farahani, R., Baird, S., Besner-Johnston, A., Lefebvre, C., Kang, X., and et al. 1995. The gene for neuronal apoptosis inhibitory protein is partially deleted in individuals with spinal muscular atrophy. Cell **80**: 167-178.

Rudnik-Shoneborn, S., Forket, R., Hahnen, E., Wirht, B. and K. Zerres. 1996. Clinical spectrum and diagnostic criteria for infantile spinal muscular atrohy: Further delineation on the basis of *SMN* gene deletion finding. Neuropediatrics **27**: 8-15.

Russman, B.S., Iannacone, S.T. and F.J. Samaha. 2003. A phase I trial of riluzole in spinal muscular atrophy. Arch. Neurol. **60**: 1601-1603.

Scharf, J. M., Endrizzi, M. G., Wetter, A., Huang, S., Thompson, T. G., Zerres, K., Dietrich, W. F., Wirth, B., and Kunkel, L. M. 1998. Identification of a candidate modifying gene for spinal muscular atrophy by comparative genomics. Nat. Genet. **20**: 83-86.

Schmalbruch, H.M.D., Jensen, H., Bjearg, M., Kamienniecka, Z. and B.S. Kurland. 1991. A new mouse mutant with progressive motor neuropathy. J. Neuropathol. Exp. **50**: 192-204.

Schrank, B., Gotz, R., Gunnersen, J. M., Ure, J. M., Toyka, K. V., Smith, A. G., and Sendtner, M. 1997. Inactivation of the survival motor neuron gene, a candidate gene for human spinal muscular atrophy, leads to massive cell death in early mouse embryos. Proc. Natl. Acad. Sci. U. S. A. **94**: 9920-9925.

Seale, P., Sabourin, L. A., Girgis-Gabardo, A., Mansouri, A., Gruss, P., and Rudnicki, M. A. 2000. Pax7 is required for the specification of myogenic satellite cells. Cell 102: 777-786.

Selenko, P., Sprangers, R., Stier, G., Buhler, D., Fischer, U. and M. Sattler. 2001. SMN tudor domain structure and its interaction with the Sm proteins. Nat Struct Biol. **8**: 27-31.

Sharrad, W.J.W. 1955. The distribution of the permanent paralysis in the lower limb in poliomyelitisw: a clinical and pathological study. J. Bone. Jt. Surg. **37B**: 540-558.

Smith, A. G. (1991) Culture and differentiation of embryonic stem cells. J. Tissue Culture Methods **13**: 89-94.

Sobue, K. 1993. Actin-based cytoskeleton in growth cone activity. Neurosci. Res. **18**: 91-102.

Soltysik-Espanola, M., Rogers, R.A., Jiang, S., Kim, T.A., Gaedigk, R., White, R.A., Avraham, H. and S. Avraham. 1999. Characterization of Mayven, a novel actin-binding protein predominantly expressed in brain. Mol. Bio. Cell **10**: 2361-2375.

Stennicke, H.R. and G.S. Salvesen. 2000. Caspases-controlling intracellular signals by protease zymogen activation. Biochim Biophys Acta **1477:**299-306.

Toyoshima, I., Sugawara, M., Kato, K., Wada, C., Hirota, K., Hasegawa, K., Kowa, H., Sheetz, M.P. and O. Masamune. 1998. Kinesin and cytoplasmic dynein in spinal spheroids with motor neuron disease. J. Neurol. Sci. **159**: 38-44.

Vukosavic, S., Dubois-Dauphin, M., Romero, N. and S. Przedborski. 1999. Bax and Bcl-2 interaction in a transgenic mouse model of familial amyotrophic lateral sclerosis. J. Neurochem. **73**: 2460-2468.

Wagey, R., Hu, J., Pelech, S.L., Raymond, R.A. and C. Krieger. 2001a. Modulation of NMDA-mediated excitotoxicity by protein kinase C. J. Neurosci. **78**: 715-716.

Wagey, R., Lurot, S., Perrlet, D., Pelech, S.L., Sagot, Y. and C. Krieger. 2001b. Phosphatidylinositol 3-kinase activity in murine motoneuron disease: the progressive motor neurophathy mouse. Neuroscience **103**: 257-266.

Warita, H., Manabe, Y., Murakami, T., Shiro, Y., Nagano, I. and K. Abe. 2001. Early decrease of survival signal-relatedproteins in spinal motor neurons ofpresymptomatic transgenic mice with a mutant SOD1 gene. Apoptosis 6: 345-352.

Wei, M.C., Lindsten, T., Mootha, V.K., Weiler, S., Gross, A., Ashiya, M., Thompson, C.B. and S.J. Korsmeyer. 2000. tBID, a membrane-targeted death ligand, oligomerizes BAK to release cytochrome c. Genes Dev. 14:2060-71.

Wei, M.C., Zong, W.X., Cheng, E.H., Lindsten, T., Panoutsakopoulou, V., Ross, A.J., Roth, K.A., MacGregor, G.R., Thompson, C.B. and S.J. Korsmeyer. 2001. Proapoptotic BAX and BAK: a requisite gateway to mitochondrial dysfunction and death. Science **292**:727-730.

Wiese S, Pei G, Karch C, Troppmair J, Holtmann B, Rapp UR, Sendtner M. 2001 Specific function of B-Raf in mediating survival of embryonic motoneurons and sensory neurons. Nat. Neurosci. **4**:137-42.

Werdnig, G. 1894. Die fruhinfantile progressive spinale muskelatrophie. Arch. Psychiat. **26**: 706-744.

Wirth, B., Hahnen, E., Morgan, K., DiDonato, C.J., Dadze, A., Rudnik-Schoneborn, S., Simard, L.R., Zerres, K. and A.H. Burghes. 1995. Allelic association and deletions in autosomal recessive proximal spinal muscular atrophy: association of marker genotype with disease severity and candidate cDNAs. Hum. Mol. Genet. **4**:1273-84.

Wingrave, J.M., Schaecher, K.E., Sribnick, E.A., Wilford, G.G., Ray, S.K., Hazen-Martin, D.J., Hogan, E.L. and N.L. Banik. 2003. Early induction of secondary injury factors causing activation of calpain and mitochondria-mediated neuronal apoptosis following spinal cord injury in rats. J. Neurosci. Res. **73**:95-104.

Wohlfart, G. 1957. Collateral regeneration from residual motor neuron fibers in amyotrophic lateral schlerosis. Neurology **7**: 124-134.

Wooten, M.W. 1999. Function of NF-kB in neuronal survival: regulation by atypical protein kinase C. J. Neurosci. Res. **58**: 607-611.

Wurmbach, E., Gonzalez-Maeso, J., Yuen, T., Ebersole, B.J., Mastaitis, J.W., Mobbs, C.V. and S.C. Seaflon. 2002. Validated genomic approach to study differentially expressed genes in complex tissues. Neurochem. Res. **27**: 1027-1033.

Yoshiyama, Y., Zhang, B., Bruce, J., Trojanowski, J.Q. and Virginia M.-Y. Lee. 2003. Reduction of detyrosinated microtubules and golgi fragmentation are linked to tau induced degeneration in astrocytes. J. Neuroscience **23**:10662–10671.

Yun-Fu, S., Li-Yung, Y., Saarma, M., Timmusk, T. and U. Arumae. 2001. Neuron-specific Bcl-2 homology 3 domain-only splice variant of Bak is anti-apoptotic in neurons, but pro-apoptotic in non-neuronal cells. J. Biol. Chem. **276**: 16240-16247.
Zhang, H.L., Singer, R.H. and G.J. Bassell. 1999. Neurotrophin regulation of b-actin mRNA and protein localization within growth cones. J. Cell Biol. **147**: 59-70.

Zhang, H.L., Eom, T., Oleynikov, Y., Shenoy, S.M., Liebelt, D.A., Dictenberg, J.B., Singer, R.H. and G.J. Bassell. 2001. Neurotrophin-induced transport of a b-actin mRNP complex increases b-actin levels and stimulates growth cone motility. Neuron **31**: 261-275.

Zhang, H.L., Pan, F., Hong, D., Shenoy, S.M., Singer, R.H. and G.J. Bassell. 2003. Active transport of the survival motor neuron protein and the role of exon-7 in cytoplasmic localization. J. Neurosci. **23**: 6627-6637.